(2)

Polytechnic UNIVERSITY

FINAL TECHNICAL REPORT

OPTIMUM AEROELASTIC CHARACTERISTICS FOR COMPOSITE SUPERMANEUVERABLE AIRCRAFT

(AFOSR CONTRACT F49620-87-C-0046)

November 27, 1988

Principal Investigator: Prof. G.A. Oyibo

Polytechnic University
Long Island Campus
Farmingdale, NY 11735

POLY AE Report No. 88-8

Unclassified

SECURITY CLASSIFICATION OF THIS PAGE

REPORT DOCUMENTATION PAGE

Form Approved OMB No. 0704-0188

1a. REPORT SECURITY CLASSIFICATION: Unclassified	1b. RESTRICTIVE MARKINGS: N/A
2a. SECURITY CLASSIFICATION AUTHORITY: N/A	3. DISTRIBUTION/AVAILABILITY OF REPORT: Approved for public release, distribution unlimited
2b. DECLASSIFICATION/DOWNGRADING SCHEDULE: N/A	
4. PERFORMING ORGANIZATION REPORT NUMBER(S): POLY AE 88-8	5. MONITORING ORGANIZATION REPORT NUMBER(S): AFOSR-TR- 89-0127
6a. NAME OF PERFORMING ORGANIZATION: Polytechnic University; 6b. OFFICE SYMBOL (If applicable):	7a. NAME OF MONITORING ORGANIZATION: [redacted]
6c. ADDRESS (City, State, and ZIP Code): Route 110, Farmingdale, NY 11735	7b. ADDRESS (City, State, and ZIP Code): same as 6c.
8a. NAME OF FUNDING/SPONSORING ORGANIZATION: USAF Air Force Office of Scientific Research; 8b. OFFICE SYMBOL (If applicable): AFOSR/NA	9. PROCUREMENT INSTRUMENT IDENTIFICATION NUMBER: F49620-[redacted] 87-C-0046
8c. ADDRESS (City, State, and ZIP Code): Bolling Air Force Base BXC9410, DC 20332-6448	10. SOURCE OF FUNDING NUMBERS: PROGRAM ELEMENT NO. 61102F; PROJECT NO. 2302; TASK NO B1; WORK UNIT ACCESSION NO.

11. TITLE (Include Security Classification): OPTIMUM AEROELASTIC CHARACTERISTICS FOR COMPOSITE SUPERMANEUVERABLE AIRCRAFT (U)

12. PERSONAL AUTHOR(S): Prof. Gabriel A. Oyibo, Prof. James Bentson and Prof. T. A. Weisshaar

13a. TYPE OF REPORT	13b. TIME COVERED	14. DATE OF REPORT (Year, Month, Day)	15. PAGE COUNT
Final Technical Report	FROM 6/1/87 TO 9/31/88	1988/11/27	

16. SUPPLEMENTARY NOTATION

17. COSATI CODES		
FIELD	GROUP	SUB-GROUP

18. SUBJECT TERMS (Continue on reverse if necessary and identify by block number): Aeroelastic optimization, aeroelasticity, aeroelastic tailoring, unsteady aerodynamics, composite materials, composite structures, structural dynamics, composite wings.

19. ABSTRACT (Continue on reverse if necessary and identify by block number)

The investigation of an aeroelastically induced constrained warping phenomenon for a composite, supermaneuverable type aircraft wing has continued in this second year of the study. The first year investigation was concentrated mainly on the static phenomena and the search for closed form solutions for free vibration of aircraft wings having constrained warping in the presence of elastic coupling. The wing is analytically modelled as a straight flat laminated plate. Various forms of highly simplified aerodynamic loads are employed in the analysis. The free vibrations and stability aspects of this phenomenon are examined to obtain some physical insights and to determine its importance and/or design implications. Analytical tools employed include an affine transformation concept which was formulated previously (by the present principal investigator) as well as a non-dimenionalization scheme. With the help of these tools, an evolution of effective warping parameters with which to study this phenomenon was carried out. The virtual work theorem and variational principles were used to derive the equations of motion based on the assumed wing displacements. The

20. DISTRIBUTION/AVAILABILITY OF ABSTRACT	21. ABSTRACT SECURITY CLASSIFICATION
☑ UNCLASSIFIED/UNLIMITED ☐ SAME AS RPT. ☑ DTIC USERS	Unclassified
22a. NAME OF RESPONSIBLE INDIVIDUAL: Dr. A. Amos	22b. TELEPHONE (Include Area Code): 202-767-4937; 22c. OFFICE SYMBOL:

DD Form 1473, JUN 86 — Previous editions are obsolete. — SECURITY CLASSIFICATION OF THIS PAGE

Unclassified

19. Abstract - Continued

existence of closed-form free vibrations solutions for composite wings with elastic coupling and constraint of warping was established. A revelation from these closed-form solutions is that, elastic coupling lowers the coupled frequencies (in fact a significant amount of coupling could reduce the first frequency to almost zero. The discovery of the closed-form solutions for the free vibration which seems to mark the first time such solutions were ever obtained, not only led to answers to a number of previously unanswered questions but also raised new unanswered questions such as "Does the aeroelastic divergence of flutter problem of such wings have any closed-form solutions".

A main goal of the second year investigation is therefore essentially to find the answer to the above mentioned question. Accordingly in the first quarter, efforts were concentrated on determining the possibility of finding closed-form solutions to the divergence problem. The investigation led to two possible methods of obtaining such solutions. These methods are (a) the "elimination" approach (which was used for the free vibration) and (b) the method of Laplace transformation. Although it's already known that (a) works, (b) was implemented in formulating the analytical expressions for the closed-form solution of the divergence problem due to an anticipated relative ease. These newly derived closed-form expressions are shown in this report. The numerical approach used for extracting the eigenvalues from the closed-form expressions for the free vibration was studied carefully to determine how it might be used to extract the eigenvalues (and eventually the divergence flight velocities) from the closed form expressions derived for the divergence phenomenon. The results extracted showed agreement with existing results and seem to establish new trends.

TABLE OF CONTENTS

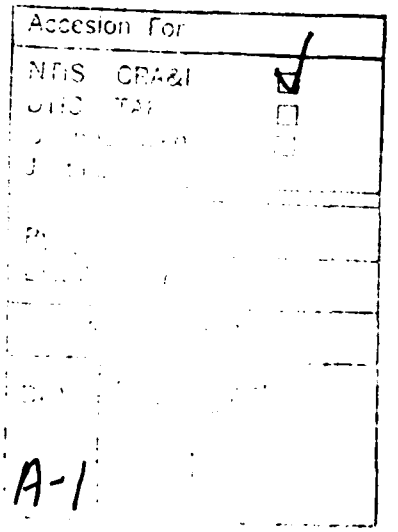

1.0 ABSTRACT

The investigation of an aeroelastically induced constrained warping phenomenon for a composite, supermaneuverable type aircraft wing has continued in this second year of the study. The first year investigation was concentrated mainly on the static phenomena and the search for closed form solutions for free vibration of aircraft wings having constrained warping in the presence of elastic coupling. The wing is analytically modelled as a straight flat laminated plate. Various forms of highly simplified aerodynamic loads are employed in the analysis. The free vibrations and stability aspects of this phenomenon are examined to obtain some physical insights and to determine its importance and/or design implications. Analytical tools employed include an affine transformation concept which was formulated previously (by the present principal investigator) as well as a non-dimensionalization scheme. With the help of these tools, an evolution of effective warping parameters with which to study this phenomenon was carried out. The virtual work theorem and variational principles were used to derive the equations of motion based on the assumed wing displacements. The existence of closed-form free vibrations solutions for composite wings with elastic coupling and constraint of warping was established. A revelation from these closed-form solutions is that, elastic coupling lowers the coupled frequencies (in fact a significant amount of coupling could reduce the first frequency to almost zero. The discovery of the closed-form solutions for the free vibration which seems to mark the first time such solutions were ever obtained, not only led to answers to a number of previously unanswered questions but also raised new unanswered questions such as

"Does the aeroelastic divergence of flutter problem of such wings have any closed-form solutions".

A main goal of the second year investigation is therefore essentially to find the answer to the above mentioned question. Accordingly in the first quarter, efforts were concentrated on determining the possibility of finding closed-form solutions to the divergence problem. The investigation led to two possible methods of obtaining such solutions. These methods are (a) the "elimination" approach (which was used for the free vibration) and (b) the method of Laplace transformation. Although it's already known that (a) works, (b) was implemented in formulating the analytical expressions for the closed-form solution of the divergence problem due to an anticipated relative ease. These newly derived closed-form expressions are shown in this report. The numerical approach used for extracting the eigenvalues from the closed-form expressions for the free vibration was studied carefully to determine how it might be used to extract the eigenvalues (and eventually the divergence flight velocities) from the closed form expressions derived for the divergence phenomenon. The results extracted showed agreement with existing results and seem to establish new trends.

2.0 NOMENCLATURE

a_i	= chordwise integrals
c_o', c_o	= affine space half-chord and chord, respectively
D_{ij}	= elastic constants
e	= parameter that measures the location of the reference axis relative to mid-chord
EI, GJ	= bending and torsional stiffness, respectively
$\bar{h}$	= wing box depth
(h_o, α_o)	= affine space bending and torsional displacement, respectively
K,So	= elastic coupling and warping stiffness, respectively
k_{ij}	= elemental stiffness parameter
k_o	= Strouhal number
L_o, M_o	= affine space running aerodynamic lift and moments, respectively
ℓ_o	= affine space half-span for the wing
m_o	= affine space mass per unit span
$(\Delta p, \Delta p_o)$	= differential aerodynamic pressure distributions in physical and affine space, respectively
t	= time
U, U_o	= virtual work expressions in physical and affine space, respectively
U_f	= flutter speed
$(x,y,z,)$, (x_o, y_o, z_o)	= physical and affine space coordinates, respectively
$\gamma_i, \delta_i, \beta_i$	= displacement shape functions
$r, L_1, L_2, D^*, D^*_o,$	= generic nondimensionalized stiffness parameters
μ_o	= affine mass ratio parameter
μ_{ij}, ε	= Poisson ratios and generalized Poisson's ratio, respectively
λ_o	= divergence parameter

ρ, ρ_∞ = affine space material and air density, respectively

θ = twisting displacements

w = displacement

ω = vibration frequency

3.0 INTRODUCTION

In the late 1960's designers began to investigate the possibility of exploiting the directional properties of composite materials to improve aeroelastic characteristics of lifting surfaces. For example, superfighter designers may aeroelastically tailor a wing so that it deforms to the optimum camber under maneuvering loads.

For instance, a wing can be tailed so that its leading edge will twist downward under the stress of a tight turn, thereby decreasing the wing's angle of attack and hence reduce drag.

Exploitation of the directional properties of composite materials to solve aeroelastic instability problems (known as aeroelastic tailoring) may enhance the performance of future high performance military aircraft, particularly the super-maneuverable concepts. This stems from the need for future military weapon systems to exhibit high performance and minimum vulnerability (e.g.; minimum radar cross-sectional area). These requirements may lead to unorthodox aircraft configurations which in turn result in unorthodox aeroelastic instability problems (e.g. the X-29 primary mode of instability, called the 'body freedom' flutter).

Perhaps the aeroelastic tailoring concept would have been discovered much earilier if the physics of anisotropic aeroelasticity were more apparent. This inherent physical intractability is largely due to the existence of numerous variables, e.g.; flight parameters, several composite directional properties, fiber orientation angles, etc., which are not even truly independent, in the aniso-

tropic system. This state of affairs is therefore analogous to that which existed in the basic rigid body aerodynamics before the advent of the similarity rule theory. This theory clearly revealed that, the utilization of non-dimensionalized groups of variables, e.g.; Reynolds, Mach, Strouhal, Froude numbers etc., provide significantly superior physical insight to the problem than the individual physical variables. The new methodology that is being used as the basic tool in this research program is basically the aeroelastic equivalent of the aerodynamic similarity rule. The expected superiority of this new approach over the state-of-the-art (SOA) counterpart, which utilizes individual physical variables, especially in terms of physical insights, has been demonstrated in references 1-10. For example, a high-aspect-ratio composite wing could behave aeroelastically like a low aspect ratio wing and vice-versa. Similarity parameters can expose conditions for which this might happen. This is significant, (for instance) in the light of the important role played by the wing aspect ratio in the aerodynamics approximations for an aeroelastic analysis. This result may therefore be suggesting some new form of coupling between the elastic and aerodynamic equations in composite wing aeroelasticity. A fundamental aspect of this new methodology has been used in studies at Purdue University[11] and MIT[12].

In this research, an investigation of a wing's spanwise sectional distortion (warping) resulting from aerodynamic forces and its influence on the wing's free vibrations, as well as (aeroelastic) stability, is being carried out. In particular, St. Venant's tor-

sional/twisting theory, which is currently widely used for estimating the wing's twisting displacements has been examined with the help of the new methodology, to determine its limitations, when applied to wings fabricated of composite materials. The relevance and significance of this study for the newly emerging supermaneuverable type aircraft may be seen in the light of the fact that (a) supermaneuverability is characterized by high angle of attack which implies high twisting aerodynamic forces, and (b) most aircraft designers believe future aircraft will be fabricated of 40-70% composite materials.

When the St. Venant's torsional theory is used to estimate a wing's twisting displacement and/or forces, the fact that the wing's root section's distortion is relatively small compared to that of other sections is ignored. However, previous investigators have determined that such an unrealistic assumption may lead to only little errors if the aspect ratio of the wing is very high.

The research has shown during the first phase that the conclusions reached by previous investigators are basically true for wings fabricated of metals or isotropic materials. A set of new theories is therefore being postulated in this research effort for accurately estimating the twisting displacements, vibrational frequencies and instability boundaries for wings fabricated of composite materials.

REFERENCES

1. Oyibo, G.A., "A Unified Flutter Analysis for Composite Aircraft Wings", AIAA paper No. 84-0906, 25th AIAA SDM Conference, Palm Springs, CA, May 1984.

2. Oyibo, G.A., "Reply by the Author to P.A.A. Laura", AIAA Journal, Vol. 22, April 1984.

3. Oyibo, G.A., "A Unified Flutter Theory for Composite Aircraft Wings" Invited Lecture, 26th Israel Annual Conference on Aviation and Astronautics, Technion, Haifa, Israel, February 1984.

4. Oyibo, G.A., and Brunelle, E.J., "Vibrations of Circular Orthotropic Plates in Affine Space", AIAA Journal, Vol. 22, October 1984.

5. Oyibo, G.A., "Generic Approach to Determine Optimum Aeroelastic Characteristics for Composite Forwardswept Wing Aircraft", AIAA Journal, Vol. 22, No. 1, January 1984, pp. 117-123.

6. Oyibo, G.A., "Unified Aeroelastic Flutter Theory for Very Low Aspect Ratio Panels", AIAA Journal, Vol. 21, No. 11, November 1983, pp. 1581-1587.

7. Brunelle, E.J., and Oyibo, G.A., "Generic Buckling Curves for Specially Orthotropic Rectangular Plates", AIAA Journal, Vol. 21, August 1983, pp. 1150-1587.

8. Oyibo, G.A., "Unified Panel Flutter Theory with Viscous Damping Effects", AIAA Journal, Vol. 21, May 1983, pp. 767-773.

9. Oyibo, G.A., "Flutter of Orthotropic Panels in Supersonic Flow Using Affine Transformations", AIAA Journal, Vol. 21, February 1983, pp. 283-289.

10. Oyibo, G.A., "The Unified Panel Flutter Theory and the Damping Effects", AFDC paper No. 82-002, presented at the Aerospace

11. Weisshaar, T.A., and Ryan, R.J., "Control of Aeroelastic Instabilities Through Elastic Cross-Coupling", AIAA paper, No. 84-0985, May 1984.

12. Jensen, D.W., and Crawley, E.F., "Frequency Determination Techniques for Cantilevered Plates with Bending-Torsion Coupling", AIAA Journal, Vol. 22, No. 3, March 1984.

4.0 RESEARCH OBJECTIVES

The overall goal of this phase of the research program is twofold: first, is to formulate closed-form solutions to the aeroelastic divergence and flutter of aircraft wings with warping contraint and elastic coupling, and use these to study the effects of constrained warping on aeroelastic response; second is to develop new plate-beam finite elements and use in modal analysis of vibration and flutter to provide an independent check on the closed-form solutions results.

The results of the efforts towards achieving this overall objective are the subject of this final technical report. Initially efforts were concentrated at conducting investigations to examine various methods (including the one already used for free vibration studies) with which to formulate the closed-form solutions to the divergence problem. Two analytical methods were thoroughly examined to determine their suitability for formulating the closed-form solutions. These are: (a) the method of "elimination", which was used to formulate the closed-form solutions to the free vibration problem during the first phase of this research, and (b) the method of Laplace Transformations. The latter method appears to invoke relatively less algebra, and so was implemented for formulating the close-form solutions during this first quarter. If correct, these expressions may be the first closed-form solutions ever derived for the divergence of composite aircraft wings having warping constraint and elastic coupling. In parallel with the analytical derivation, the numerical approach used during the first phase of the study for extracting the eigenvalues from the closed-form expressions for the free vibration, have been carefully studied to determine how it (numerical approach) may be

used for extracting the eigenvalues (and hence flight divergence speeds) from the closed-form expressions just derived. The results extracted were found to be in agreement with previously published results. This provided the necessary confidence in the new trends predicted by the new theory. Also in parallel is the development of a new plate beam finite elements, with which to independently check the closed form solutions being generated.

5.0 STATUS OF RESEARCH EFFORTS

5.1 INTRODUCTION

During the year, the research program progressed according to plan resulting in the accomplishment of the goals defined for the year. These goals, which have been defined in Section 4 of this report, basically include a preliminary formulation and investigation of closed-form solutions to the aeroelastic divergence problems of supermanuverable type aircraft wings (fabricated of composite materials) in order to determine an effective and efficient means with which to accurately estimate and study the effects of the "restraint of warping" on their mechanism of aeroelastic instability.

In the first quarter, during the preliminary study, Prof. G. A. Oyibo investigated and eventually formulated the expressions which seem to represent the closed form solutions to the divergence problems of aircraft wings having warping constraint and elastic coupling. Prof. J. Bentson explored the numerical approach used for the vibration problem in order to determine how it (numerical approach) may be used to extract the divergence eigenvalues from the closed form expressions just derived. Prof. T. A. Weisshaar is also continuing his investigations into how a new beam-plate finite elements may be formulated to capture the constraint of warping effect in order to provide results which may be used to independently check the closed-form solutions which have been, and are being generated.

In the second quarter significant programming work was accomplished on the divergence problem and this effort is still continuing. Meanwhile exciting results were obtained in the part of the research work that calls for an independent verification of the analytical closed form results obtained thus far in this research program. Therefore it is a pleasure to report the following:

(i) independent results obtained from MIT seem to accurately verify our closed form results as is shown in Figure 6 in the copy of the paper, shown below, that has been sent to the AIAA Journal to be considered for publication.

(ii) an elaborate, very careful, independent study by Prof. T. A. Weisshaar and his team at Purdue University (which is included in this report as their contribution to the program) has accurately verified our closed form results and some of their implications. For example, it verified our proposed physical explanation (perhaps the very first explanation) to the phenomenon of "modal transfer" reported previously by Purdue and MIT.

In the third quarter, more exciting conclusions began to unfold, that might potentially change the way dynamicists look at dynamics: it is normally thought that the usual way one gets a complex determinant when a vibration eigenvalue problem is formulated is when one has damping in the system. In this research we have shown that that is not always the case. We have now seen

that the elastic coupling (D_{26} (or D_{16}) introduces perhaps some "conservation" damping characteristics into the free undamped vibration of an anisotropic wing. This results from the complex nature of the determinant and the consequential fact that the bending and torsion modes are out of phase with each other. While this discovery seems to puzzle many experienced dynamicists, a look at the basic equations of motion would indicate that, the term containing D_{26} (or D_{16}) is an <u>odd</u> derivative (similar to the damping terms). Therefore, it would seem that this physical insight which is perhaps most easily extracted using an analytical method, is not only meaningful but very important.

In the final quarter, the divergence problem was studied more carefully to evolve the physical insight into the mechanism of divergence instability in the presence of warping restraint and elastic coupling. This study revealed the following:

First, it is seen that the view held by many analysts that elastic coupling plays a significant role in aeroelastic tailoring is verified.

Second it is seen that another view that, higher aeroelastic stability boundaries are feasible with negative elastic coupling (than positive elastic coupling), is basically true, but up to a point. It is further seen that there seems to be a limit to how negative the elastic coupling can be made to obtain better stability boundaries - after this limit a further negative increment in elastic coupling would seem to result in lower stability boundaries.

Third it is found that the effective aspect ratio defined in the first phase of this research program (λ_c) for simpler models can still be used in this relatively more complex model, to measure the effect of warping restraint on the phenomenon of divergence instability. The results show that ignoring the warping restraint would lead to conservative estimates for the divergence instability boundaries. It is also seen that the restraint of warping effects are more important for small effective aspect ratios and/or large elastic coupling.

5.2 ACCURATE DIVERGENCE THEORY FOR COMPOSITE SUPERMANEUVERABLE AIRCRAFT WINGS

5.2.1 INTRODUCTION

Modern supermaneuverable aircraft concepts benefit a great deal from, among other things, significant advances in materials technology and the availability of more accurate aerodynamic prediction capabilities. Supermaneuverability as a design goal invariably calls for an optimization of the design parameters. Optimization may be partially accomplished for example, by using composite materials to minimize weight. Indeed, it has been known that these composite materials can be tailored properly to resolve the dynamic or static instability problems of these types of aircraft. The concept is referred to as aeroelastic tailoring.

While aeroelastic tailoring has tremendous advantages in the design of an aircraft, the analysis which provides the basis for the aeroelastic tailoring itself is generally very involved. This is rather unfortunate since a good fundamental physical insight of the tailoring mechanism is required for accurate and reliable results.

In this investigation an attempt is made to look at some dynamics theories that can be used to understand the aeroelastic tailoring mechanism. Specifically, the accuracy of the St. Venant torsion theory which is relatively simple and frequently used in aeroelastic analysis is examined with particular reference to the effects of the wings aspect ratio as well as other design parameters.

An accurate torsion/twist theory is particularly significant for supermaneuverable aircraft wings since supermaneuverability is basically characterized by high angle of attack.

Although earlier studies (1,2,3) have indicated that the St. Venant's torsion theory is reasonably accurate except for aircraft wings with fairly low aspect ratios, the theory supporting that conclusion was based on the assumption that the wing is constructed of isotropic materials. Basically the St. Venant's torsion theory assumes that the rate of change of the wing's twist angle with respect to the spanwise axis is constant. This assumption is hardly accurate particularly for modern aircraft construction in which different construction materials are employed and the aerodynamic loads vary significantly along the wing's span. However, References 1-3 have shown that (in spite of such an inaccurate assumption) the main parameter that determines the accuracy of the St. Venant's theory is the wing's aspect ratio. Thus, it was determined that the theory is fairly accurate for moderate to high aspect ratio wings constructed of isotropic materials. In recent studies (4,5,6) however, it has been shown that for wings constructed of orthotropic composite materials, the conclusion of References 1-3 need to be modified. Rather than using the geometric aspect ratio of the wing to determine the accuracy of St. Venant's twist theory, it was suggested that a generic stiffness ratio as well as an effective aspect ratio which considers the wing's geometry and the ratio of the principal directional stiffness should be considered in establishing the accuracy of St. Venant's theory.

The present investigation is related to the studies that were initiated in References 5 and 6. In this study the first task was to examine the role of coupling (both mass and elastic coupling) on the accuracy of St. Venant's theory applied to static problems. It was discovered that coupling plays a very significant role on the accuracy of St. Venant's twist theory. The second task was to investigate the torsional vibration for a flat plate model of an aircraft wing fabricated of composite materials in which the constrained warping phenomenon is more realistically represented, with particular emphasis on higher frequencies and to compare results with those from a representation based on St. Venant's theory.

5.2.2 FORMULATION

Consider an aircraft wing fabricated of composite materials and mathematically idealized as a cantilevered plate subjected to an aerodynamic flow over its surfaces. The mathematical statement of the virtual work theorem for such a plate model is well known and documented. It is also known that such mathematical statements of the virtual work theorem for a laminated plate model are characterized with the existence of so many variables (in the statement), reflecting the various directional properties for the laminated plate model, which would tend to interfere with any physical insight that might be desired from a phenomenological analysis employing such a mathematical statement. The newly discovered affine transformation concept (5,6 and 7) was developed principally to resolve such a problem.

This new concept therefore can be used to evolve the mathematical statement of the virtual work theorem in an affine space given by the following equation.

$$\delta \bar{U}_o = 0 = 2\int_0^t \iint_A \Big\{ (w,_{x_o x_o})^2 + 2D^* \Big[(1-\epsilon)(w,_{x_o y_o})^2 + \epsilon\, w,_{x_o x_o} w,_{y_o y_o} \Big] + (w,_{y_o y_o})^2 + L_1 w,_{x_o x_o} w_{x_o y_o} + L_2 w,_{y_o y_o}\, w,_{x_o y_c} \Big\} dx_o dy_o dt$$
$$- \frac{\delta}{2}\int_0^t \iint_A \rho_o \dot{w}^2 dx_o dy_o dt + \int_0^t \iint_A \Delta p_o \delta w dx_o dy_o dt \qquad (1)$$

where:

$$\bar{U}_o = \frac{\bar{U}}{D_{22}}\left(\frac{D_{22}}{D_{11}}\right)^{1/4} \quad ; \quad D^* = \frac{D_{12} + 2D_{66}}{(D_{11}D_{22})^{1/2}} \quad ; \quad \epsilon D^* = \frac{D_{12}}{(D_{11}D_{22})^{1/2}}$$

$$L_1 = \frac{4D_{16}}{(D_{11})^{3/4}(D_{22})^{1/4}} \; ; \; L_2 = \frac{4D_{26}}{(D_{11})^{1/4}(D_{22})^{3/4}} \qquad (2)$$

$$\Delta p_o = \frac{\Delta p}{D_{22}} \; ; \; \rho_o = \frac{\rho \bar{h}}{D_{22}}$$

D_{ij} are the elastic constants, ρ, is the material density, Δp is the differential pressure distribution, w is the displacement, t is the time, A integrals represent area integrals and $\bar{h}$ is the wing box depth.

Equations (1) and (2) therefore form the basis of the newly developed methodology. The equations of motion of a plate model of an aircraft wing can now be derived by prescribing a realistic wing displacement and using Equation (1).

When Equation (1) is compared to its physical space counterpart, it is seen that Equation (1) has fewer variables. It is also seen that Equation (1) contains only non-dimensionalized stiffness quantities (compared to dimensional stiffness quantities in its physical space counterpart). Another feature of this new methodology which makes it unique is that the non-dimensionalization (a consequence of the affine transformation) is accomplished before assuming the wing deformations. This means that the non-dimensionalization is independent of how the wing deforms. A non-dimensionalization scheme that depends on a particular assumption of the wings deformations could lead the analyst to an incorrect physical interpretation of results, since the wing's deformations assumptions have inherent errors because they are based on the analyst's judgments and experience. This observation may become clearer during the evolution of a warping parameter with which to study the effects of the warping constraint phenomenon on the status and dynamics of a wing fabricated of composite materials later in this study.

If the chordwise curvature is neglected in an initial approximation, the wing's deformation may be assumed as follows:

$$w(t,x_o,y_o) = h_o(t,y_o) + x_o\alpha_o(t,y_o) \tag{3}$$

where h_o and α_o are the bending and twisting displacements, respectively.

It can be shown that when Equation (3) is substituted into Equation (1) and the variational calculus is carried out for arbitrary h_o and α_o, the following equations of motion are obtained:

$$a_1 h_o^{iv} + a_2 \alpha_o^{iv} + a_5 \alpha_o^{iii} + \rho_o a_1 \ddot{h}_o + \rho_o a_2 \ddot{\alpha}_o = L_o$$

$$a_2 h_o^{iv} - a_5 h_o^{iii} + a_3 \alpha_o^{iv} - a_4 \alpha_o'' + \rho_o a_3 \ddot{\alpha}_o + \rho_o a_2 \ddot{h}_o = M_o \tag{4}$$

where:

$$a_1 = \int_{e\bar{c}_o}^{\bar{c}_o} dx_o \quad ; \quad a_2 = \int_{e\bar{c}_o}^{\bar{c}_o} x_o\, dx_o$$

$$a_3 = \int_{e\bar{c}_o}^{\bar{c}_o} x_o^2 dx_o \quad ; \quad a_4 = 2\int_{e\bar{c}_o}^{\bar{c}_o} D^*(1-\epsilon)dx_o \qquad (5)$$

$$L_o = \int_{e\bar{c}_o}^{\bar{c}_o} \Delta p_o dx_o \quad ; \quad a_5 = \int_{e\bar{c}_o}^{\bar{c}_o} L_2 dx_o$$

$$M_o = \int_{e\bar{c}_o}^{\bar{c}_o} x_o \Delta p_o dx_o$$

$$-\infty < e < 0 \quad ; \qquad \bar{c}_o = \frac{c_o}{1-e}$$

$$(\,)' = \frac{\partial}{\partial y_o}, \; (\dot{}) = \frac{\partial}{\partial t} \qquad (6)$$

5.2.3 EVOLUTION OF WARPING PARAMETERS

The evolution of the warping parameter with which to study the constrained aeroelastic warping phenomenon for wings fabricated of composite materials is a process that depends on the sophistication of the wing's mathematical model; whether coupling effects are included, whether the wing's chordwise curvatures are included and so on. Therefore, any warping parameter is as good as the corresponding wing's displacements assumptions. However, Equation (1) makes it possible for the analyst to determine its effective independent variables even before the displacement assumptions are made.

By non-dimensionalizing the spanwise space variable in Equation (4), depending on whether one is interested in the static, dynamic, coupled or uncoupled displacements, one of the following warping parameters may be useful.

$$\lambda_c = \frac{\ell_o}{c_o}\sqrt{\frac{3}{2}D_o^*} \tag{7}$$

$$\bar{\lambda}_c = \frac{\ell_o}{c_o}\sqrt{\frac{3}{2}\left(D_o^* - \frac{L_2^2}{8}\right)} \tag{8}$$

$$\bar{\lambda}_c = \frac{\ell_o}{c_o}\sqrt{\frac{3}{2}\,\frac{D_o^*}{1-3\tilde{a}_2^2}} \tag{9}$$

where:

$$D_o^* = D^*(1 - \epsilon) \quad ; \qquad \bar{a}_2 = \frac{a_2}{c_o^2} \tag{10}$$

(ℓ_o/c_o) is defined as the wing's effective aspect ratio and D_o^* and L are the generalized stiffness and coupling ratios, respectively (defined in earlier work such as References 5 and 6).

Equations (7) thru (9) represent the appropriate warping parameter for dynamic deformation, static displacement with elastic cross-coupling, and static deformation with "geometric" coupling ($e \neq 1$), respectively.

It was discovered in this study that evolving the warping parameter in a manner shown in Equations (1) thru (3), should enable one to investigate the effects of warping on the composite wing's dynamics (or the accuracy of St. Venant's theory) effectively. From the lamination theory for composites it is known that while D_o^* and (ℓ_o/c_o) are always positive, L and $\bar{a}_2$ can be positive or negative. However, from Equations (1) and (3), it is clear that whether a composite wing has positive or negative coupling, the warping effect (in terms of $\bar{\lambda}_c$) is unchanged.

Using the Laplace transform method on the divergence form of equations 4 in which strip aerodynamic theory is used, the following Laplace function becomes important in the divergence problem,

$$F_1(s) = 9_{13}\,[s^7 - a_{14}s^5 + a_{15}s^4 + a_{16}s^3 + a_{17}s^2 + a_{18}] \qquad (7)$$

where

$$a_{13} = \bar{a}_1\bar{a}_3,\quad a_{14} = -\frac{(\bar{a}_1\bar{a}_4 - \bar{a}_5^2)}{\bar{a}_1\bar{a}_3},\quad a_{15} = \frac{\bar{F}_2\bar{a}_3}{\bar{a}_1\bar{a}_3}$$

$$a_{16} = \frac{\bar{F}_4 a_5 - \bar{F}_3\bar{a}_1}{\bar{a}_1\bar{a}_3},\quad a_{17} = \frac{\bar{F}_1\bar{a}_5 - \bar{F}_2\bar{a}_4}{\bar{a}_1\bar{a}_3}$$

$$a_{18} = \frac{\bar{F}_1\bar{F}_4}{\bar{a}_1\bar{a}_3},\quad s \text{ is Laplace variable,}$$

$\bar{F}_i$ $(i=1,2,3,4)$ are aerodynamic forces and moments

Let

$$F_1(s) \equiv a_{13}[(s+b)^2+a_1^2]\,[(s+\underline{b}_2)^2+a_2^2]\,[(s+b_3)^2+a_3^2]\,[s+b_4] \qquad (8)$$

$$T_{01}(s) = a_{13}[s^4 + 9_{01}2^2 + a_{02}s + a_{03}] \qquad (9)$$

$$a_{01} = \frac{\bar{a}_5}{\bar{a}_1\bar{a}_5},\quad a_{02} = \frac{\bar{a}_3\bar{F}_2}{\bar{a}_1\bar{a}_3},\quad a_{03} = \frac{\bar{a}_5 F_4}{\bar{a}_1\bar{a}_3}$$

$$F_{014}(s) = [F_1(s)/(s+b_4)]$$

$$p_{014} = \frac{T_{01}(-b_4)}{F_{014}(-b_4)}$$

$$F_{011}(s) = F_1(s)/[(s+b_1)^2+a_1^2]$$

$$P_{0115} + iP_{0116} = \frac{T_{01}(-b_1+ia_1)}{F_{011}(-b_1+ia_1)}$$

$$f_{011} = \frac{P_{0116}}{a_1} \quad , \quad p_{011} = P_{0115} + \left(\frac{b_1}{a_1}\right) P_{0116} \tag{10}$$

$$F_{012}(s) = F_1(s)/[(s+b_2)^2+a_2^2]$$

$$P_{0115}+iP_{0116} = \frac{T_{01}(-b_1+ia_1)}{F_{011}(-b_1+ia_1)}$$

$$f_{011} = \frac{P_{0116}}{a_1} \quad , \quad p_{011} = P_{0115} + \left(\frac{b_1}{a_1}\right) P_{0116}$$

$$F_{012}(s) = F_1(s)/(s+b_2)^2+a_2^2]$$

$$P_{0125} + iP_{0126} = \frac{T_{o1}(-b_2+ia_2)}{F_{012}(-b_2+ia_2)} \tag{11}$$

$$f_{012} = \frac{P_{0126}}{a_2} \quad , \quad p_{012} = P_{0125} + \left(\frac{b_2}{a_2}\right) P_{0126}$$

$$F_{013}(s) = F_1(s)/[(s+b_3)^2+a_3^2]$$

$$P_{0135} + iP_{0136} = \frac{T_{01}(-b_3 + ia_3)}{F_{013}(-b_3+ia_3)} \tag{12}$$

$$f_{013} = \frac{P_{0136}}{a_3} \quad , \quad P_{013} = P_{0135} + \left(\frac{b_3}{a_3}\right) P_{0136}$$

$$T_{02}(s) = a_1 a_3 \, [a_{04} s + a_{05}]$$

$$a_{04} = \frac{\bar{a}_1 \bar{F}_4}{\bar{a}_1 \bar{a}_3} \quad , \quad a_{05} = - \frac{\bar{a}_5 \bar{F}_2}{\bar{a}_1 \bar{a}_3} \tag{13}$$

$$P_{024} = T_{02} \, (-b_4) / F_{014} \, (-b_4)$$

$$P_{0215} + iP_{0216} = \frac{T_{02}(-b_1 + ia_1)}{F_{011}(-b_1 + ia_1)} \quad ; \tag{14}$$

$$f_{021} = \frac{P_{0216}}{a_1} \quad ; \; P_{021} = P_{0215} + \left(\frac{b_1}{a_1}\right) P_{0216}$$

$$P_{0225} + iP_{0226} = \frac{T_{02}(-b_2 + ia_2)}{F_{012}(-b_2 + ia_2)} \tag{15}$$

$$f_{022} = \frac{P_{0226}}{a_2} \quad , \quad P_{022} = P_{0225} + \left(\frac{b_2}{a_2}\right) P_{0226}$$

$$P_{0235} + iP_{0236} = \frac{T_{02}(-b_3 + ia_3)}{F_{013}(-b_3 + ia_3)} \tag{16}$$

$$f_{023} = \frac{P_{0236}}{a_3} \quad , \quad P_{023} = P_{0235} + \left(\frac{b_3}{a_3}\right) P_{0236}$$

$$T_{03}(s) = \bar{a}_1 \bar{a}_3 \, [s^3 + a_{06}] \quad , \quad a_{06} = \frac{\bar{a}_3 \bar{F}_2}{\bar{a}_1 \bar{a}_3} \tag{17}$$

$$P_{034} = \frac{T_{03}(-b_4)}{F_{014}(-b_4)}$$

$$P_{0315} + iP_{0316} = \frac{T_{03}(-b_1+ia_1)}{F_{011}(-b_1+ia_1)} \quad ; \quad f_{031} = \frac{P_{0316}}{a_1} \quad ,$$

$$P_{031} = P_{0315} + \left(\frac{b_1}{a_1}\right) P_{0316} \tag{18}$$

$$P_{0325} + iP_{0326} = \frac{T_{03}(-b_2+ia_2)}{F_{012}(-b_2+ia_2)} \quad , \quad f_{032} = \frac{P_{0326}}{a_2} \quad ;$$

$$P_{032} = P_{0325} + \left(\frac{b_2}{a_2}\right) P_{0326} \tag{19}$$

$$P_{0335} + iP_{0336} = \frac{T_{03}(-b_3+ia_3)}{F_{013}(-b_3+ia_3)} \quad ; \quad f_{033} = \frac{P_{0336}}{a_3} \quad ;$$

$$P_{033} = P_{0335} + \left(\frac{b_3}{a_3}\right) P_{0336} \tag{20}$$

$$T_{04} = \bar{a}_1\bar{a}_3 \left[a_{08}s^2 + a_{09}\right] \quad , \quad a_{08} = \frac{\bar{a}_5\bar{a}_1}{\bar{a}_1\bar{a}_3} \quad ; \quad a_{09} = \frac{a_1\bar{F}_4}{\bar{a}_1\bar{a}_3}$$

$$P_{044} = \frac{T_{04}(-b_4)}{F_{04}(-b_4)} \tag{21}$$

$$P_{0415} + iP_{0416} = \frac{T_{04}(-b_1+ia_1)}{F_{011}(-b_1+ia_1)} \quad ; \quad f_{041} = \frac{P_{0416}}{a_1} \quad ,$$

$$P_{041} = P_{0415} + \left(\frac{b_1}{a_1}\right) P_{0416} \tag{22}$$

$$P_{0425} + iP_{0426} = \frac{T_{04}(-b_2+ia_2)}{F_{012}(-b_2+ia_2)} \quad ; \quad f_{042} = \frac{P_{0426}}{a_2} \quad ; \tag{23}$$

$$P_{042} = P_{0425} + \left(\frac{b_2}{a_2}\right) P_{0426}$$

$$P_{0435} + iP_{0436} = \frac{T_{04}(-b_3+ia_3)}{F_{013}(-b_3+ia_3)} \quad , \quad f_{043} = \frac{P_{0436}}{a_3} \quad ; \tag{24}$$

$$P_{043} = P_{0435} + \left(\frac{b_3}{a_3}\right) P_{0436}$$

$$T_{21}(s) = \bar{a}_5 F_1(s) - (\bar{F}_1 + \bar{a}_5 s^3) T_{01}(s) \tag{25}$$

$$T_{210}(s) = s(\bar{a}, s^3 + \bar{F}_2) F_1(s)$$

Let

$$F_{210}(s) \equiv s[(s+\beta_1)^2 + \alpha_1^2]\ [(s+\beta_2)^2+\alpha_2^2]\ [(s+\beta_3)^2+\alpha_3^2] \tag{26}$$

$$[s+\beta_4]\ [s+\beta_5]\ [(s+\beta_6)^2+\alpha_6^2]$$

$$F_{21}(s) = \frac{T_{21}(s)}{F_{210}(s)} \equiv \frac{P_7}{s} + \frac{P_4}{s+\beta_4} + \frac{P_5}{s+\beta_5} + \sum_{n=1,2,3,6} \frac{f_h^+ s + P_h}{(s+\beta_n)^2+\alpha_n^2} \tag{27}$$

or in proper notation

$$F_{21}(s) \equiv \frac{p_{217}}{s} + \frac{p_{214}}{s+\beta_{14}} + \frac{p_{215}}{s+\beta_{15}} + \sum_{n=1,2,3,6} \frac{f_{21n}s + p_{21n}}{(s+\beta_n)^2+\alpha_n^2} \tag{28}$$

or

$$F_{MN}(s) = \frac{p_{MN7}}{s} + \frac{p_{MN4}}{s+\beta_4} + \frac{p_{MN5}}{s+\beta_5} + \sum_{n=1,2,3,6} \frac{f_{MNh}s + p_{MNh}}{(s+\beta_n)^2+\alpha_n^2} \tag{29}$$

$MN = 21,22,23,24$

Define

$$F_{21n}(s) = F_{210}(s)/[(s+\beta_n)^2+\alpha_n^2] \quad , \quad n = 1,2,3,6$$

$$F_{21n}(s) = F_{22n}(s) = F_{23n}(s) = F_{24n}(s) \tag{30}$$

$$F_{217}(s) = F_{210}(s)/s \quad , \quad F_{214}(s) = F_{210}(s)/(s+\beta_4)$$

$$F_{215}(s) = F_{210}(s)/(s+\beta_5) \tag{31}$$

$$p_{217} = \frac{T_{21}(0)}{F_{217}(0)} \quad , \quad p_{214} = \frac{T_{21}(-\beta_4)}{F_{214}(-\beta_4)}$$

$$p_{215} = \frac{T_{21}(-\beta_5)}{F_{215}(-\beta_5)} \tag{32}$$

$$p_{2115} + i\, p_{2116} = \frac{T_{21}(-\beta_1+\alpha_1)}{F_{211}(-\beta_1+i\alpha_1)} \tag{33}$$

$$f_{211} = \frac{p_{2116}}{\alpha_1} \quad , \quad p_{211} = p_{2115} + \left(\frac{\beta_1}{\alpha_1}\right) p_{2116}$$

or

$$p_{21n5} + ip_{21n6} = \frac{T_{21}(-\beta_n+i\alpha_n)}{F_{21n}(-\beta_n+i\alpha_n)} \qquad n = 1,2,3,6 \tag{34}$$

$$f_{21r} = \frac{p_{21n6}}{\alpha_n} \quad ; \quad p_{21n} = p_{21n5} + \left(\frac{\beta_n}{\alpha_n}\right) p_{21n6} \tag{35}$$

Similarly

$$T_{22}(s) = (\bar{F}_1+\bar{a}_5 s^3)\ (\bar{a}_1\bar{F}_4 s - \bar{a}_5\bar{F}_2)\ - \bar{a}_1 s F_1(s) \tag{36}$$

$$p_{227} = \frac{T_{22}(0)}{F_{217}(0)} \quad p_{224} = \frac{T_{22}(-\beta_4)}{F_{214}(-\beta_4)}$$

$$p_{225} = \frac{T_{22}(-\beta_5)}{F_{215}(-\beta_5)} \tag{37}$$

$$P_{22n5}+iP_{22n6} = \frac{T_{22}(-\beta_n}{F_{21n}(-\beta_n+i\alpha_n)}$$

$$f_{22n} = \frac{P_{22n6}}{\alpha_n} \quad , \quad P_{22n} = P_{22n5} + \left(\frac{\beta_n}{\alpha_n}\right) P_{22n6} \tag{38}$$

$$T_{23}(s) = \bar{a}_3 \ (\bar{F}_1+\bar{a}55^3) \ (\bar{a}_1 s^3+\bar{F}_2)$$

$$P_{237} = \frac{T_{23}(0)}{F_{217}(0)} \quad , \quad P_{234} = \frac{T_{23}(-\beta_4)}{F_{214}(-\beta_4)} \quad , \quad P_{235} = \frac{T_{23}(-\beta_5)}{F_{215}(-\beta_5)}$$

$$P_{23n5}+ \ iP_{23n6} = \frac{T_{23}(-\beta_n+i\alpha_n)}{F_{21n}(-\beta_n+i\alpha_n)} \tag{39}$$

$$P_{23n} = \frac{P_{23n6}}{\alpha_n} \quad , \ P_{23} = P_{23n5} + \left(\frac{\beta_n}{\alpha_n}\right) P_{23n6} \tag{40}$$

$$T_{24}(s) = \bar{a}_1 F_1(s) - (\bar{F}_1+\bar{a}_5 s^3)(\bar{a}_5 s^2+\bar{F}_4)$$

$$P_{247} = \frac{T_{24}(o)}{F_{217}(o)} \quad , \quad P_{244} = \frac{T_{24}(-\beta_4)}{F_{214}(-\beta_4)} \quad , \quad P_{245} = \frac{T_{24}(-\beta_5)}{F_{215}(-\beta_5)}$$

$$P_{24n5} + iP_{24n6} = \frac{T_{24}(-\beta_n+i\alpha_n)}{F_{21n}(-\beta_n+i\alpha_n)} \quad ; \quad f_{24n} = P_{\frac{24n6}{\alpha}} \quad ; \tag{41}$$

$$P_{24n} = P_{24n5} + \left(\frac{\beta_n}{\alpha_n}\right) P_{24n6}$$

$$F''_{01}(11) = b_4^2\, p_{014} e^{-b_4} - \sum_{n=1,2,3} F_{oin}^{1/2} A_n e^{-b_n} \sin(a_n + g_{oin} + 2\bar{g}_n)$$

$$F_{oin} = f_{oin}^2 + \bar{f}_{oin}^2 \; ; \quad \bar{f}_{oin} = \frac{p_{oin} - f_{oin} b_n}{a_n}$$

$$A_n = a_n^2 + b_n^2 \; , \; \sin\bar{g}_n = b_n / A_n^{1/2}, \quad \cos\bar{g}_n = \frac{a_n}{A_n^{1/2}} \tag{42}$$

$$\sin g_{oin} = \frac{f_{oin}}{F_{oin}^{1/2}} \; , \; \cos g_{oin} = \frac{f_{oin}}{F_{oin}^{1/2}}$$

or

$$F''_{om}(1) = b_4^2\, p_{om4} e^{-b_4} - \sum_{n=1,2,3} F_{omn}^{1/2}\, A_n e^{-b_n} \sin(a_n + g_{omn} + 2\bar{g}_n)$$

$$\boxed{m = 1,2,3,4} \tag{43}$$

$$F_{omn} = f_{omn}^2 + \bar{f}_{omn}^2 \; ; \quad \bar{f}_{omn} = \frac{p_{omn} - f_{omn} b_n}{a_n}$$

$$A_n = a_n^2 + b_n^2 \; , \; \sin\bar{g}_n = b_n / A_n^{1/2} \; , \; \cos\bar{g}_n = \frac{a_n}{A_n^{1/2}}$$

$$\sin g_{omn} = \frac{f_{omn}}{F_{omn}^{1/2}} \; ; \quad \cos g_{omn} = \frac{\bar{f}_{omn}}{F_{omn}^{1/2}}$$

$$F'_{om}(1) = -b_4 p_{om4} e^{-b_4} + \sum_{n=1,2,3} F_{om}^{1/2}\, A_n^{1/2} e^{-b_n} \cos(a_n + g_{omn} + \bar{g}_n) \tag{44}$$

$$m = 1,2,3,4$$

$$F'''_{om}(1) = b_4^3 p_{om4} e^{-b_4} - \sum_{n=1,2,3} F_{om}^{1/2} A_n^{3/2} e^{-b_n} \cos(a_n + g_{omn} + 3\bar{g}_n) \tag{45}$$

$m = 1,2,3,4$

$$F''_{MN}(1) = \sum_{m=4,5} \beta_m^2 p_{MNm} e^{-\beta_n} - \sum_{n-1,2,3,6} \bar{F}_{MNn}^{1/2} \bar{A}_n e^{-\beta_n} \sin(2_n + G_{MNn} + 2\bar{G}_n) \tag{46}$$

$\boxed{MN = 21,22,23,24}$

$$\bar{F}_{MNn} = f_{MNn}^2 + \bar{f}_{MNn}^2 \quad , \quad \bar{A}_n = \alpha_n^2 + \beta_n^2 \quad , \quad \bar{f}_{MNn} = \frac{p_{MNn} - f_{MNn}\beta_n}{\alpha_n} \tag{47}$$

$$\text{Sin}G_{MNn} = \frac{f_{MNn}}{\bar{F}_{MNn}^{1/2}} \quad ; \quad \cos G_{MNn} = \frac{\bar{f}_{MNn}}{\bar{F}_{MNn}^{1/2}} ; \quad \sin\bar{G}_n = \frac{\beta_n}{\bar{A}_n^{1/2}} \quad ,$$

$$\cos\bar{G}_n = \frac{\alpha_n}{\bar{A}_n^{1/2}}$$

$$F'''_{MN}(1) = -\sum_{m=4,5} \beta_m^3 p_{MNm} e^{-\beta_m} - \sum_{n=1,2,3,6} \bar{F}_{MNn}^{1/2} \bar{A}_n^{3/2} e^{-\beta_n} \cos(\alpha_n + G_{MNn} + 3G_n \tag{48}$$

$n = 1,2,3,6$

$$\bar{F}_{11} = F_{21}'''(1) \; ; \; \bar{F}_{12} = F_{22}'''(1) \; ; \; \bar{F}_{13} = F_{23}'''(1) \; ; \; \bar{F}_{14} = F_{24}'''(1)$$

$$\bar{F}_{21} = -F_{01}''(1) \; ; \; \bar{F}_{22} = F_{02}''(1) \; ; \; \bar{F}_{23} = F_{03}''(1) \; ; \; \bar{F}_{24} = -F_{04}''(1)$$

$$\bar{F}_{31} = \bar{a}_1 F_{21}''(1) + \bar{a}_5 F_{01}'(1) \; ; \; \bar{F}_{32} = \bar{a}_1 F_{22}''(1) - \bar{a}_5 F_{02}'(1) \; ;$$

$$\bar{F}_{33} = \bar{a}_1 F_{23}''(1) - \bar{a}_5 F_{03}'(1) \qquad (49)$$

$$\bar{F}_{34} = \bar{a}_1 F_{24}''(1) + \bar{a}_5 F_{04}'(1)$$

$$\bar{F}_{41} = \left(\bar{a}_4 - \frac{a_5^{-2}}{\bar{a}_1}\right) F_{01}'(1) - \bar{a}_3 F_{01}'''(1) \; ; \; \bar{F}_{42} = \bar{a}_3 F_{02}'''(1) - \left(\bar{a}_4 - \frac{a_5^{-2}}{\bar{a}_1}\right) F_{02}'(1)$$

$$\bar{F}_{43} = \bar{a}_3 F_{03}'''(1) - \left(\bar{a}_4 - \frac{\bar{a}_5^{\,2}}{\bar{a}_1}\right) F_{03}'(1) \; ; \; \bar{F}_{44} = \left(\bar{a}_4 - \frac{\bar{a}_5^{\,2}}{\bar{a}_1}\right) F_{04}'(1) - \bar{a}_3 F_{04}'''(1)$$

Determine eigenvalues that makes the following determinant zero

$$\begin{vmatrix} \bar{F}_{11} & \bar{F}_{12} & \bar{F}_{13} & \bar{F}_{14} \\ \bar{F}_{21} & \bar{F}_{22} & \bar{F}_{23} & \bar{F}_{24} \\ \bar{F}_{31} & \bar{F}_{32} & \bar{F}_{33} & \bar{F}_{34} \\ \bar{F}_{41} & \bar{F}_{42} & \bar{F}_{43} & \bar{F}_{44} \end{vmatrix} = 0 \qquad (50)$$

Equation 50 is therefore expected to represent the closed-form expression for the divergence eigenvalues. Numerical methods are now being used to extract these eigenvalues in order to obtain the divergence speeds.

RESULTS

The results obtained so far seem to verify existing results and establish new trends. Due to the fact that the evolution of these new trends are yet to be fully completed, only a summary of these results are presented below.

The results obtained by solving equation 50 were carefully to evolve the physical insight into the mechanism of divergence instability in the presence of warping restraint and elastic coupling. This study revealed the following, as can be seen from figures 1-6.

First, it is seen that the view held by many analysts that elastic coupling plays a significant role in aeroelastic divergence tailoring is verified.

Second, it is seen that another view that, higher aeroelastic divergence stability boundaries are feasible with negative elastic coupling (than positive elastic coupling), is basically true, but up to a point. It is further seen that there seems to be a limit to how negative the elastic coupling can be made to obtain better stability boundaries - after such a limit, a further negative increment of elastic coupling would seem to lower the stability boundaries.

Third, it is found that the effective aspect ratio defined in the first phase of this research program ($)_c$), for simpler models can still be used in this relatively more complex model, to measure

the effect of warping restraint on the phenomenon of divergence instability. The results show that ignoring the warping restraint would lead to conservative estimates for the divergence instability boundaries. It is also seen that the restraint of warping effects are more significant for small effective aspect ratio (λ_c) and/or large elastic coupling.

REFERENCES

1. Reissner, E. and Stein, M., "Torsion and Transverse Bending of Cantilevered Plates", NACA TN 2369, June 1951.
2. Bisplinghoff, R.L., Ashley, H. and Halfman, R.L., "Aeroelasticity", Addison Wesley, 1955.
3. Petre, A., Stanescu C., and Librescu, L., "Aeroelastic Divergence of Multicell Wings (Taking their Fixing Restraints into Account)", Aeromecanique, 1962, pp. 689-698.
4. E. F. Crawley and J. Dugundji, "Frequency Determination and Non-dimensionalization for Composite Cantilever Plates", Journal of Sound and Vibration, Vol. 72, No. 1, pp. 1-10, 1980.
5. Oyibo, G.A. and Berman, J.H., "Influence of Warpage on Composite Aeroelastic Theories", AIAA Paper No. 85-0710, April 1985.
6. Oyibo, G.A. and Berman, J.H., "Anisotropic Wing Aeroelastic Theories with Warping Effects", DGLR Paper No. 85-57, Second International Symposium on Aeroelasticity and Structural Dynamics, Technical University of Aachen, West Germany, April 1985.

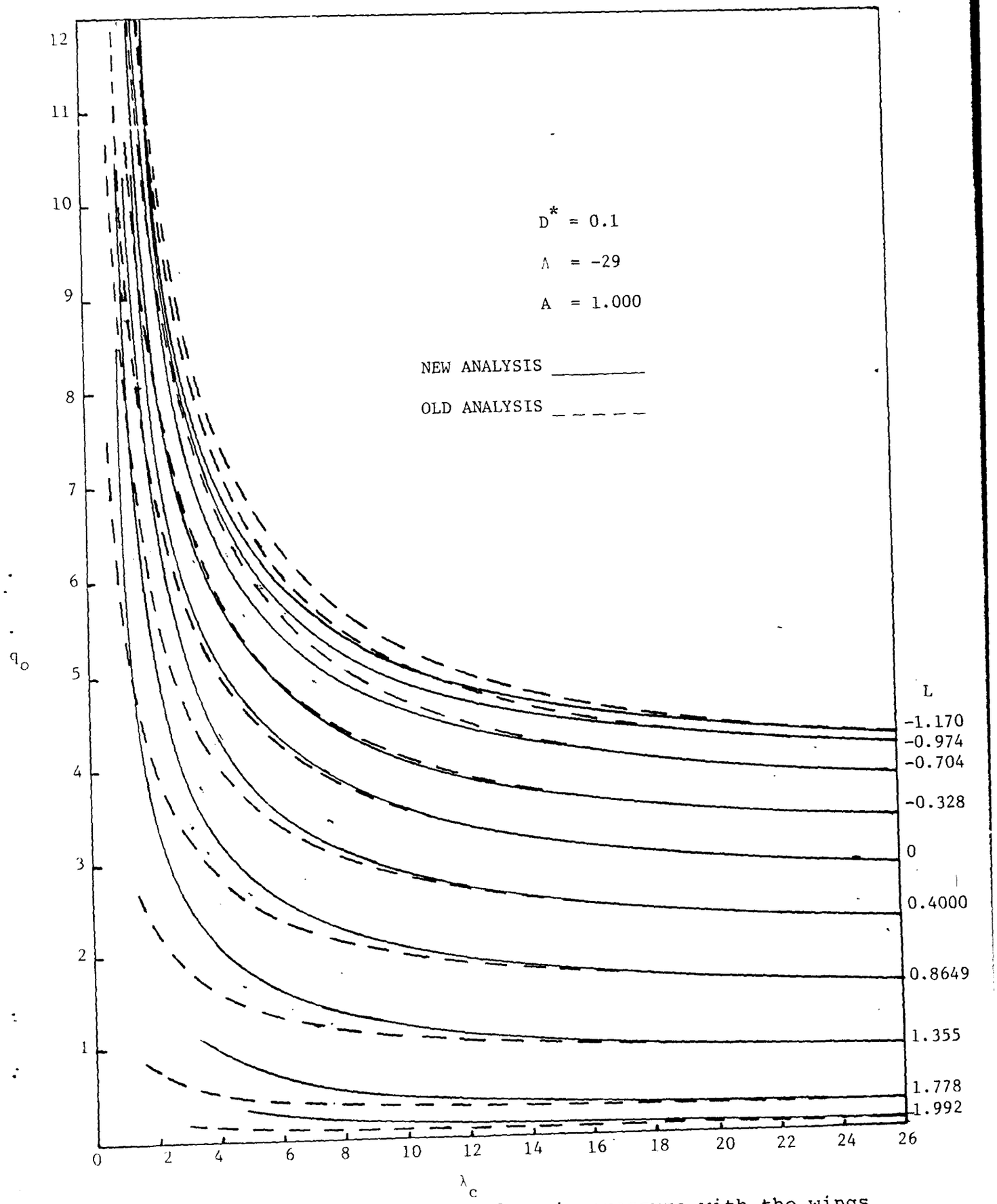

Figure 1 Variation of Divergence dynamic pressure with the wings Effective Aspect ratio

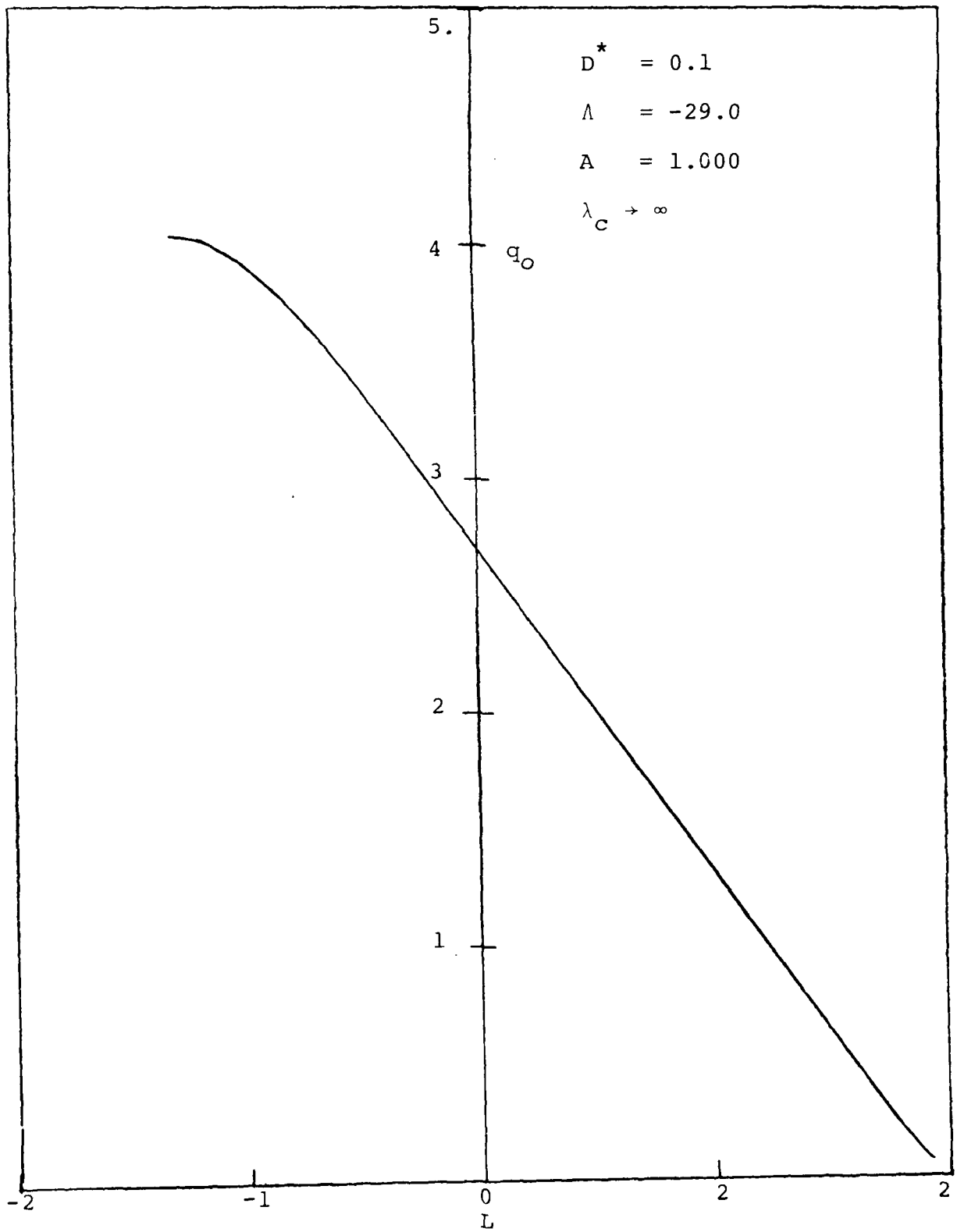

Figure 2 Variation of divergence dynamic pressure with coupling for large effective wing aspect ratio

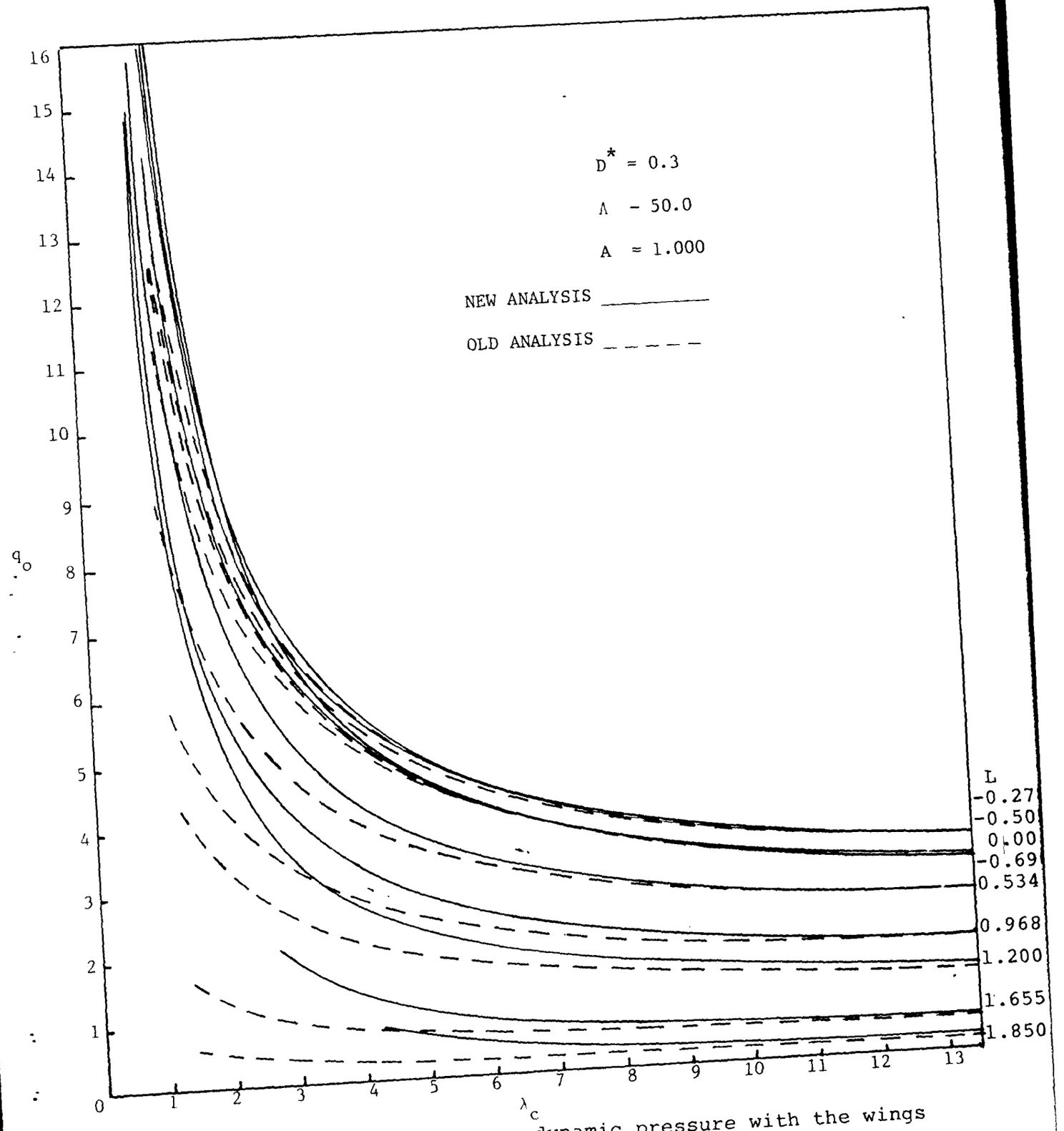

Figure 3 Variation of divergence dynamic pressure with the wings effective aspect ratio

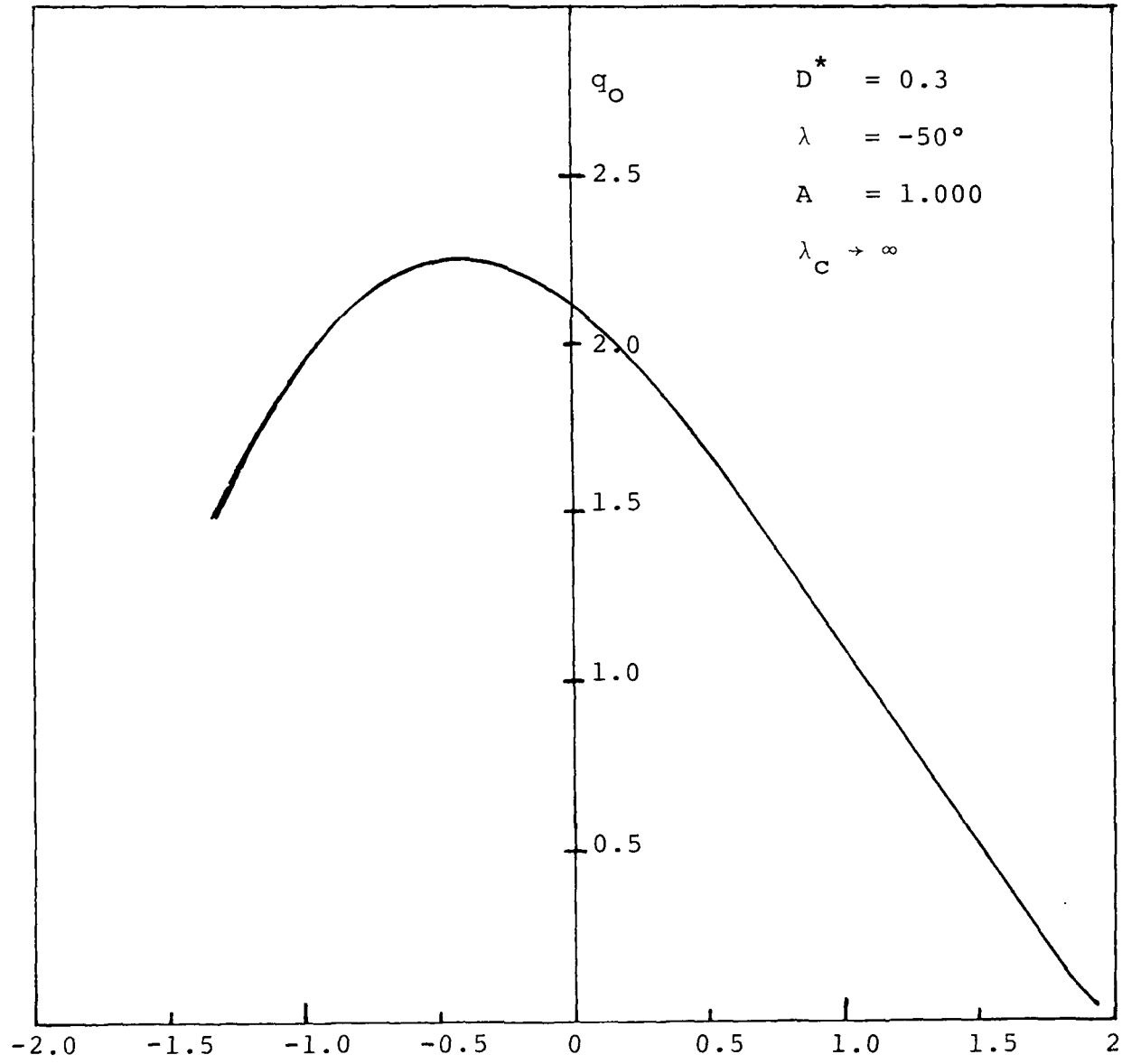

Figure 4 Variation of divergence dynamic pressure with coupling for large effective wing aspect ratio

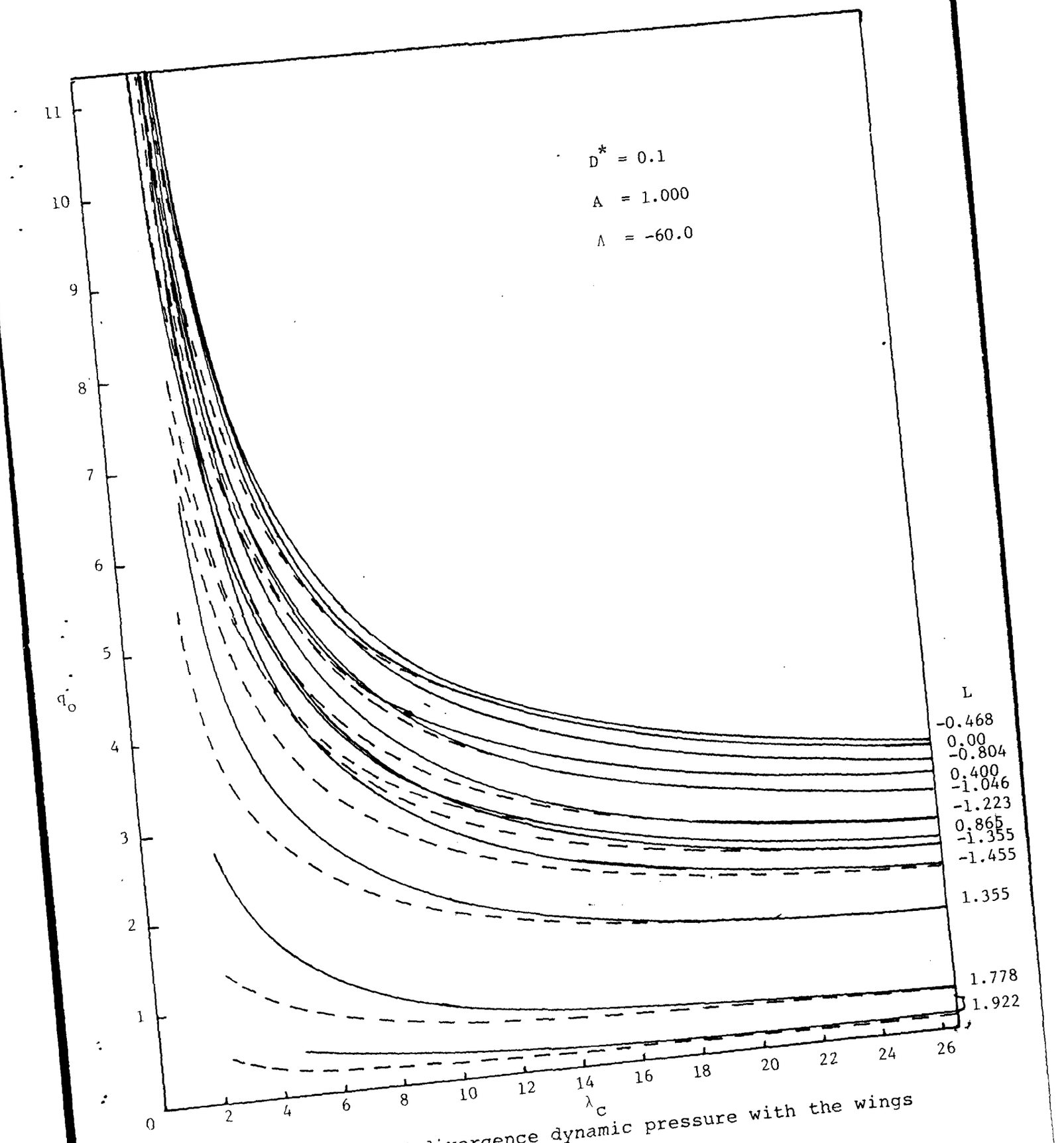

Figure 5 Variation of divergence dynamic pressure with the wings effective aspect ratio

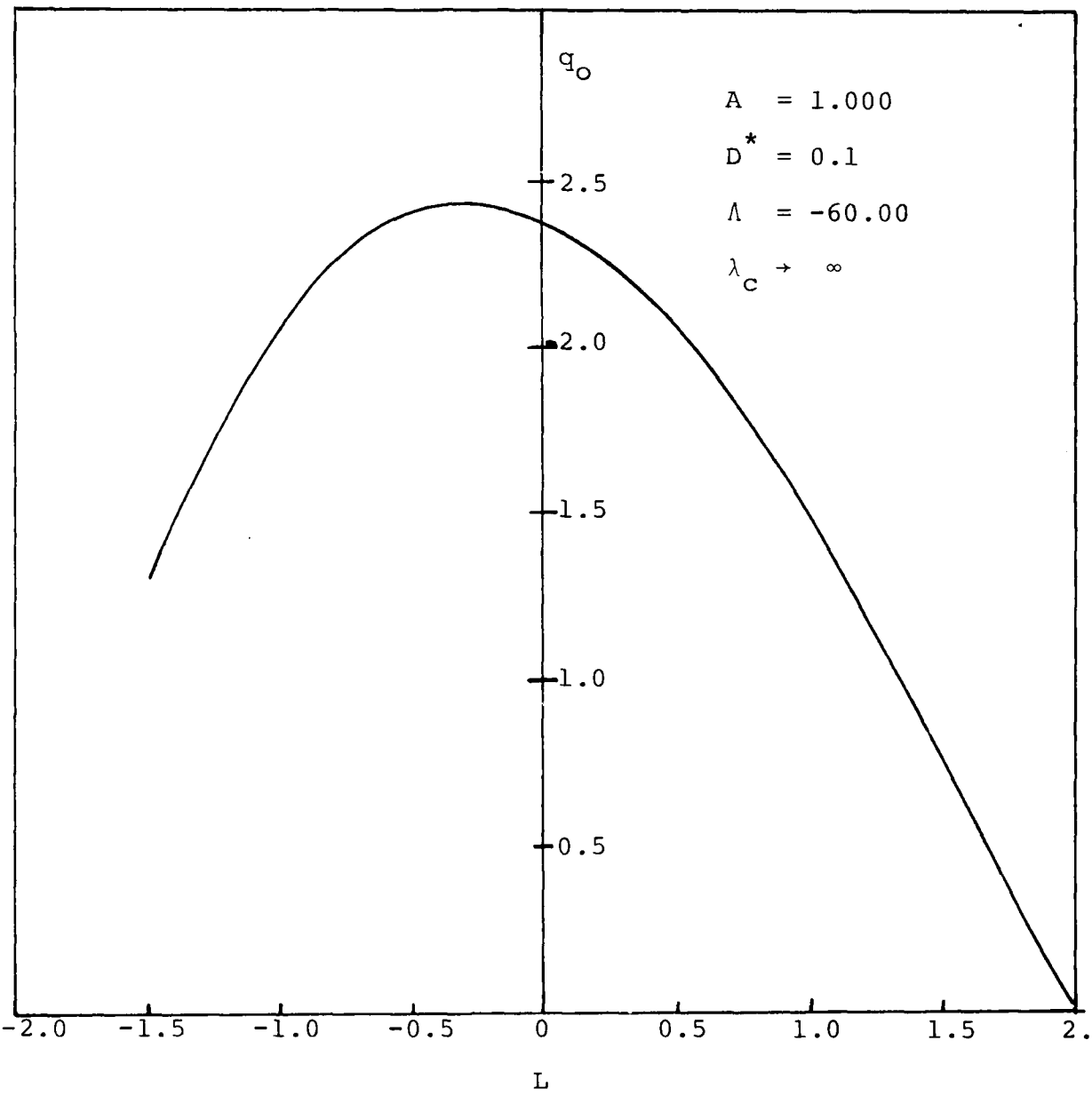

Figure 6 Variation of divergence dynamic pressure with coupling for large effective wing aspect ratio

5.3

Exact Solutions to Aeroelastic Oscillations of Composite Aircraft Wings with Warping Constraint and Elastic Coupling†

Gabriel A. Oyibo* and James Bentson*
Polytechnic University
Farmingdale, New York

Abstract

Exact solutions within the framework of standard aeroelastic bending and twisting assumptions are found to the free oscillations of composite aircraft wings having warping constraint and elastic coupling. The problem is treated as a regular boundary value problem consisting of two fourth order partial differential equations coupled by the presence of elastic coupling. This system, which is linear, therefore is equivalent to an eighth order ordinary differential equation . Classical linear "operator" method is therefore used to extract fundamental solutions which are superimposed appropriately to obtain an exact functional form for the mode shapes. These mode shapes are therefore made to satisfy the necessary boundary conditions, a process that leads to the formulation of the required eigenvalue problem. The eigenvalues are extracted numerically by using appropriate ordering of the eight roots of the operator equation. The bending-torsion frequencies obtained as a result of this analysis are compared favorably with existing results. New insights made possible by these results which are preliminary, ap-

†Research sponsored by the Air Force Office of Scientific Research (AFOSR), under Contracts F49620-85-C-0090 and F49620-87-C-0046.

*Associate Professor Dept. of Aerospace Engineering

pear to be that (a) the first coupled frequency decreases with increasing coupling and (b) the phenomenon of modal transformations found by earlier investigators is explainable in terms of some conservative inter-modal energy transfer.

5.3.1 NOMENCLATURE

a_i	= chordwise integrals
c_o', c_o	= affine space half-chord and chord, respectively
D_{ij}	= elastic constants
e	= parameter that measures the location of the reference axis relative to mid-chord
EI, GJ	= bending and torsional stiffness, respectively
$\bar{h}$	= wing box depth
(h_o, α_o)	= affine space bending and torsional displacement, respectively
K,So	= elastic coupling and warping stiffness, respectively
k_{ij}	= elemental stiffness parameter
k_o	= Strouhal number
L_o, M_o	= affine space running aerodynamic lift and moments, respectively
ℓ_o	= affine space half-span for the wing
m_o	= affine space mass per unit span
$(\Delta p, \Delta p_o)$	= differential aerodynamic pressure distributions in physical and affine space, respectively
t	= time
U, U_o	= virtual work expressions in physical and affine space, respectively
U_f	= flutter speed
$(x,y,z,), (x_o, y_o, z_o)$	= physical and affine space coordinates, respectively
$\gamma_i, \delta_i, \beta_i$	= displacement shape functions
$r, L_1, L_2, D^*, D^*_o,$	= generic nondimensionalized stiffness parameters
μ_o	= affine mass ratio parameter
μ_{ij}, ε	= Poisson ratios and generalized Poisson's ratio, respectively
λ_o	= divergence parameter

ρ, ρ_∞	= affine space material and air density, respectively
ϑ	= twisting displacements
w	= displacement
ω	= vibration frequency

5.3.2
Introduction

Perhaps one of the more elusive aspects of supermaneuverability as a design concept is its aeroelastic implications. One generally accepted definition of supermaneuverable aircraft is that it is designed to operate at high angles of attack. Strictly speaking high angle of attack problems are nonlinear. However due to the high degree of complexities involved in dealing with nonlinear aeroelastic problems, an average aeroelastician would prefer to deal with a linearized version of the problem (at least as a first approximation). If linear aeroelastic equations are used under such conditions, at least it should be assumed that the high angle of attack would introduce large twisting displacements which would imply that terms containing twisting displacement should be retained. Even under low angle of attack assumptions, the early works of Reissner and Stein[1] and later works of Libescu et al[2] have shown that for metal wings there are conditions under which the so called St. Venant's torsion principle is inapplicable. This is when the restraint of warping effect is important and a more accurate analysis would need to include a higher order term involving the twisting displacement. Although the retention of such a term implies solving fourth order (instead of second order) differential equations for the twisting and bending displacements, the equations can be easily decoupled for metal wings. However for composite wings, the decoupling of these equations is neither easy practically nor is it even desirable from aeroelastic tailoring standpoint.[3-7] These studies have also shown that the restraint of warping is very important

in composite wings. Therefore it would seem that an aeroelastic analysis of a supermaneuverable (high angle of attack) aircraft wing fabricated of composite materials would need to consider the effects of restraint of warping as well as elastic coupling.

Previous investigation of this latter problem (free vibration) at MIT[3,4] used analytical methods to solve the decoupled problem, while numerical methods were utilized to solve the coupled problems. Consequently general results were presented for the decoupled problem while representative results were presented for the coupled problem.

In this paper the coupled free vibration is treated analytically as a pair of coupled fourth order (differential equations) boundary value problem to which exact closed form eigen-solutions are sought. The enforcement of the necessary boundary conditions resulted in a fairly complicated transcendental function to be used to determine the required eingenvalues from which the natural frequencies are to be obtained. This transcendental function was complex in contrast to its decoupled counterpart (which is real). That should be indicating the presence of the phase angle that exists between the twisting and bending displacements. A comparison with a damped (decoupled) system in which complex determinant signifies phase angles between damping and other forces, led us to the formulation of an explanation for the "modal transformation" phenomenon which was reported in studies at MIT[3,4] and Purdue[8] (which seemed to have lacked explanation until this study). The explanation is that the modal transformation may be viewed as a form of steady state conservative (energy stays in this system

since there is no damping) inter-

modal energy transfer between the vibration modes. In fact work currently in progress at Purdue[8] seem to support and confirm this explanation. The results which favorably compared with those obtained at MIT,[3,4] also revealed that coupling has a tendency to lower the first coupled natural frequency of a composite aircraft wing. In fact it is seen that a substantial amount of coupling could reduce the first coupled frequency to almost zero (hence a possibility of coupling with rigid body modes).

5.3.3

Problem Statement

For a composite aircraft wing cantilevered at the root as shown in Figure 1, the virtual work theorem in the physical space is given by

$$\delta\bar{U} = 0 = \frac{\delta}{2}\int_0^t\int_A\int \Big[D_{11}(w_{,xx})^2 + 2D_{12}\, w_{,xx}\, w_{,yy} + D_{22}(w_{,yy})^2\Big] + 4D_{16}\, w_{,xx}\, w_{,xy} + 4D_{26}\, w_{,yy} + 4D_{66}\,(w_{,xy})^2 \; dxdydt - \frac{\delta}{2}\int_0^t\int_A\int \rho\,\bar{h}\,\dot{w}^2 dxdydt + \int_0^t\int_A\int \Delta p\,\delta w\; dxdydt \tag{1}$$

where:

D_{ij} are the elastic constants, ρ, is the material density, Δp is the differential pressure distribution, w is the displacement, t is the time, A integrals represent area integrals and h is the wing box depth.

Using the following affine transformation of variables;

$$x = \left(\frac{D_{11}}{D_{22}}\right)^{1/4} x_o \quad ; \quad y = y_o \quad ; \quad z = z_o \tag{2a}$$

then in affine space the virtual work theorem becomes:

$$\delta\bar{U}_o = 0 = 2\int_0^t\iint_A \Big\{ (w,_{x_o x_o})^2 + 2D^* \Big[(1-\varepsilon)(w,_{x_o y_o})^2 + \varepsilon w,_{x_o x_o} w,_{y_o y_o}\Big] + (w,_{y_o y_o})^2 + L_1 w,_{x_o x_o} w_{x_o y_o} + L_2 w,_{y_o y_o} w,_{x_o y_o}\Big\} dx_o dy_o dt - \frac{\delta}{2}\int_0^t\iint_A \rho_o \dot{w}^2 dx_o dy_o dt + \int_0^t\iint_A \Delta p_o \delta w dx_o dy_o dt \tag{2b}$$

where

$$\bar{U}_o = \frac{\bar{U}}{D_{22}}\left(\frac{D_{22}}{D_{11}}\right)^{1/4} \quad ; \quad D^* = \frac{D_{12} + 2D_{66}}{(D_{11}D_{22})^{1/2}}$$

$$; \ \varepsilon D^* = \frac{D_{12}}{(D_{11}D_{22})^{1/2}} \quad ; \quad L_1 = \frac{4D_{16}}{(D_{11})^{3/4}(D_{22})^{1/4}} \quad ; \tag{3}$$

$$L_2 = \frac{4D_{26}}{(D_{11})^{1/4}(D_{22})^{3/4}} \quad ; \ \Delta p_o = \frac{\Delta p}{D_{22}} \quad ; \quad \rho_o = \frac{\rho\bar{h}}{D_{22}}$$

If the affine space equivalent of the standard aeroelastic displacement assumptions is made, i.e.,

$$w(x_o, y_o, t) = h_o(y_o, t) + x_o \alpha_o(y_o, t) \ .. \tag{4}$$

where h_o and α_o are the bending and twisting displacements respectively, then it can be shown through the use of the calculus of variations that a coupled set of aeroelastic equations of motion for the composite aircraft wing, in which the restraint of warping and elastic coupling effects are accounted for is given by

$$a_1 h_o^{iv} + a_2 \alpha_o^{iv} - a_5 \alpha_o^{iii} + \rho_o a_1 \ddot{h}_o + \rho_o a_2 \ddot{\alpha}_o = L_o$$

$$a_2 h_o^{iv} + a_5 h_o^{iii} + a_3 \alpha_o^{iv} - a_4 \alpha_o'' + \rho_o a_3 \ddot{\alpha}_o + \rho_o a_2 \ddot{h}_o = M_o \qquad (5)$$

$$\text{at } y_o = 0$$

with boundary conditions

$$h_o = 0,\ h_o' = 0,\ \alpha_o = 0,\ \alpha_o' = 0 \qquad (6)$$

$$\text{at } y_o = \ell_o$$

$$a_3 \alpha_o'' + a_2 h_o'' - L_2 a_2 \alpha_o' = 0,\ a_1 h_o'' - a_5 \alpha_o' + a_2 \alpha_o'' = 0$$

$$a_2 \alpha_o''' + a_1 h_o''' - a_5 \alpha_o'' = 0$$

$$a_2 h_o''' + a_3 \alpha_o''' + a_5 h_o'' - a_4 \alpha_o' = 0$$

where:

$$a_1 = \int_{e\bar{c}_o}^{\bar{c}_o} dx_o \quad ; \quad a_2 = \int_{e\bar{c}_o}^{\bar{c}_o} x_o\, dx_o$$

$$a_3 = \int_{e\bar{c}_o}^{\bar{c}_o} x_o^2 dx_o \quad ; \quad a_4 = 2\int_{e\bar{c}_o}^{\bar{c}_o} D^*(1-\epsilon)dx_o$$

$$L_o = \int_{e\bar{c}_o}^{\bar{c}_o} \Delta p_o dx_o \quad ; \quad a_5 = \int_{e\bar{c}_o}^{\bar{c}_o} L_2 dx_o \qquad (7)$$

$$M_o = \int_{e\bar{c}_o}^{\bar{c}_o} x_o \Delta p_o dx_o$$

$$-\infty < e < 0 \quad ; \quad \bar{c}_o = \frac{c_o}{1-e}$$

$$(\,)' = \frac{\partial}{\partial y_o}; \quad (\dot{}) = \frac{\partial}{\partial t}$$

For free vibrations, if a_2 (through the geometric construction of the wing) is made to be zero, equations 5 reduce to

$$a_1 h_o^{iv} - a_5 \alpha_o''' + \rho_o a_1 \ddot{h}_o = L_o$$

$$a_3 \alpha_o^{iv} + a_5 h_o''' - a_4 \alpha'' + \rho_o a_3 \ddot{\alpha}_o = M_o \qquad (8a)$$

with boundary conditions

at $y = 0$,

$$h_o = 0,\ h_o' = 0,\ \alpha_o = 0,\ \alpha' = 0$$

at $y_o = \ell_o$

$$a_1 h_o''' = a_5 \alpha_o''' = 0,\ a_1 h_o'' - a_5 \alpha_o' = 0 \qquad (8b)$$

$$a_3 \alpha_c''' + a_5 h_o''' - a_4 \alpha_o' = 0$$

It may be stated here that the restraint of warping effect is represented by the product of α^{IV} and a_3 while the elastic coupling effect is represented by the a_5 terms.

5.3.4

Methods of Solution

Two methods for solving equations 8 are examined in this paper. These are (a) an "exact closed form" approach and (b) a "semi-exact closed form" approach. The exact closed form approach is defined here as one in which explicit expressions are derived for the eight roots of the eighth order operator equations representing equations 8a, and through the superimposition of fundamental solutions corresponding to each of the eight operator roots, the boundary conditions 8b are satisfied. The semi-exact closed form approach is the same as (a) except that the roots of the operator equation are determined numerically through the usage of some standard root extraction subroutines.

In either case, to solve for the operator roots of equation 8a, it may be rewritten in operator form as follows,

$$\bar{L}_1\bar{h}_o - \bar{L}_2\bar{\alpha}_o = 0 \tag{9a}$$

$$\bar{L}_2\bar{h}_o + \bar{L}_3\bar{\alpha}_o = 0 \tag{9b}$$

where the operators $\bar{L}_n$ (n = 1,2,3) are given by

$$\bar{L}_1 = a_1 \frac{\partial^4}{\partial \bar{y}_o^4} - a_1\omega^2\rho_o \qquad \bar{L}_2 = a_5 \frac{\partial^3}{\partial \bar{y}_o^3}$$

$$\bar{L}_3 = a_3 \frac{\partial^4}{\partial \bar{y}_o^4} - a_4 \frac{\partial^2}{\partial \bar{y}_o^2} - a_3\omega^2\rho_o \tag{10}$$

and $h_o = \bar{h}_o e^{i\omega t}$

$\alpha_o = \bar{\alpha}_o e^{i\omega t}$

ω is vibration frequency

Following the method used in Hilderbrand,[9] if $\bar{L}_1$ and $\bar{L}_2$ are commutative (i.e., $\bar{L}_1\bar{L}_2 = \bar{L}_2\bar{L}_1$) or $\bar{L}_2$ and $\bar{L}_3$ are commutative (i.e., $\bar{L}_2\bar{L}_3 = \bar{L}_3\bar{L}_2$) either $\bar{h}_o$ or $\bar{\alpha}_o$ may be eliminated and equations 9 is reduced to one eighth order operator equation in either $\bar{\alpha}_o$ or $\bar{h}_o$, respectively. This can be accomplished by using $\bar{L}_2$ to operate on 9(a) and $\bar{L}_1$ to operate on 9(b) and subtracting 9(a) from 9(b) or by using $\bar{L}_3$ to operate on 9(a) and $\bar{L}_2$ to operate on 9(b) and subtracting 9(a) from 9(b). The result of such an operation in which $\bar{h}_o$ is eliminated is given by

$$(\bar{x}^4 + F_3\bar{x}^3 + F_2\bar{x}^2 + F_1\bar{x} + F_o)\ \alpha_o = 0$$

where, $F_3 = -16\bar{\lambda}_c^2$, $F_2 = -\bar{k}^2$, $F_1 = 8(\bar{k}\lambda_c)^2$ (11)

$$F_o = \frac{\bar{k}^4}{4}, \quad \bar{x} = \left(\frac{\partial}{\partial y_o}\right)^2$$

It should be noted here that because the method of elimination of $\bar{h}_o$ is through a differential operator, superfluous solutions are to be expected (e.g., operator equation 11 is eighth order instead of fourth order). These superfluous solutions are eliminated by enforcing some consistency conditions on the solutions as described below. Based on equation 11, an appropriate form for the exact-closed form (or complete) solution for the mode shapes of the free vibration problem proposed in this paper, which can also be made to satisfy the necessary boundary conditions is given by,

$$h_o = A_1 \cosh\beta_1 y_o + A_2 \sinh\beta_1 y_o + A_3 \cos\beta_2 y_o + A_4 \sin\beta_2 y_o + A_5 \cosh\beta_3 y_o + A_6 \sinh\beta_3 y_o + A_7 \cos\beta_4 y_o + A_8 \sin\beta_4 y_o \quad (12(a))$$

$$\alpha_o = B_1 \cos\beta_1 y_o + B_2 \sinh\beta_1 y_o + B_3 \cos\beta_2 y_o + B_4 \sin\beta_2 y_o + B_5 \cosh\beta_3 y_o + B_6 \sinh\beta_3 y_o + B_7 \cos\beta_4 y_o + B_8 \sin\beta_4 y_o \quad (12(b))$$

where

$$\beta_n = \bar{x}_n^{1/2} \qquad n = 1,2,3,4 \tag{13}$$

and $\bar{x}_n$ can be obtained either from the numerical solution of equation 11 or according to the method described in Abramowitz and Stegun,[10] as follows

Define

$$\lambda_c = (\ell_o/c_o)\sqrt{\frac{3}{2}D_o^*} \qquad \bar{\lambda}_c = (\ell_o/c_o)\sqrt{\frac{3}{2}(D_o^* - \frac{L_2^2}{2})} \tag{14}$$

$$P_1 = 4(\bar{\lambda}_c^4 + \lambda_c^4) - 8/3\bar{\lambda}_c^2\lambda_c^2 + \frac{\bar{k}^2}{27}$$

$$P_2 = \frac{1}{6}(32\bar{\lambda}_c^2\lambda_c^2 + \frac{\bar{k}^2}{3}) \tag{15}$$

$$S_1 = 2\bar{k}\left[\bar{k}P_1 + (\bar{k}^2P_1^2 - 8P_2^3)^{\frac{1}{2}}\right]^{\frac{1}{3}}$$

$$S_2 = 2\bar{k}\left[\bar{k}P_1 - (\bar{k}^2P_1^2 - 8P_2^3)^{1/2}\right]^{1/3} \tag{16}$$

$$u_1 = S_1 + S_2 - \frac{\bar{k}^2}{3}$$

$$u_2 = -\frac{1}{2}(S_1+S_2) - \frac{\bar{k}^2}{3} + i\frac{\sqrt{3}}{2}(S_1-S_2) \tag{17}$$

$$u_3 = -\frac{1}{2}(S_1+S_2) - \frac{\bar{k}^2}{3} - i\frac{\sqrt{3}}{2}(S_1-S_2)$$

$$f_{3,4} = -8\bar{\lambda}_c^2 \mp \left[64\bar{\lambda}_c^4 + u_i + \bar{k}^2 \right]^{\frac{1}{2}}$$

$$f_{5,6} = \frac{u_i}{2} \pm \left[\left(\frac{u_i}{2}\right)^2 - \frac{\bar{k}^4}{4} \right]^{\frac{1}{2}} \qquad (18)$$

$$\bar{x}_{1,2} = \frac{-f_3 \pm \sqrt{f_3^2 - 4f_5}}{2}$$

$$\bar{x}_{3,4} + \frac{-f_4 \pm \sqrt{f_4^2 - 4f_6}}{2} \qquad (19)$$

where u_i $(i = 1,2,3)$ is the root that makes $f_{3,4,5,6}$ all real.

5.3.5
Consistency Conditions

From equations 12(a) and 12(b) it is seen that there are sixteen arbitrary integration constants as opposed to the expected eight constants. The additional eight constants have been introduced superfluously as a result of the differential operation which was done in order to eliminate one of the dependent variables in the two coupled differential equations (equations 9). In order to get rid of these superfluous solutions it is necessary to enforce some consistency conditions. This may be accomplished by

substituting equations 12(a) and 12(b) into one of the equations 9 and requiring the equation to be satisfied identically. This procedure shall establish a set of explicit relationships between the constants A_n and B_n in which A_n can be determined in terms of B_n or vice-versa.

When the superfluous solutions are eliminated, equations 12 can now be used to satisfy the boundary conditions for this problem (equations 8b). Consequently the condition for nontrivial solutions is enforced to obtain the transcendental functional expression for determining the eigenvalues of this problem.

5.3.6

Eigenvalues

The following steps and definitions are carried out in order to obtain the transcendental functional expression for determining the necessary eigenvalue (for this eighth order boundary value problem) from which the coupled natural frequencies may be obtained

Define

$$h_n = \beta_n^4 - \frac{\bar{k}2}{2} \quad ; \quad t_n = \beta_n^2 - \frac{1}{\beta_n^2} h_n$$

$$\bar{h}_n = \frac{h_n}{\beta_n^3} \qquad h_n' = \frac{h_n}{\beta_n} \tag{20}$$

$$\bar{t}_n = 16(\lambda_c^2 - \bar{\lambda}_c^2)\ \beta_n^2 + (-1)^{n+1} \frac{h_n}{\beta_n^2} [\beta_n^2 + (-1)^n 16\lambda_c^2] \tag{21}$$

$$a_{15} = \frac{\bar{h}_3+\bar{h}_2}{\bar{h}_1+\bar{h}_2} \qquad a_{17} = \frac{\bar{h}_4-\bar{h}_2}{\bar{h}_1+\bar{h}_2} \qquad a_{35} = \frac{\bar{h}_3-\bar{h}_1}{\bar{h}_1+\bar{h}_2}$$

$$a_{37} = \frac{\bar{h}_1+\bar{h}_4}{\bar{h}_1+\bar{h}_2} \qquad a_{26} = \frac{\bar{h}_3-\bar{h}_2}{\bar{h}_2-\bar{h}_1} \qquad a_{28} = \frac{\bar{h}_4-\bar{h}_2}{\bar{h}_2-\bar{h}_1} \tag{22}$$

$$a_{46} = \frac{\bar{h}_1-\bar{h}_3}{\bar{h}_2-\bar{h}_1} \qquad a_{48} = \frac{\bar{h}_1-\bar{h}_4}{\bar{h}_2-\bar{h}_1}$$

$$F_{51} = -\beta_1{}^3 a_{15}\sinh\beta_1+\beta_2{}^3 a_{35}\sin\beta_2+\beta_3{}^3\sinh\beta_3$$

$$F_{61} = \beta_1{}^3 a_{26}\cosh\beta_1-\beta_2{}^3 a_{46}\cos\beta_2+\beta_3{}^3\cosh\beta_3$$

$$F_{71} = \beta_1{}^3 a_{17}\sinh\beta_1-\beta_2{}^3 a_{37}\sin\beta_2+\beta_4{}^3\sin\beta_4 \tag{23}$$

$$F_{81} = \beta_1{}^3 a_{28}\cosh\beta_1-\beta_2{}^3 a_{48}\cos\beta_2-\beta_4{}^3\cos\beta_4$$

$$F_{52} = h_1' a_{15}\sinh\beta_1-h_2' a_{35}\sin\beta_2-h_3'\sinh\beta_3$$

$$F_{62} = -h_1' a_{26}\cosh\beta_1+h_2' a_{46}\cos\beta_2-h_3'\cosh\beta_3$$

$$F_{72} = -h_1' a_{17} \sinh\beta_1 + h_2' a_{37} \sin\beta_2 - h_4' \sin\beta_4$$

$$F_{82} = -h_1' a_{28} \cosh\beta_1 + h_2' a_{48} \cos\beta_2 + h_4' \cos\beta_4$$

$$F_{53} = -t_1 a_{15} \cosh\beta_1 - t_2 a_{35} \cos\beta_2 + t_3 \cosh\beta_3$$

$$F_{63} = t_1 a_{26} \sinh\beta_1 - t_2 a_{46} \sin\beta_2 + t_3 \sinh\beta_3$$

$$F_{73} = t_1 a_{17} \cosh\beta_1 + t_2 a_{37} \cos\beta_2 - t_4 \cos\beta_4$$

(24)

$$F_{83} = t_1 a_{28} \sinh\beta_1 - t_2 a_{48} \sin\beta_2 - t_4 \sin\beta_4$$

$$F_{54} = \bar{t}_1 a_{15} \cosh\beta_1 + \bar{t}_2 a_{35} \cos\beta_2 - \bar{t}_3 \cosh\beta_3$$

$$F_{64} = -\bar{t}_1 a_{26} \sinh\beta_1 + \bar{t}_2 a_{46} \sin\beta_2 - t_3 \sinh\beta_3$$

$$F_{74} = -\bar{t}_1 a_{17} \cos\beta_1 - \bar{t}_2 a_{37} \cos\beta_2 + \bar{t}_4 \cos\beta_4$$

$$F_{84} = -\bar{t}_1 a_{28} \sinh\beta_1 + \bar{t}_2 a_{46} \sin\beta_2 + \bar{t}_4 \sin\beta_4$$

$$a_{57} = \frac{F_{61}F_{72}-F_{62}F_{71}}{F_{51}F_{62}-F_{52}F_{61}} \qquad a_{58} = \frac{F_{61}F_{82}-F_{62}F_{81}}{F_{51}F_{62}-F_{52}F_{61}}$$

$$a_{67} = \frac{F_{52}F_{71}-F_{51}F_{72}}{F_{51}F_{62}-F_{52}F_{61}} \qquad a_{68} = \frac{F_{52}F_{81}-F_{51}F_{82}}{F_{51}F_{62}-F_{52}F_{61}} \tag{25}$$

Then, $\bar{k}_n$ are given by the roots of

$$\bar{F} = (F_{53}a_{57}+F_{63}a_{67}+F_{73})(F_{54}a_{58}+F_{64}a_{68}+F_{84}) - (F_{54}a_{57}+F_{64}a_{67}+F_{74})(F_{53}a_{58}+F_{63}a_{68}+F_{83}) = 0 \tag{26}$$

Equation 26 is therefore the exact closed form transcendental functional expression from which the eigenvalues $\bar{k}_n$ may be extracted. The coupled natural frequencies are related to these eigenvalues by the following expression,

$$\omega_n = \left(\frac{D_{22}}{\rho}\right)^{1/2} \frac{\bar{k}_n}{\ell_o^2} (\lambda_c, \bar{\lambda}_c/\lambda_c) \ \ldots \tag{27}$$

5.3.7
Computations

The extraction of the eigenvalues from the exact-closed form transcendental expression in equation 26 proved to be a very challenging computational exercise due mainly to its complex nature, the existence of branch points, the necessity to order the operator roots appropriately and the existence of numerical noise.

The characteristic roots for the equations of motion, $\bar{x}_n$, were extracted in two different ways in order to assure accuracy: one method was by using a Jenkins-Traub computational method from the IMSL library. The second method was by using an exact-closed form approach outlined in Abramowitz and Stegun.[10] When these roots are being extracted numerically, they do not necessarily come out in a continuous manner. Therefore a subroutine that reorders them so that they become continuous with respect to the eigenvalue $\bar{k}_n$ is also employed. Once this reordering of these roots is completed, the parameters needed for computing the transcendental function, $\bar{F}$, in equation 26 are computed. Finally, the transcendental expression itself is computed and the roots, $\bar{k}_n$, are found numerically.

One interesting result is that the values of $\bar{F}$ are complex here. It is known, however, that each of the two uncoupled problems (bending or torsion) when treated separately has a real transcendental expression for extracting the eigenvalues. This behavior of the transcendental expression for extracting the coupled eigenvalues (i.e., being complex as opposed to being real) was the first hint that led the first author to examine any possible mathematical similarity between the problem at hand (a coupled non-damped oscillations problem) and simple damped oscillations problem in which the expression for determining the eigenvalues is in general complex due to the need to determine the oscillation frequency and the amount of damping in the mode, etc. In the coupled problem the complex nature of this transcendental expression for extracting the eigenvalues seems to be basically a reflection of

the phase that normally should exist between the bending and torsional modes. Realizing that in the damped case, there is a non-conservative energy transfer between the oscillating system and its environment as well as intermodal energy transfer, it became clear to the first author that in the undamped coupled system there may be a conservative energy transfer in the oscillating system. At the time of this thought it seemed to the first author that if it made sense, the idea should provide an explanation for the modal changes which were noticed during the studies at Purdue and MIT[3,4] as coupling in the system was changed. This prediction which turns out to be useful and confirmed by other recent studies from Purdue University[8] shall be discussed in more detail below.

The most convenient way to obtain the eigenvalues, $\bar{k}_n$, was found to be by graphical means. Thus the values of the real and imaginary parts of the complex transcendental function $\bar{F}$ are plotted against the values of $\bar{k}_1$ on the same curve as shown in Figure 2. The values of $\bar{k}_n$ at which the real and imaginary parts of the transcendental function are simultaneously equal to zero corresponds to the desired eigenvalues for this coupled problem.

One of the problems with the computational model described above is that, when the coupling parameter, L_2, becomes identically zero, the coupled system of equations becomes computationally ill conditioned and unsolvable. To circumvent this the results for the uncoupled case ($\bar{\lambda}_c/\lambda_c = 1$) are obtained from a series of calculations using successively smaller values for the coupling parameter, L_2. This led us to accept the values of eigenvalues

for zero coupling as the value corresponding to the limit as the coupling approaches zero. Although this continuity assumption seems to make sense, it is not backed by a rigorous mathematical proof. Luckily it was possible to check these results with results generated for an isotropic/metal aluminum/wing by MIT,[3,4] and the agreement was found to be good for the cases checked.

5.3.8
Results and Discussions

The natural frequencies ω_n for the coupled bending-torsion oscillations for a composite aircraft wing in the presence of elastic coupling and warping restraint is found (as shown by equation 27) to be a function of the ratio $(D_{22}/\rho)^{1/2}$, the length ℓ_o and the nondimensionalized frequency parameter $\bar{k}_n$ for the wing. In this problem, $\bar{k}_n$, is a function of only two parameters, i.e., λ_c which may be considered as an effective nondimensionalized aspect ratio and $\bar{\lambda}_c/\lambda_c$, which in a way, measures the amount of elastic coupling in the wing ($\bar{\lambda}_c/\lambda_c = 1$ for zero coupling). It is therefore seen from equation 27 that in order to increase ω_n one needs to make ℓ_o as small as possible and/or make (D_{22}/ρ) and $\bar{k}_n$ as large as possible. Such an exercise may be necessary when a tailoring of the frequency is needed to avoid instabilities (e.g., very low structural frequencies may provide an atmosphere for a coupling between the flexible modes and rigid body motions, which in turn has a potential to result in instability). This kind of tailoring is made convenient through the use of equation 27 in which, for a particular wing configuration and composite material, every variable in the equation shall be known ex-

cept $\bar{k}_n$ and D_{22}. Obviously if we want high ω_n, as we said earlier, D_{22} should be made to be as high as possible (and of course ρ as low as possible). Once this is done the only other parameter to be tailored is $\bar{k}_n$.

The plot of $\bar{k}_1$ as a function of λ_c and $\bar{\lambda}_c$ is shown in Figure 3 for all configurations having low camber to twisting coupling, and all values of bending to twisting coupling. The results computed at MIT,[3,4] which were used to verify the present results, are shown in Figure 3 as well. The important trend made visible is this investigation as shown in Figure 3, is that $\bar{k}_1$ (and hence ω_1) decreases with increasing nondimensionalized coupling L_2, which perhaps may be a more effective way to actually measure and compare elastic couplings, D_{16} and D_{26}. For example, the results from MIT[3,4] which were computed for some representative configurations, in dimensionalized form seem to represent systems with a fairly significant variation in coupling D_{26} or D_{16} (depending on the coordinate system). However when nondimensionalized, the results as shown in Figure 3 seem to show little variation in coupling. In fact they appear to be so close to the zero coupling case ($\bar{\lambda}_c/\lambda_c = 1$) or isotropic (or metal) case, that $\bar{k}_1$ for a metal or isotropic wing should be a good approximation (if it was necessary to make an approximation). The low value for the effective coupling was also evident in the nondimensionalized results from MIT[3,4] where the bending frequency hardly varied with material changes. The question that could be asked is therefore "Do all possible composite wing configurations result in very low effective nordimensionalized coupling, ($\bar{\lambda}_c/\lambda_c \approx 1$)?" If the answer is "yes",

then it may be proposed that for $\lambda_c > .5$, $\bar{k}_1\ (\lambda_c, \bar{\lambda}_c/\lambda_c)$ may be approximated as $\bar{k}_1(\lambda_c, 1)$, which is also the isotropic or metal value. For this case it is seen that the computation of the natural frequencies of composite aircraft wing having aeroelastic oscillations, merely requires the computation of (D_{22}/ρ) for a given wing half span ℓ_o, since $\bar{k}_n\ (\lambda_c, \bar{\lambda}_c/\lambda_c)$ is approximately equal to $\bar{k}_n\ (\lambda_c, 1)$ which is approximately equal to a constant (3.5) for n = 1. This result should make frequency computations for the bending mode significantly easier.

The problem with an affirmative answer which may likely be a "practical" answer, to the question posed above, is that there doesn't seem to be a theoretical or rigorous analytical reason (to the best of the authors' knowledge) why $\bar{\lambda}_c/\lambda_c$ must always be approximately 1. Therefore, if on the other hand, the answer to our question is negative, then the following observations may be made: (a) significant variation in $\bar{k}_1$ is possible with variations in effective nondimensionalized coupling $(\bar{\lambda}_c/\lambda_c)$. In fact it can be seen from Figure 3 that if $\bar{\lambda}_c/\lambda_c$ approaches zero, k_1 (and hence ω_1) approaches zero. (b) The values of $\bar{k}_1$ vary significantly with λ_c for low λ_c but approach asymptotic values for large λ_c. (c) The highest values of $\bar{k}_1$ is for isotropic (metals) or quasi-isotropic configurations. (d) For large values of λ_c, there appears to be a simple approximate (hopefully linear relationship) between $\bar{k}_1$ and $\bar{\lambda}_c/\lambda_c$ (or a measure of coupling). (e) For very large coupling $(\bar{\lambda}_c/\lambda_c \to 0)$, $\bar{k}_1$ approaches zero, which may provide the ingredient necessary for coupling between the elastic and rigid motions.

Perhaps a number of implications of some of these observations should be examined: Observation (c) seems to imply that the highest first frequency would correspond to isotropic or quasi-isotropic configurations if (D_{22}/ρ) and ℓ_o are the same. It is known however the metals have lower values of (D_{22}/ρ) than composites. It therefore means that quasi-isotropic or orthotropic configurations are desirable for such a design goal. Observation (e) would seem to imply that if a designer, interested in tailoring the wing frequencies, arbitrarily introduces large effective nondimensionalized coupling $(\bar{\lambda}_c/\lambda_c \to 0)$, then $\bar{k}_1$ (and hence ω_1) would approach zero. This may result in coupling between flexible and rigid motions which may or may not lead to instabilities. Could this have happened in the case of the X-29 Forward Swept Composite Wing Aircraft for which one of the primary modes of instability results from the coupling between flexible and rigid body motions? In other words was "too much" coupling (effective) inadvertently built into the wing during the design process? If that is the case, is there an alternative, equivalent design without any penalties (weight or otherwise) that could have been explored? Although the answers to these questions can, strictly speaking, only be possible after carrying the necessary aeroelastic analysis in which unsteady aerodynamic forces are considered, it appears from Figure 3 that a rough idea of the final picture may be obtained from the natural frequency analysis. Afterall, it is a common belief that the phenomena that actually lead to aeroelastic instabilities are linked to damping and coupling.

5.3.9

Modal Transformation

Earlier in this paper it was mentioned that previous studies by other investigators have found what appeared to be some kind of modal transformations as ply orientation was changed in a design process for a composite wing. While variation in ply orientation may change several directional stiffness parameters for the wing, the coupling stiffness parameter, L_2, may be singled out as a significant design parameter, because it may vary considerably (orthotropic configurations have zero values while it may be fairly significant in other configurations). Furthermore it should be remembered that the main reason for ply orientation variation is for 'tailoring', which is believed to be primarily tied to couplings (D_{16} and D_{26}). The absence (or the presence) of these couplings is basically what differentiates orthotropic configurations from anisotropic configurations. From these observations, and the fact that the entity that ties the bending and torsional equations is the coupling, it became clear that the role of coupling in modal transformations should be significant.

In order to see the role of coupling therefore in this study, the modal assumptions for the coupled problem were made similar to those normally made for the uncoupled problem (e.g., the frequency was assumed to be real) so as to provide an opportunity to compare, contrast and discern the final results easily. When this was done and the eigen-problem was formulated resulting in a complex transcendental expression from which the eigenvalue are to be extracted, a careful examination began.

A significant difference between the coupled and uncoupled

problems was that (as shown in Figure 2) the transcendental expression from which the eigenvalues are extracted is complex for the coupled problem while it is real for uncoupled problems. The complex nature of this transcendental expression basically reflects the fact that the bending and twisting oscillations are generally out of phase. Therefore the resultant coupled frequency that represents both the bending and twisting oscillation may be viewed as some kind of vector representation of the individual contributions. In order to formulate some explanations for the phenomenon of modal transformation in coupled (conservative) system, it may be necessary to compare and contrast coupled systems with damped systems. Damped systems, by definition are nonconservative, i.e., the system experiences a net loss or gain in energy. It is well known that in a damped system the transcendental expression for extracting the eigenvalues is complex, again, due to the phase angle that exists between the damping force and the conservative forces in the system. It is also known that some damping (desirable types) would tend to reduce the oscillation of the system (the non-desirable type tend to make the oscillations diverge). Therefore since damping is linked to some energy transfer which in turn tend to lead to a change in the oscillation frequencies, it was thought that the complex nature which is common to the coupled and damped system determinants (transcendental functions) from which the eigenvalues are extracted may be a similarity that may provide some explanations to the modal transformations in coupled systems. Using the similarity argument, the coupled system which for the present problem, is conservative, may

be viewed as having some conservative inter-modal energy transfer within the system when the coupling is changed, resulting in steady state changes or transformations of the modal energy content of a coupled mode compared to the uncoupled case. It may be worthwhile to point out that some results recently obtained at Purdue University[8] and communicated to the authors seem to strongly support this hypothesis.

5.3.10
Empirical Relations

A careful study of Figure 3 has led the authors to propose the following closed form asymptotic relationship that may be useful for some preliminary design consideration:

$$\bar{k}_1 = 3.5\ (\bar{\lambda}_c/\lambda_c) \quad , \quad \lambda_c > 3{\cdot}0 \tag{28}$$

Equation 28 was derived from Figure 4. Equation 28 as well as equation 27 show that the first coupled frequency decreases with increasing coupling, a trend that seems to be supported by new results from Purdue University[8] and the data from MIT.[3] In reference 3 for example, the first nondimensionalized frequency computed by Raleigh-Ritz (in which coupling is zero) had a value of 3.52, which is consistently higher than those computed by finite element method in which coupling is finite (not equal to zero). Equations 27 and 29 which are closed form (generally rare for anistropic systems) should be easy to use.

Before this discussion is concluded, it is probably necessary to explain why only the results of the first mode are shown in this paper. First of all it should be pointed out that some second mode data have been generated but are still being studied very critically to understand the general trends. It may also be pointed out that the extraction of the eigenvalues is a little challenging since some care is needed in ordering the roots of the operator equations.

5.3.11

Concluding Remarks

This paper has attempted to present exact closed form solutions to the coupled bending-torison vibration problem for a simplified model of composite aircraft wings with war ping constraint. Increasing the coupling was found to decrease the first coupled frequency. A comparison between the coupled problem and a sample damped problem led the authors to propose some explanation to the "modal transformation" phenomenon found by earlier investigators. Some simplified closed form expressions are provided for the first coupled frequencies which may be useful for fast applications.

5.3.12

Acknowledgement

The authors acknowledge valuable discussions with Drs. A. Amos, and A. Nachman who are monitors for the AFOSR Contracts F49620-85-C-0090/F49620-87-C-0046 under which this study was conducted. We also appreciate Professor T. A. Weisshaar's efforts in providing the data for validating the results presented here. Finally we acknowledge the programming efforts of Mr. John Calle-

ja, a graduate student in the department and we thank Mrs. B. Hein for patiently typing the manuscript.

REFERENCES

1. Reissner, E. and Stein, M., "Torsion and Transverse Bending of Cantilevered Plates," NACA TN 2369, June 1951.

2. Petre, A., Stanescu, C., and Librescu, L., "Aeroelastic Divergence of Multicell Wings (Taking their Fixing Restraints into Account,)" Aeromecanique, 1962, pp. 689-698.

3. E. F. Crafley and J. Dugundji, "Frequency Determination and Non-dimensionalization for Composite Cantilever Plates," Journal of Sound and Vibration, Vol. 72, No. 1, pp. 1-10, 1980.

4. Jensen, D.W. and Crawley, E.F., "Frequency Determination Techniques for Cantilevered Plates with Bending-Torsion Coupling," AIAA Journal, Vol. 22, No. 3, March 1984, pp. 415-420.

5. Oyibo, G.A. and Berman, J.H., "Influence of Warpage on Composite Aeroelastic Theories," AIAA Paper No. 85-0710, April 1985.

6. Oyibo, G.A. and Berman, J.H., "Anisotropic Wing Aeroelastic Theories with Warping Effects," DGLR Paper No. 85-57, Second International Symposium on Aeroelasticity and Structural Dynamics, Technical University of Aachen, West Germany, April 1985.

7. Oyibo, G.A., and Weisshaar, T.A., "Optimum Aeroelastic Characteristics for Composite Supermaneuverable Aircraft," Final Technical Report, AFOSR Contract F49620-85-C-0090, Report No. AE002V7407, July 31, 1986.

8. Weisshaar, T.A., "Vibration Tailoring", AFOSR Contract F49620-87-0046 Second Quarterly Technical Report, POLY AE Report 88-2, December, 1987.

9. Hildebrand, F.B., "Advanced Calculus for Applications," Prentice-Hall, Inc., Englewood Cliffs, New Jersey, 1976.

10. Abramowitz, M., and Stegun, I. A., "Handbook of Mathematical Functions" National Bureau of Standards, US Printing Office, 1965.

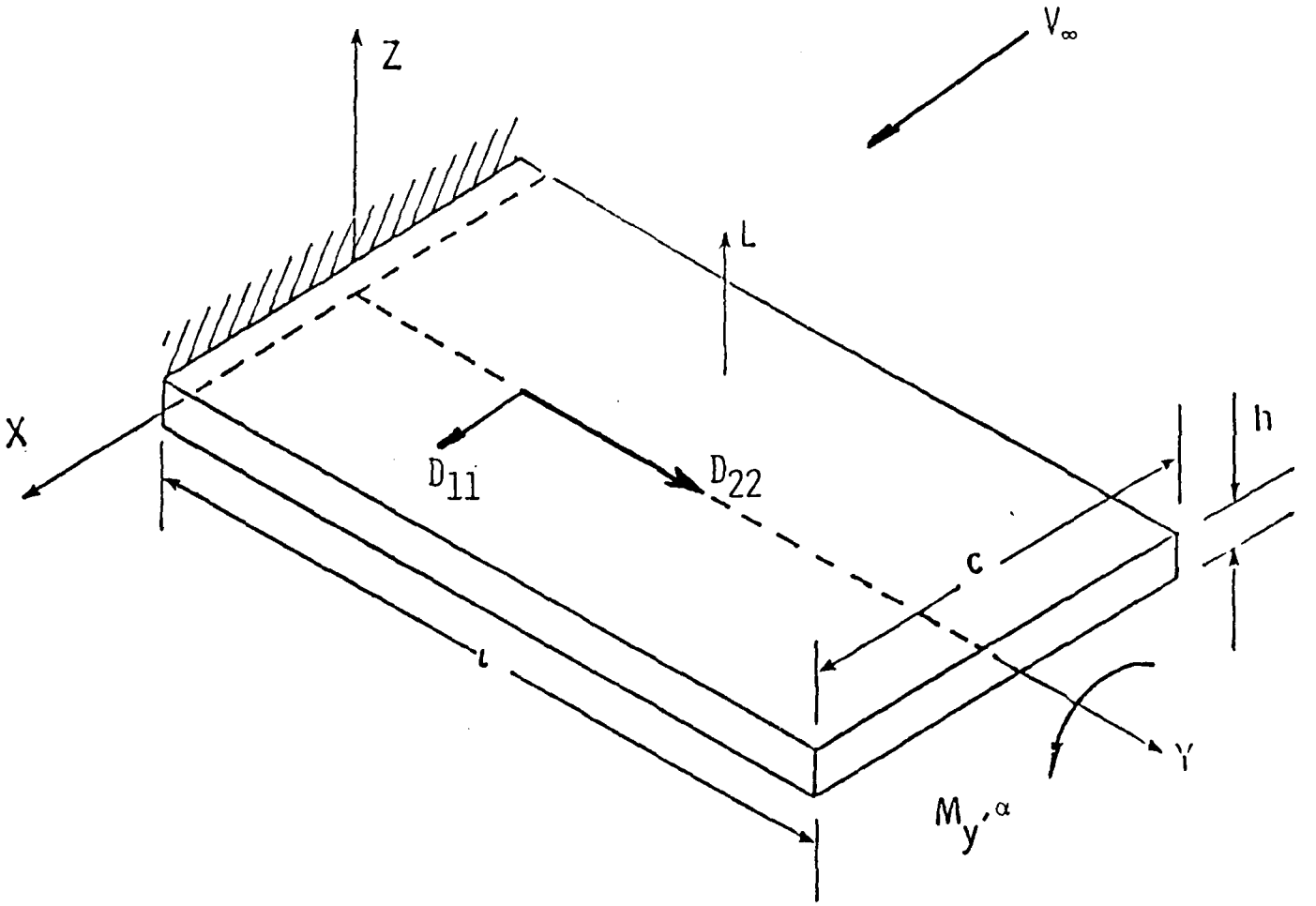

Figure 1: A Laminated Plate Model of a Composite Aircraft Wing

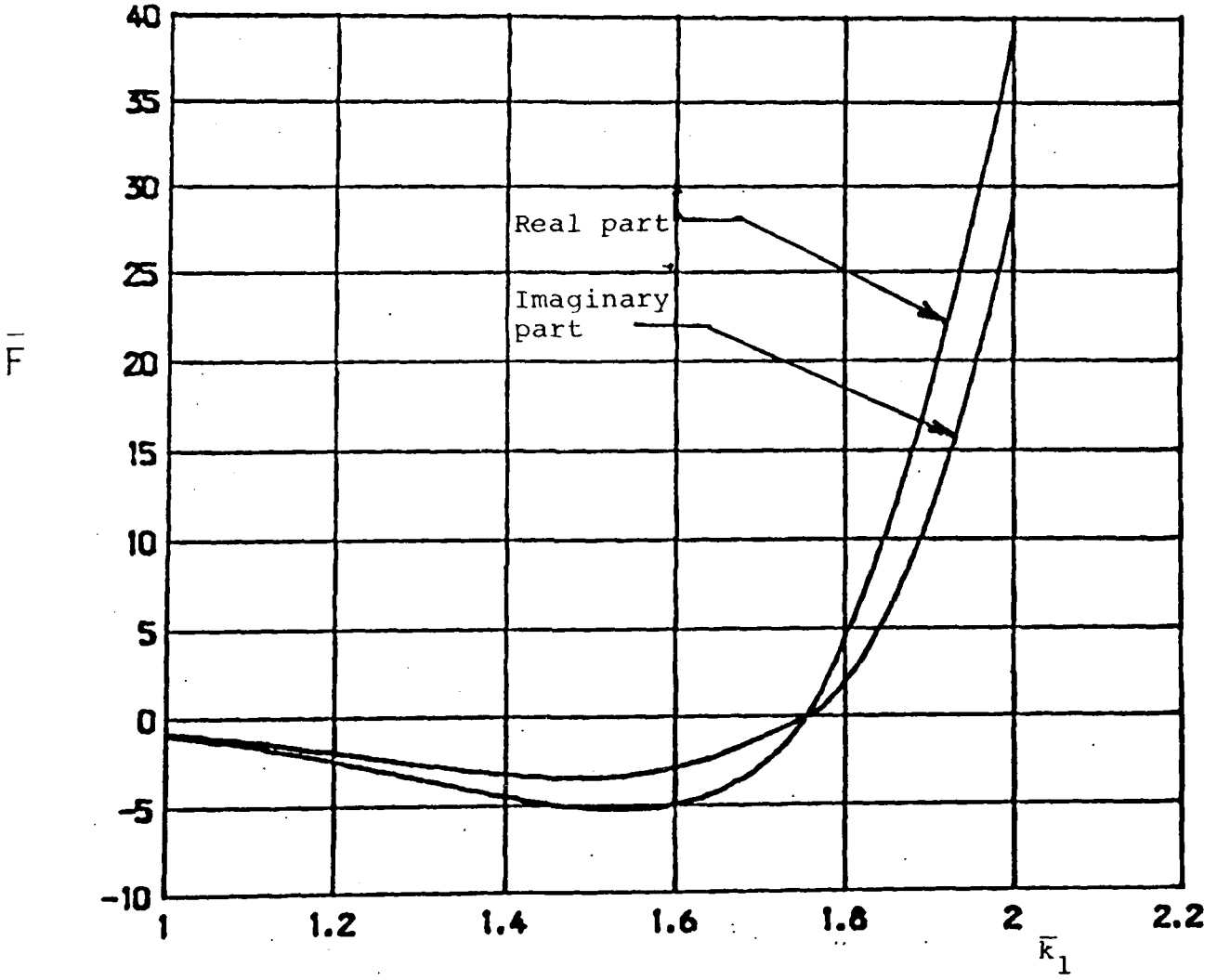

Figure 2: Variation of the Transcendental Function $\bar{F}$ with the Eigenvalue $\bar{k}_1$ ($\bar{\lambda}_c/\lambda_c = .638$, $\lambda_c = .732$)

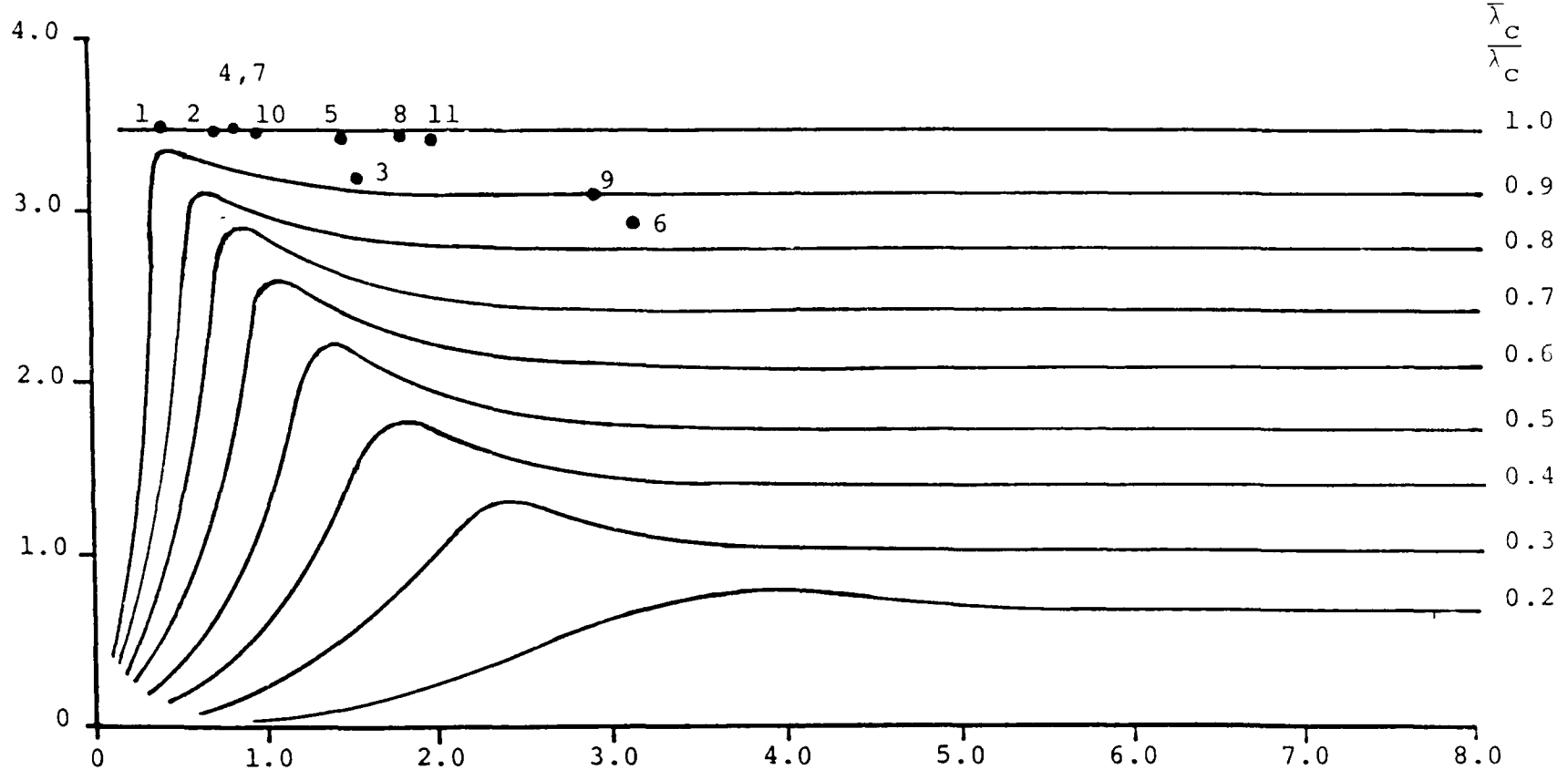

	1	2	3	4	5	6	7	8	9	10	11
$\frac{\bar{\lambda}_c}{\lambda_c}$ =	.971	.958	.955	.971	.958	.955	1.00	.993	.999	1.00(Aℓ)	1.00(Aℓ)

Figure 3 Variation of the first modal eigenvalue with effective aspect ratio

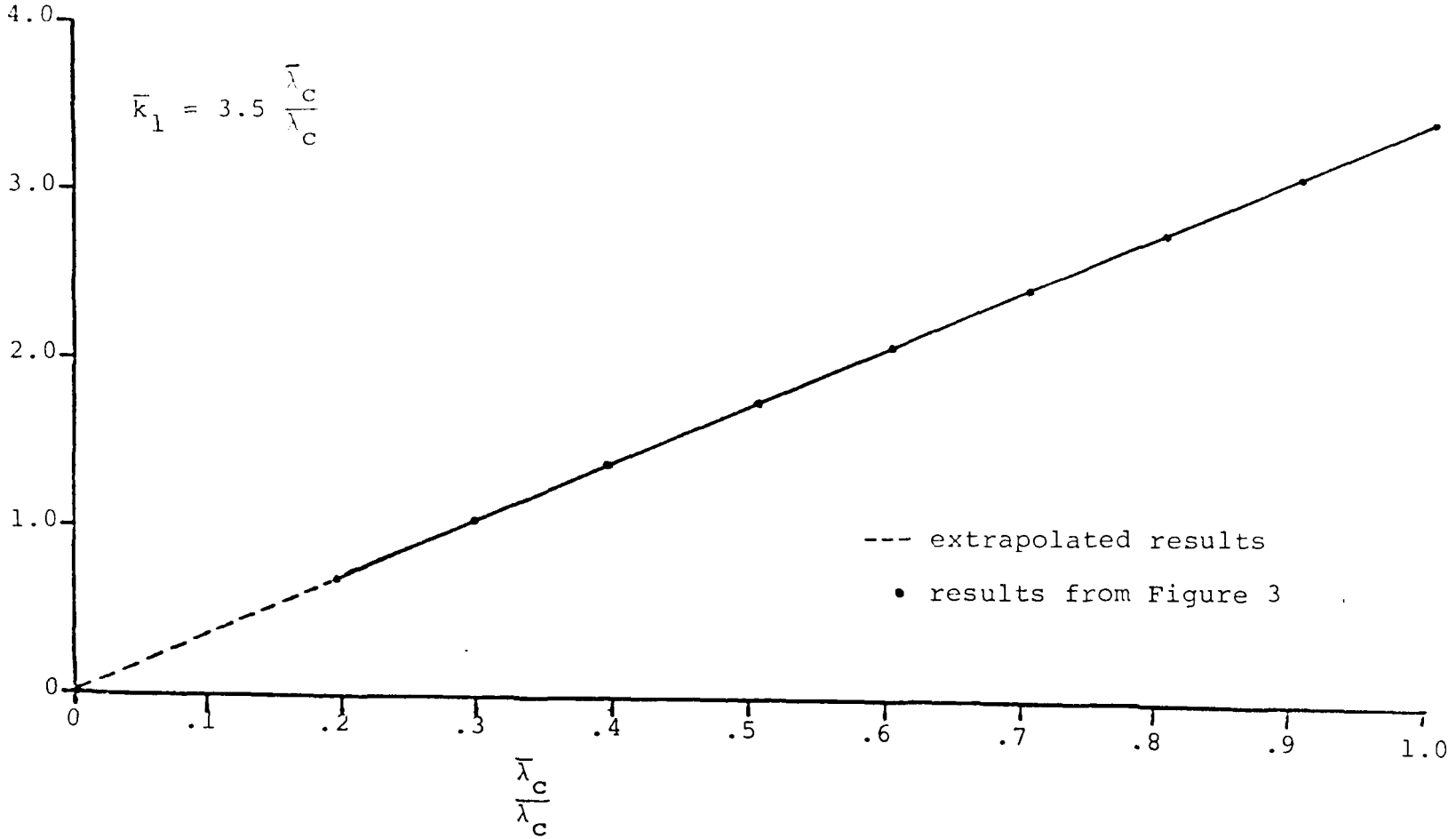

Figure 4 Empirical (asymptotic) relationship between the first modal eigenvalue and effective coupling ($\lambda_c \to \infty$)

5.4

VIBRATION TAILORING

T. A. Weisshaar**
Purdue University
West Lafayette, Indiana

5.4

1. Introduction

The analytical study of free vibration of a multi-degree-freedom system presents itself in the form of an eigenvalue problem, in which the eigenvalues yield the natural frequencies and the corresponding eigenvectors are the mode shapes. Together the natural frequencies and the mode shapes constitute the "fingerprints" that uniquely characterize a dynamic system. Moreover, the solu ion of a forced vibration problem relies predominantly upon the technique based on modal series expansion which, as implied by the name, requires the determination of eigenvalues and modal vectors. Indeed, the forced response is obtained as a superposition of the system's normal modes, each one of them being multiplied by a time-dependent generalized coordinate. In the area of dynamic aeroelasticity, the knowledge of natural modes is also essential. The modal matrix formed by columns of eigenvectors is used as a transformation matrix to reduce the number of degrees of freedom in the flutter analysis. By modifying the mode shapes of a system through aeroelastic tailoring, the flutter margin can be changed for better or for worse. It is therefore instructive to examine the influence of the tailoring

**Professor of Aeronautics and Astronautics

parameters upon the vibration modes. In previous work tailoring parameters were suggested nondimensioned in terms of combinations of the plate bending stiffnesses. When these parameters are varied within the constraint of their applicable bounds, the natural frequencies and mode shapes change. The magnitude and extent of these changes are the subject of this chapter.

5.4

2. Effect of Cross Stiffnesses on the Natural Frequencies

To illustrate and to discern the probable extent of the influence of dimensionless parameters on plate natural frequencies, a cantilevered, rectangular, flat plate of differing aspect ratios was chosen for the study. The geometry of the plate is shown in Figure 1. The deformation of this planform is modelled by classical plate theory using the Rayleigh-Ritz method. For this part of the tailoring work, the assumed displacement function is a polynomial in x and y coordinates, i.e.

$$w(x,y) = \sum_{i=1}^{m+1} \sum_{j=1}^{n+1} a_{ij}\, x^{i-1}\, y^{j-1} \qquad \text{for } m, n = 1,2,\ldots,8 \qquad (1)$$

If both the integers m and n take on the same value, say 4, then the displacement function is said to be biquartic (similarly, bihextal for $m = n = 6$, bioctal for $m = n = 8$, etc...). For the plate in Figure 1, it has one chordwise edge built-in and the rest of edges free. The geometric boundary conditions (displacement and slope) are enforced along $y = 0$, and the displacement function is reduced to

$$w(x,y) = \sum_{i=1}^{m+1} \sum_{j=3}^{n+1} a_{ij}\, x^{i-1}\, y^{j-1} \qquad \text{for} \begin{cases} m = 1,2,\ldots,8 \\ n = 2,3,\ldots,8 \end{cases} \tag{2}$$

The advantage in using polynomials versus beam mode shape functions lies in the relative ease of integration over the trapezoidal planform for which a rectangle is a special case. For the particular planform of interest, the largest exponent order in chordwise displacement (x-direction) is qradratic, i.e. $m = 2$. This provides for a chordwise curvature or camber effect with a parabolic shape. The largest spanwise order (y-direction) is quartic, i.e. $n = 4$. This arrangement of terms is made for two reasons. First, the plate is supported along $y = 0$, thus restricting the freedom in chordwise distorsion. Secondly, the fewer number of terms included in the assumed displacement allows greater computational efficiency. Another case study discussed later will show that no significant loss of numerical accuracy is entailed by using an approximation of these orders.

Now applying Eqn (2) to Ritz analysis which seeks a stationary solution to the variational condition on the energy expression

$$\delta\,(V - T) = \frac{\partial(V-T)}{\partial a_{ij}} = 0 \tag{3}$$

where V and T are respectively the strain and kinetic energies of the flexural laminated plate, and are written as follows:

Returning to our discussion, Figures 2 through 9 display the non-dimensionalized frequency associated with the first four modes plotted against the cross-stiffness tailoring parameters, ζ_1, ζ_2 and γ. The specimen considered is the aforementioned cantilevered rectangular planform with varying aspect ratios (Figure 1). The reference frequency used for the non-dimensionalization, denoted as ω_{iref} (where i = 1,2,3,4), corresponds to that which would be computed with zero cross-stiffness at each aspect ratio and each i^{th} mode. Note that the parameters ζ_1, ζ_2 and γ measure, respectively, the degree of camber/twist, bend/twist and camber/bend interaction present. In every figure, one of these parameters is changing, while the other two are kept constant. Care was exercised to vary the tailoring parameters within their allowable ranges. In addition to the relation which defines the parameter's upper and lower bounds, another constraint was also satisfie Noncompliance with these constraints would not cause computational troubles in most cases, but it would deprive the analysis of any physical meaningfulness.

Observing the figures, one can discern the general trend that, for small values of the tailoring parameters (e.g. below 0.3 $\sim$ 0.4), stiffness cross-coupling has little influence on the natural frequencies. As the parameters approach their bounds, then the dependence of the frequencies on the coupling is extremely evident for most cases. Frequencies generally decline significantly as the couplings accentuate their effects, although there are several instances showing opposite behavior to this trend. In the cases where frequencies do increase with stronger couplings, the magnitude of the increase is not as substantial as that of the decrease with larger couplings. Compared

to previous investigations by Weisshaar, frequencies of a beam model were found to be relatively unaffected in small couplings, but decline when ψ attains high values. Furthermore, in Figures 2 and 3, one does not observe any symmetry of the frequency curves with respect to $\psi_1 = 0$. However slightly distorted, this symmetry begins to take shape when ψ_2 and ψ are variables, as depicted in Figures 4 through 7. When one of the elastic couplings is removed, such as camber/twist interaction in Figures 8 and 9, then the frequency curve symmetry with respect to $\psi_2 = 0$ is perfect. Finally, as seen in the pattern of variations, no observation can be drawn on the influence of the aspect ratios.

5.4.3

3. Effect of Cross Stiffnesses on the Mode Shapes

Of key interest to an aeroelastician is the effect of structural deformations of a lifting surface upon the aerodynamic loads. In the dynamic environment, the surface deformations associated with the mode shapes exert a strong bearing on the flutter stability. Hence, tailoring for desirable modal shapes is a passive flutter prevention technique. The most significant alteration of a mode shape is the repositioning of nodal line contours. A nodal line is a locus of zero displacement present on the structure when that structure vibrates at a particular natural frequency. Biot and Arnold reported computations wherein zero airspeed flutter occurs for a two-dimensional airfoil when a node (point in this case) is located at the 3/4 chord position aft of the leading edge. They also stated that in a vortex-free flow, i.e. flow without circulation, flutter occurs at all airspeeds when a node coincides with the 3/4 chord position. In this latter case, frequency merging

takes place, and the ratio of pure bending to pure torsion frequencies is nearly unity. The authors concluded that, in designing an airfoil, it is recommended to place the nodal lines as far away as possible from the 3/4 chord "danger zone". This is an illustration of the importance of mode shapes to flutter occurrence.

The potential for modifying mode shapes through stiffness cross-coupling is illustrated in Figures 10 through 12. In these figures, the modes are represented in terms of nodal lines. Using the same specimen, nodal lines for the first six mo[illegible] of the fixed-aspect-ratio planform are reproduced for a number of values of ψ_1 and ψ_2. These nodal lines are generated from the Rayleigh-Ritz analysis. In each of the figures, two of the three cross-coupling parameters ψ_1, ψ_2 and [illegible] are held constant, while the third ranges within the constraints imposed. Note that the spanwise length of the rectangular planform has been scaled down, so that displacement data in one mode shape are displayed on one computer output page. Two comments are in order. The different modes are not symmetric with respect to $\psi_1 = 0.0$ in Figure 10. However, in the following two figures where ψ_2 is varying, modal symmetry is clearly discernible. As a matter of fact, this symmetry appears perfect in Figure 12 where, again, the camber-twist modes are decoupled. The above situation is consistent [illegible]ith that observed for the frequency curves. Based on the observations made, one can therefore infer that the camber/twist interaction can behave very differently when the sign of the elastic coupling changes. This is in sharp contrast to the other two types of couplings.

As the second comment, a reordering of the modes occurs between, for instance, the second and third modes in Figure 10. The reordering occurs

when ψ_1 changes its value from 0.6 to 0.8. At $\psi_1 = 0.6$, the second mode is predominently a second bending mode, while the third mode is predominently a first torsion mode. At $\psi_1 = 0.8$, the second mode becomes predominently a first torsion mode, while the third mode predominently a second bending mode. This change in modal identification is sometimes referred to as a modal exchange or modal transfer. The tendency for the two modes in question to interchange their order can also be seen in the extreme negative range of ψ_1 in Figure 10. In Figure 11 and 12, modal exchange involves the fourth and fifth modes as ψ_2 increases. In all the examples cited, modal exchange occurs as the result of changes in one of the cross-stiffnesses (ψ_1 or ψ_2). This is important to dynamic behavior because, while the modal frequency is relatively unaffected by changes in these parameters, the modal forces (also called generalized forces), that arise as a result of deformation in that mode, may be affected significantly.

The need now arises to analyze and to explain the phenomenon of modal transfer in a more quantitative manner. Oyibo in a study funded by AFOSR Contract F49620-85-C-0090, first proposed that this phenomenon can be explained in terms of inter-modal energy transfer. In the next sections an independent approach shall be used to try to verify Oyibo's theoretical explanation.

5.4.4

4. Modal Content Analysis

For a vibrating anisotropic plate, the mode shapes are composed of a number of intricately coupled fundamental shapes. As a result of the presence of cross-coupling, the distinct categorization of coupled modes as pure bending or pure torsion modes is not possible. A previous work discusses the idea of expression of mode shapes for a cross-coupled structure in terms of a set of modes generated from a baseline configuration.

This decomposition may be accomplished in terms of so-called modal participation factors as explained in the following discussion.

Consider the equation of motion for free vibration of a special plate, called the baseline structure. This baseline structure has no stiffness cross-coupling between the bending and torsion modes (i.e. $\psi_1 = \psi_2 = 0$). The equation is written as:

$$-\omega_o^2 [M_o] \{\eta\} + [K_o] \{\eta\} = \{0\} \tag{7}$$

where $[M_o]$ and $[K_o]$ are, respectively, the mass and stiffness matrices of the elastically uncoupled system. The solution to the above eigenvalue problem provides the modal vectors $\{\eta^{(i)}\}$ of the elastically uncoupled system. The full modal matrix $[\eta]$, a square matrix, can be constructed by assembling columns of eigenvectors $\{\eta^{(i)}\}$ in ascending order of the natural frequencies. Consider now a plate with nonzero cross-couplings. Let $[\bar{K}]$ be the portion of the stiffness matrix due to the effects of rotating the ply angle to create stiffness cross-coupling. This matrix may be added to the uncoupled portion $[K_o]$ of the baseline structure. As a result, we encounter a new eigenvalue problem, for which ψ_1 and ψ_2 are nonzero, as follows:

$$-\omega^2 [M_o] \{\xi\} + [K_o + \bar{K}] \{\xi\} = \{0\} \tag{8}$$

The eigenvalues and eigenvectors of the free-vibration problem, Eqn (5.7), are different than those found in Eqn (8) because of the modified stiffnesses. A coordinate transformation using $[\eta]$ may be performed to obtain the following

approximation for the new modal vectors $\{\xi\}$ of the elastically coupled system:

$$\{\xi^{(j)}\} = [\eta]\ \{P^{(j)}\} \tag{9}$$

The i^{th} element of $\{P^{(j)}\}$, denoted as P_{ij}, is the contribution of the i^{th} uncoupled mode $\{\eta^{(i)}\}$ to the j^{th} coupled mode $\{\xi^{(j)}\}$. Thus we see that the j^{th} modal vector of the coupled structure, $\{\xi^{(j)}\}$, is a linear combination of the modal vectors of the uncoupled baseline structure, the coefficients in the combination being the elements of $\{P^{(j)}\}$. This vector is called the moda content vector. Now inserting Eqn (9) into Eqn (8), premultiplying throughout by $[\eta]^T$, and normalizing the modal amplitude so that the following two relationships hold:

$$[\eta]^T\ [M_o]\ [\eta] = [\ I\ ] \tag{10}$$

$$[\eta]^T\ [K_o]\ [\eta] = [\lceil \omega_o^2 \rfloor] \tag{11}$$

where $[\ I\ ]$ is the identity matrix and $[\lceil \omega_o^2 \rfloor]$ a diagonal matrix whose nonzero elements are the natural frequencies of the baseline structure. We now find that Eqn (8) becomes

$$-\omega_j^2\ \{P^{(j)}\} + [\lceil \omega_o^2 \rfloor]\ \{P^{(j)}\} + [\eta]^T\ [\bar{K}]\ [\eta]\ \{P^{(j)}\} = \{0\} \tag{12}$$

If we further define

$$[\eta]^T [\bar{K}] [\eta] = [\tilde{K}] \qquad (13)$$

then we can rewrite Eqn (12) as

$$-\omega_j^2 \{P^{(j)}\} + [\omega_o^2] \{P^{(j)}\} + [\tilde{K}] \{P^{(j)}\} = \{0\} \qquad (14)$$

To determine the elements of the modal content vector $\{P^{(j)}\}$ associated with the j^{th} coupled mode, we begin first by solving Eqn (7), finding ω_o^2 and $\{\eta\}$ for all uncoupled modes. Next ω_j^2 of j^{th} coupled mode is determined from the eigenvalue problem, Eqn (8). Finally the vector $\{P^{(j)}\}$, which is itself an eigenvector of Eqn (12), can be calculated from the system of homogeneous equations, Eqn (12) if one of its elements is arbitrarily chosen. There is, however, a more convenient way to obtain $\{P^{(j)}\}$. Solving for all the modal vectors $\{\eta^{(i)}\}$ (where i = 1,2,...,n) and the j^{th} mode $\{\xi^{(j)}\}$ of Eqns (7) and (5.8) respectively, premultiplying Eqn (9) by $[\eta]^T [M_o]$ and normalizing in accordance with Eqn (10) we get

$$\{P^{(j)}\} = [\eta]^T [M_o] \{\xi^{(j)}\} \qquad (15)$$

If we normalize $\{P^{(j)}\}$ by dividing its elements by the largest absolute value in $\{P^{(j)}\}$, then we get the relative contribution of each mode $\{\eta^{(i)}\}$ to make up the content of each $\{\xi^{(j)}\}$. Using the above technique to determine modal content, we can pinpoint those modes that may be important to the flutter analysis.

The modal content vector $\{P^{(j)}\}$ can also be applied to the energy approach of the vibration problem. Consider once more the elastically coupled free vibration equation:

$$-\omega_j^2 [M_o] \{\xi^{(j)}\} + [K_o + \bar{K}] \{\xi^{(j)}\} = \{0\} \tag{8}$$

Substituting Eqn (9) - the relationship between the uncoupled and coupled eigenvectors - into Eqn (8) and proceeding as before, we obtain Eqn (12). Then, premultiplying Eqn (12) throughout by the row vector $_{[}P^{(j)}_{]}$, we get

$$-\omega_j^2 \, {}_{[}P^{(j)}_{]} \{P^{(j)}\} + {}_{[}P^{(j)}_{]} [\omega_o^2] \{P^{(j)}\} + {}_{[}P^{(j)}_{]} [\tilde{K}] \{P^{(j)}\} = \{0\} \tag{16}$$

At this point, we can form the Rayleigh's quotient from Eqn (16) as follows:

$$\omega_j^2 = \frac{{}_{[}P^{(j)}_{]} [\omega_o^2] \{P^{(j)}\} + {}_{[}P^{(j)}_{]} [\tilde{K}] \{P^{(j)}\}}{{}_{[}P^{(j)}_{]} \{P^{(j)}\}} \tag{17}$$

By adopting the notation

$$\{P^{(j)}\} = \begin{Bmatrix} P_1^{(j)} \\ P_2^{(j)} \\ \vdots \\ P_n^{(j)} \end{Bmatrix} = \begin{Bmatrix} P_{1j} \\ P_{2j} \\ \vdots \\ P_{nj} \end{Bmatrix} \tag{18}$$

we can rewrite Eqn (17) in summation form, i.e.

$$\omega_j^2 = \frac{\sum_{i=1}^{n} \omega_{oi}^2 P_{ij}^2 + \sum_{i=1}^{n} \sum_{k=1}^{n} \tilde{K}_{ik} P_{ij} P_{kj}}{\sum_{i=1}^{n} P_{ij}^2} \qquad (19)$$

For the j^{th} mode of the elastically coupled system, the numerator in Eqn (19) represents the strain energy. The first term can be viewed as the primary strain energy of the baseline structure, while the second term is interpreted as the strain energy due to stiffness cross-coupling. The denominator represents a measure of the kinetic energy.

In the previous section, we observed the phenomenon of modal transfer. To examine this phenomenon from an energy viewpoint, we focus our attention on the kinetic energy expression $\sum_{i=1}^{n} P_{ij}^2$. First we define each element P_{ij}^2 of $[P^2]$ matrix as the contribution of the kinetic energy of the i^{th} uncoupled mode of the baseline structure to the total kinetic energy of the j^{th} mode of the coupled structure. To facilitate further the numerical interpretation of P_{ij}^2, each i^{th} element of the j^{th} column of $[P^2]$ is divided by the sum of the elements in that column. As a result, we get the sum $\sum_{i=1}^{n} P_{ij}^2 = 1$ for the j^{th} column and obtain a normalized energy contribution of each i^{th} uncoupled mode to that of the j^{th} coupled mode.

As an illustrative example, a cantilevered laminate of rectangular planform with the stacking sequence $[\theta_2/0]_s$ was chosen. The plies are of equal thickness; the ply orientation θ is measured from the longitudinal axis and takes on values from 0 to 90 degrees. The baseline structure is defined as $[0_2/0]_s$; it is orthotropic ($D_{16} = D_{26} = 0$) and elastically uncoupled. There are

$$[P^2]_{\theta=21.5^\circ} = \begin{bmatrix} 0.99 & 0.01 & 0 & 0 & 0 & 0 & 0 & 0 & 0 \\ 0.01 & 0.49 & 0.49 & 0 & 0 & 0 & 0 & 0 & 0 \\ 0 & 0.49 & 0.48 & 0.03 & 0 & 0 & 0 & 0 & 0 \\ 0 & 0.01 & 0.02 & 0.83 & 0.11 & 0 & 0.02 & 0.01 & 0 \\ 0 & 0 & 0 & 0.09 & 0.68 & 0.20 & 0 & 0.02 & 0 \\ 0 & 0 & 0 & 0.04 & 0.02 & 0.28 & 0.62 & 0.04 & 0 \\ 0 & 0 & 0 & 0.01 & 0.01 & 0.14 & 0.23 & 0.61 & 0 \\ 0 & 0 & 0 & 0 & 0.17 & 0.35 & 0.12 & 0.29 & 0.06 \\ 0 & 0 & 0 & 0 & 0.01 & 0.01 & 0 & 0.04 & 0.94 \end{bmatrix} \quad (20)$$

As θ increases further, the bending kinetic energy begins to predominate, while the torsional kinetic energy gradually declines. Finally, near $\theta = 65^\circ$, mode 2 becomes a nearly pure flexural mode ($P_{32}{}^2 = 1$). Similar comments can be made with respect to mode 3 in Figure 14 where it is the second pure bending mode at $\theta = 0^\circ$ ($P_{33}{}^2 = 1$) and transmutes into the first pure torsion mode at $\theta = 65^\circ$ ($P_{23}{}^2 = 1$). Thus, through an evolutionary process which consists of changing gradually the stiffness characteristics, we observe a reciprocal switch or exchange of modal character, and in the context of kinetic energy, this modal exchange is rendered possible by an exchange of modal kinetic energies.

For higher modes, say $\{\xi^{(4)}\}$ and $\{\xi^{(5)}\}$, the deformation pattern is more complex. As a result, there are a larger number of uncoupled modes participating in the motion of the coupled system. Hence, modal content is more distributed, as is depicted in Figures 16 and 17. A further remark is in order here. The fact that the coupled modes $\{\xi^{(2)}\}$ and $\{\xi^{(3)}\}$ involve only the interaction of first torsion and second bending is well demonstrated by the equalities $P_{32}{}^2 = P_{23}{}^2$ and $P_{22}{}^2 = P_{33}{}^2$ in Figures 13 and 14. Such equalities do not exist in Figures 16 and 17. For $\{\xi^{(4)}\}$, there are three modes of the baseline structure that are coupled together when $\theta \neq 0^\circ$, while

two reasons for selecting this particular laminate: (a) the layup is unbalanced, hence it has a greater inherent coupling of deformations as compared to the balanced counterpart; (b) the dynamic behavior of this particular laminate has been documented previously by Jensen, et al. [MIT]. This permits correlation of our study to established results. Another advantage to using this unbalanced laminate is that modes 2 and 3 involve only an interplay between the first torsion and second bending behavior of the baseline structure. The number of terms considered in Eqn (2) were again set to m = 2 and n = 4, resulting in a nine-degree-of-freedom system (see Eqn (2)). These orders of the exponent yield numerical results in satisfactory agreement with those obtained experimentally by Jensen; this is demonstrated in Figure 18 to be commented shortly. Now referring to Figure 13 and starting at $\theta = 0^\circ$, mode 2 is observed as having all the kinetic energy of the pure first torsion mode ($P_{22}{}^2 = 1$ at $\theta = 0^\circ$); there is no contribution of the kinetic energy from the second bending mode ($P_{32}{}^2 = 0$ at $\theta = 0^\circ$). The nodal line patterns at $\theta = 0^\circ$ are sketched in Figure 15 along with those corresponding to other ply angles.

In Figure 13, it is noted that, as θ is increased, mode 2 becomes more coupled; there occurs a gradual decrease of the torsional modal kinetic energy $P_{22}{}^2$ with the corresponding increase of the bending modal kinetic energy $P_{32}{}^2$. At about $\theta = 21.5^\circ$, the modal energy curves cross each other, and mode 2 has 49% of first torsional energy and another 49% of second bending energy, the remainder being contributed by other fundamental modes. For purpose of illustration of the modal energy distribution, the normalized kinetic energy matrix for $\theta = 21.5^\circ$ is shown as follows:

for $\{\xi^{(5)}\}$, there are four modes. Because of the same number and type of fundamental modes participating in the motion, the crossings of the energy curves in Figures 13 and 14 occur at the same angle θ and indicate the occurrence of a modal transfer. If the modal participation is different, as it is the case in Figures 16 and 17, then the crossings of the energy curves do not take place at the same angle θ, however they still suggest the occurrence of modal transfer somewhere in the vicinity of the crossing angles θ.

We now turn attention to the behavior of the natural frequencies as the plies rotate. Of interest in Figure 18 is the tendency the frequencies of the second and third modes to approach each other in the neighborhood of $\theta = 21.5^\circ$. However the frequency curves do not cross each other and are observed never to do so. This non-crossing behavior of the frequency curves is even more dramatically illustrated by Ritchie, et al. and Weisshaar, et al. In particular, Ritchie mentions a so-called "non-crossing rule" in conjunction with the frequency curves. Ritchie states that the non-crossing rule forbids the tuning of coupled oscillators, whether mechanical or electrical, to the same frequency. Although efforts were made by the present author to find all the stipulations, if any, associated with this rule, the search has revealed only that the term "non-crossing rule" is well established in physics. Specifically, it refers to the non-crossing of electrical potential versus internuclear distance in the context of two electronic states. However we are unable so far to relate this rule with either mechanical or electrical oscillators found in the literature. It appears that Ritchie used the terminology in a very loose manner and that, in lieu of a rule, he really meant the "non-crossing behavior".

On the other hand, if we compute the natural frequencies of the structure versus the fiber orientation (see Figure 19), but only take into account values of D_{11}, D_{12}, D_{22} and D_{66} and disregard D_{16} and D_{26}, then the frequency curves of second and third modes do cross at $\theta = 21.5^\circ$. Although such a system is uncoupled, it is not the baseline structure defined earlier. Instead, the present configuration refers to the structure that is always elastically uncoupled by intentionally setting $D_{16} = D_{26} = 0$, or $\nu_1 = \nu_2 = 0$ for all θ's. For the baseline structure we have $D_{16} = D_{26} = 0$ only for $\theta = 0^\circ$. In Figure 19, the crossing of the uncoupled frequency curves indicates that a modal transfer or reordering takes place. The same can be said with respect to Figure 20 where the double crossings between the fourth and fifth modes suggest two modal transfers. An examination of the nodal patterns confirms the above remark.

In summary, we can draw several conclusions, based on the above discussion:

i. Modal transfer of an elastically-coupled laminated plate can be viewed and charted by examining baseline modal kinetic energies; as first proposed by Oyibo [AFOSR Contract F49620-85-C-0090*].

ii. The frequency curves of two modes plotted against ply angle can approach each other, but appear never to cross each other as evidenced by a number of plots of natural frequency versus ply angle;

iii. The ply angle at which modal transfer occurs can be deduced by the crossing of the plots of frequency versus ply angle of the elastically uncoupled system ($D_{16} = D_{26} = 0$ for all θ's).

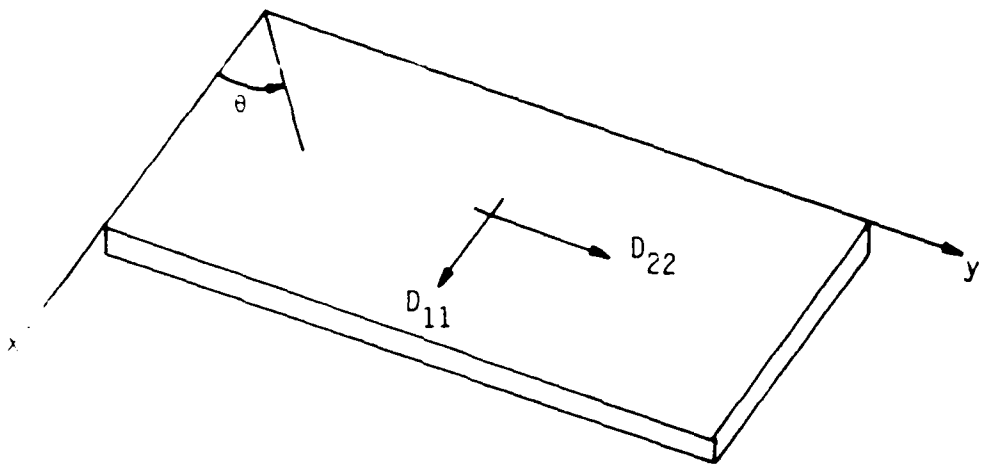

Graphite/Epoxy

Laminate: $[90/135/45/180]_s$

D_{11} = 79.04 lb·in Density: ρ = 0.055 lb/in^3

D_{22} = 21.71 lb·in Ply thickness: t = 0.0052 in

D_{66} = 14.14 lb·in

D_{12} = 12.64 lb·in

D_{16} = 4.78 lb·in

D_{26} = 4.78 lb·in

Figure 1. **Geometry and Material Properties of a Laminated Plate**

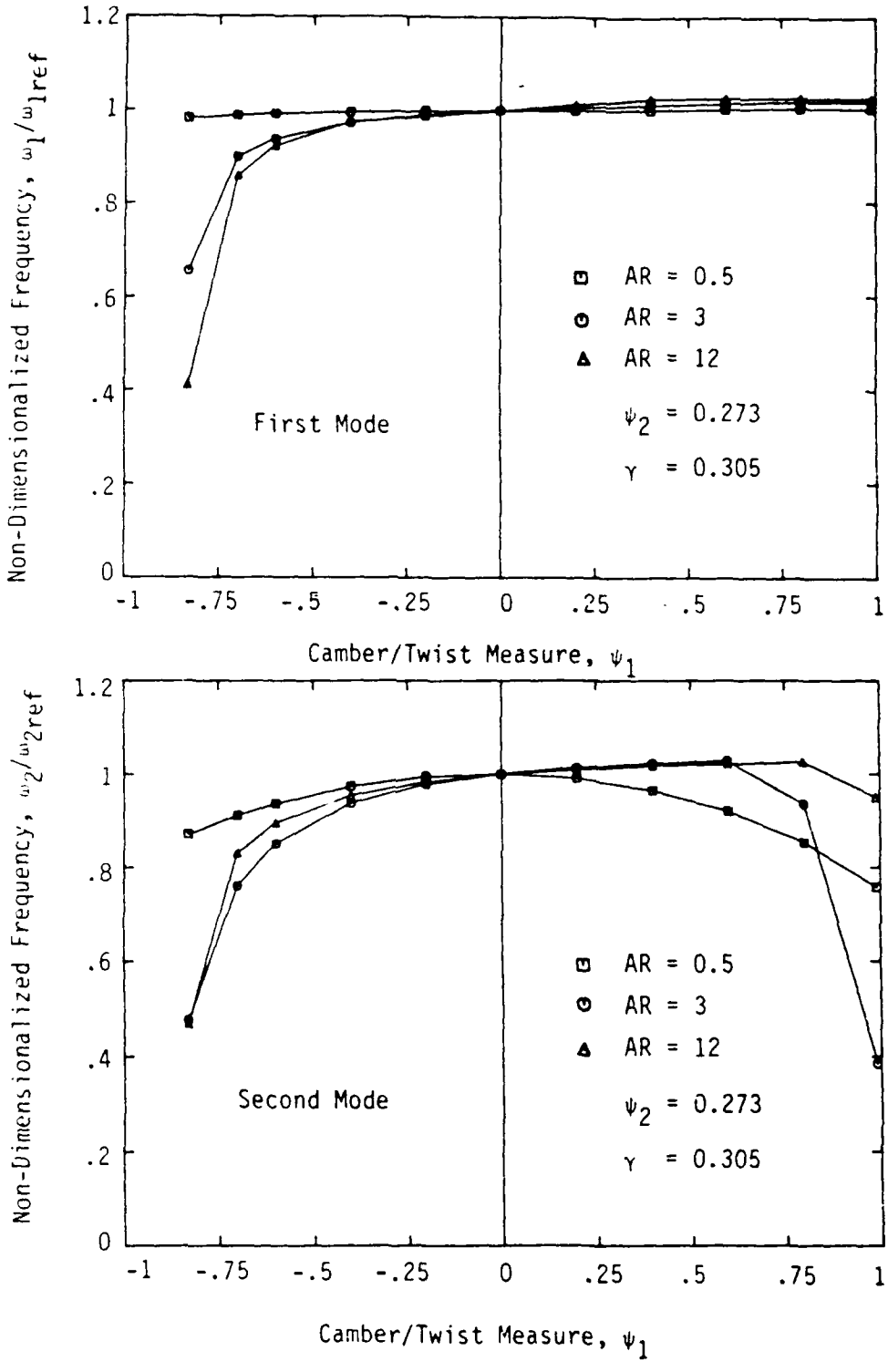

Figure 2. Frequency Variation as a Function of Camber/Twist Tailoring Parameter, ψ_1, in First and Second Modes with Different Aspect Ratios (AR)

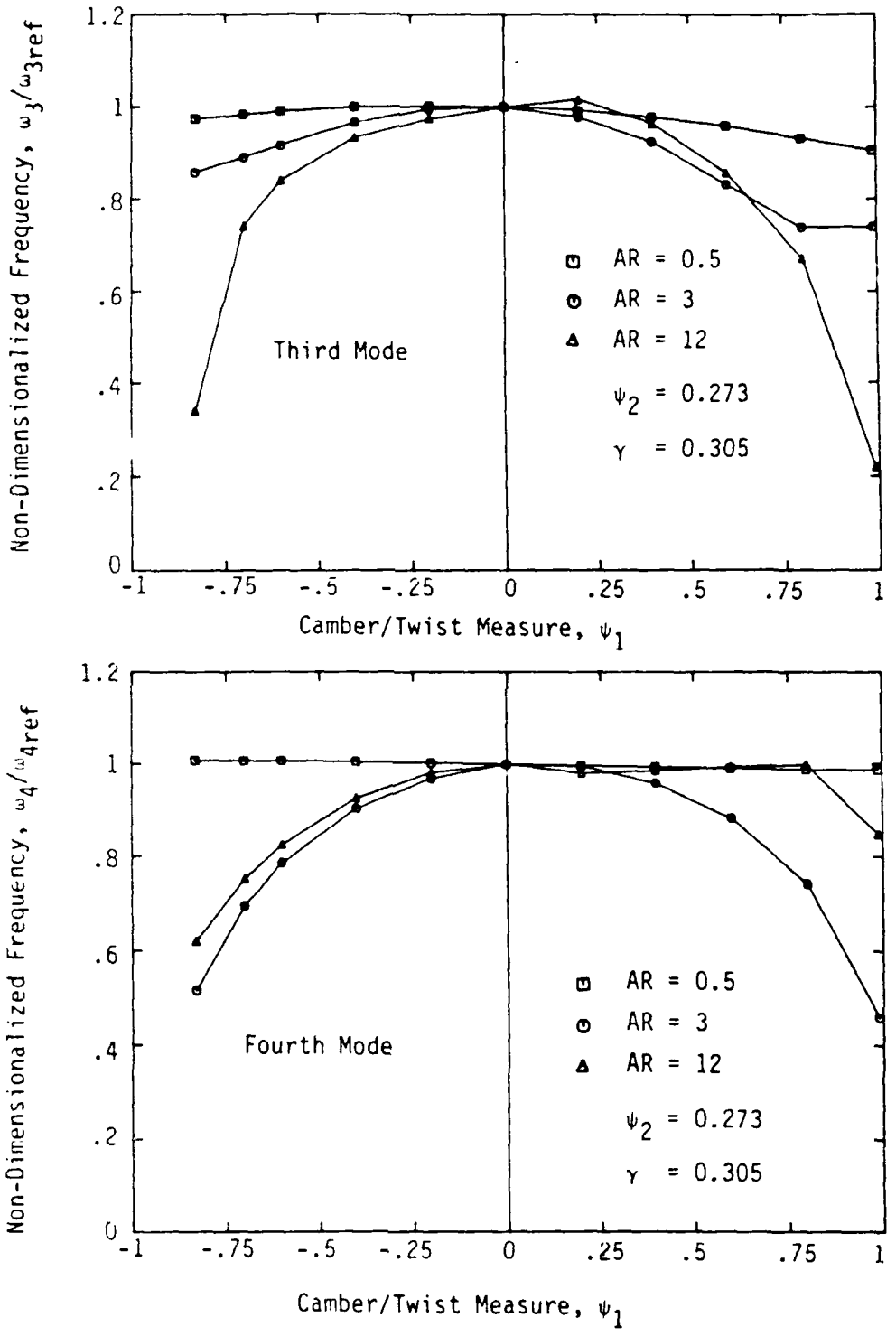

Figure 3. Frequency Variation as a Function of Camber/Twist Tailoring Parameter, ψ_1, in Third and Fourth Modes with Different Aspect Ratios (AR)

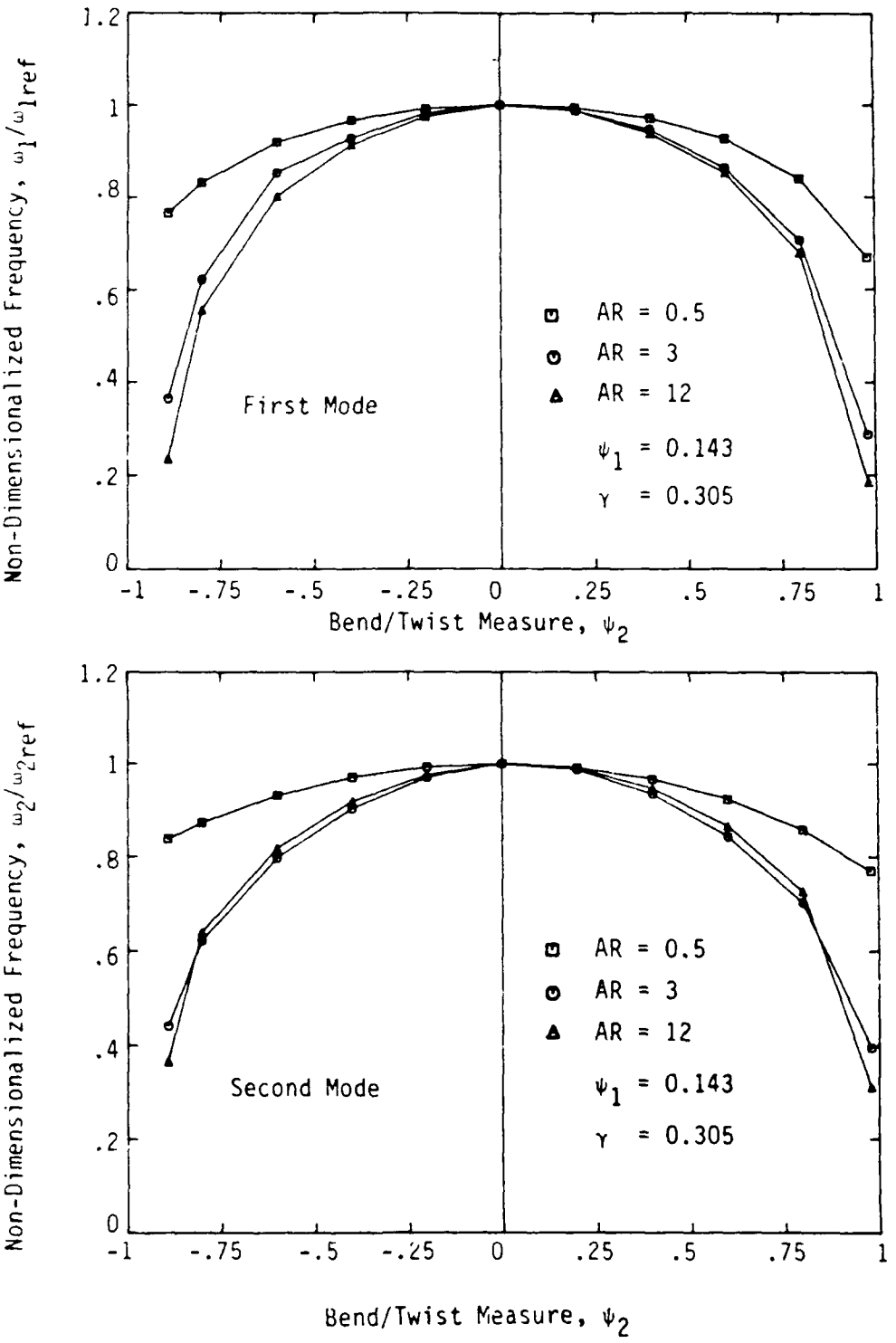

Figure 4. Frequency Variation as a Function of Bend/Twist Tailoring Parameter, ψ_2, in First and Second Modes with Different Aspect Ratios (AR)

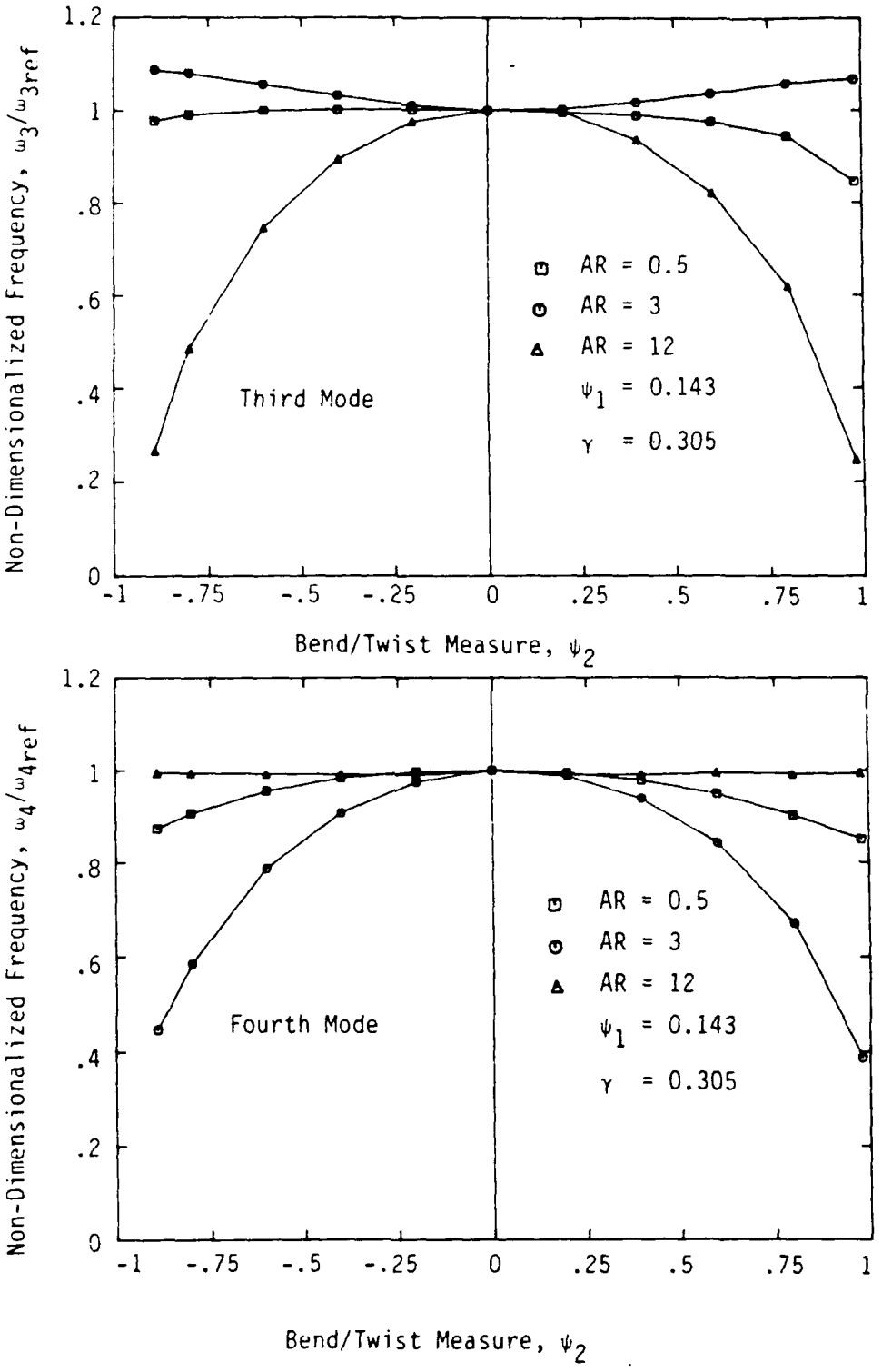

Figure 5. Frequency Variation as a Function of Bend/Twist Tailoring Parameter, ψ_2, in Third and Fourth Modes with Different Aspect Ratios (AR)

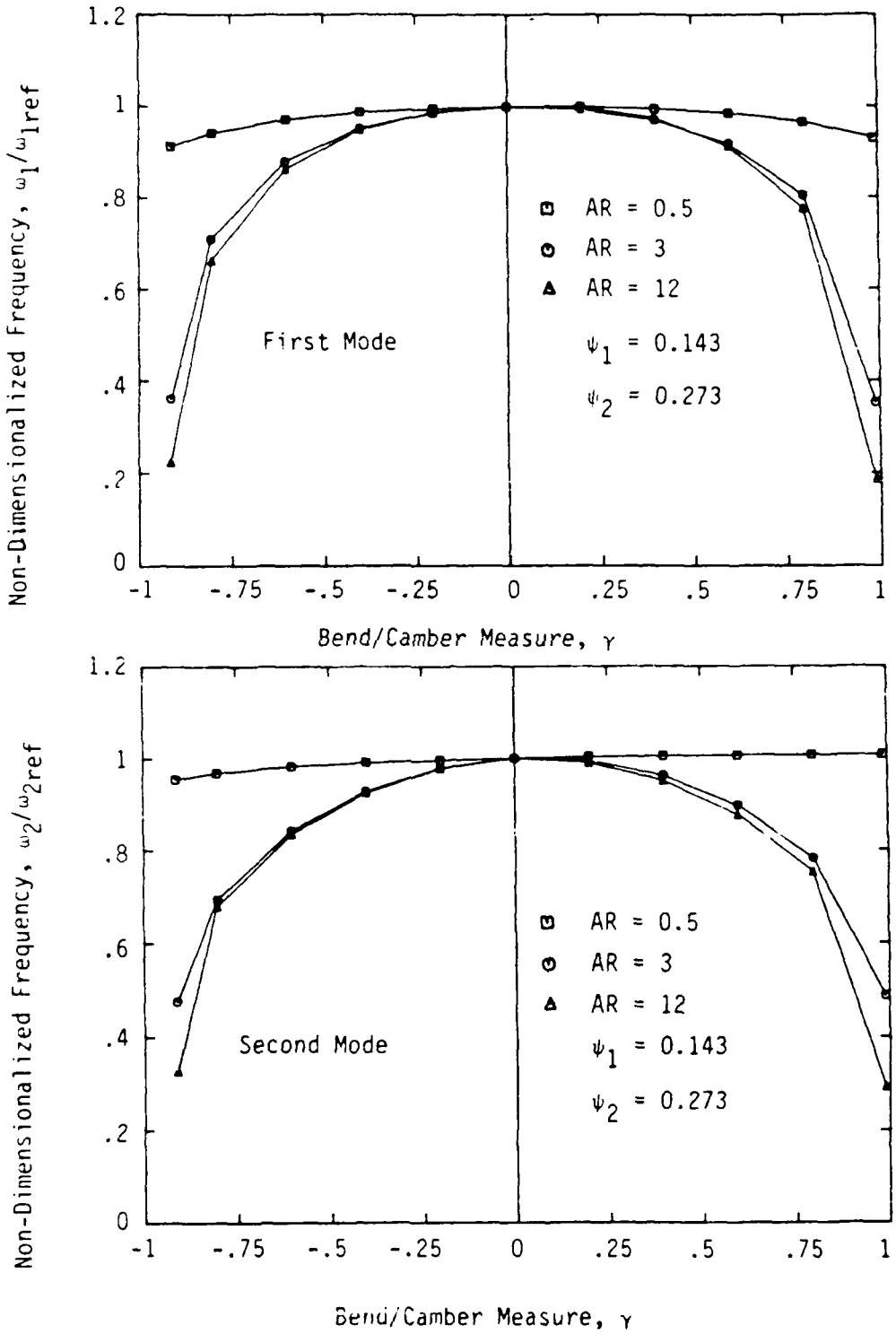

Figure 6. Frequency Variation as a Function of Bend/Camber Tailoring Parameter, γ, in First and Second Modes with Different Aspect Ratios (AR)

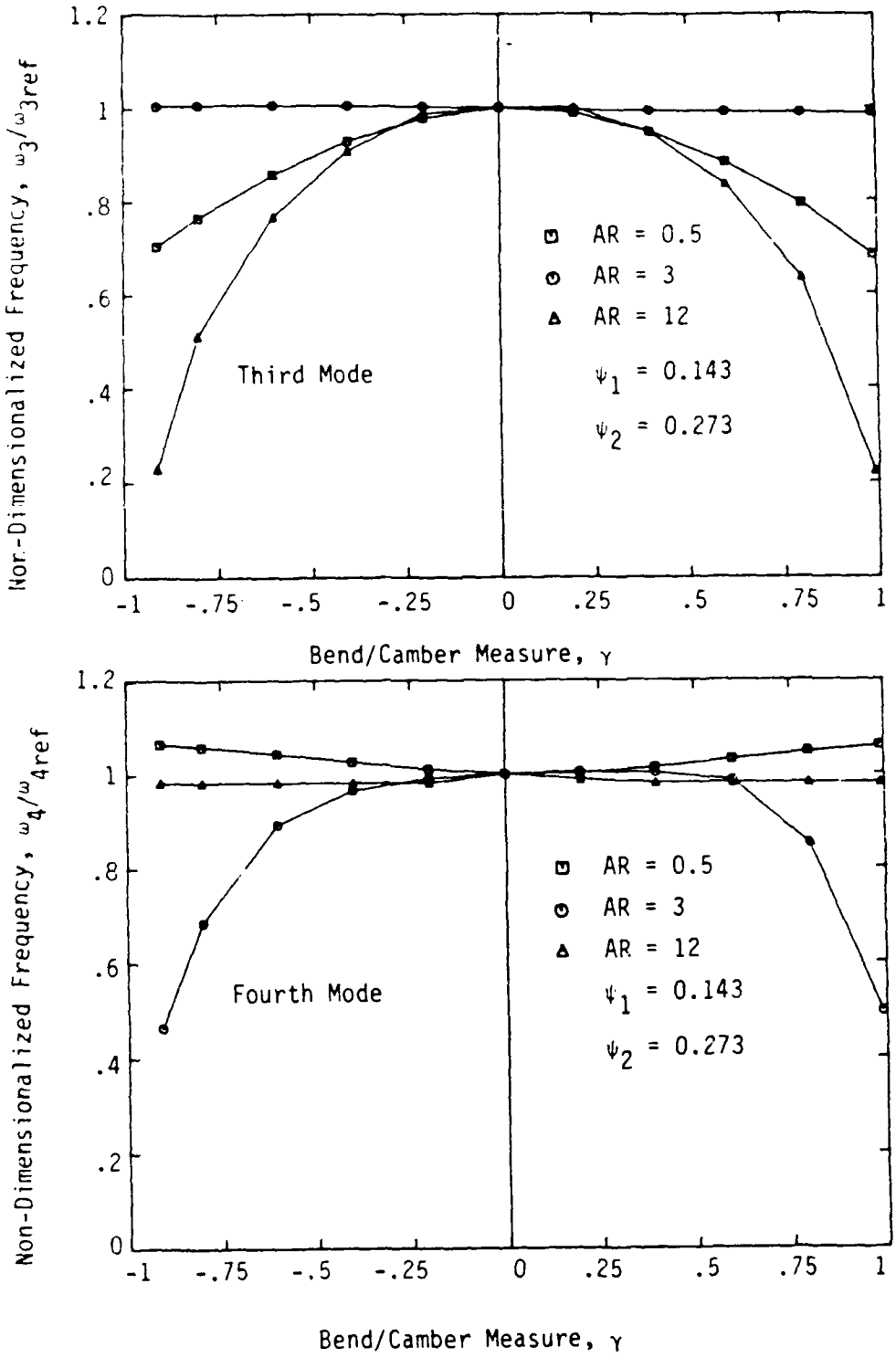

Figure 7. Frequency Variation as a Function of Bend/Camber Tailoring Parameter, γ, in Third and Fourth Modes with Different Aspect Ratios (AR)

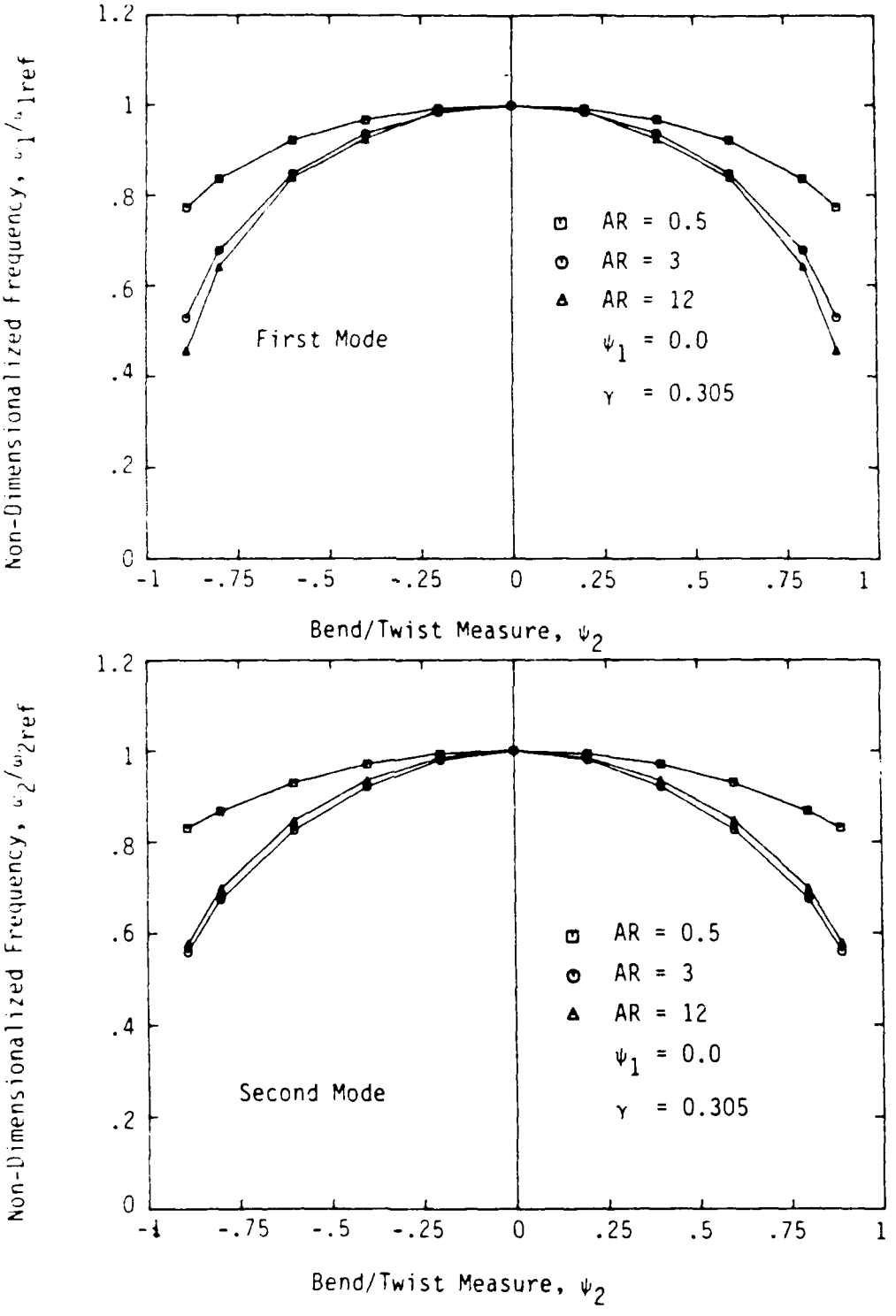

Figure 8. Frequency Variation as a Function of Bend/Twist Tailoring Parameter, ψ_2, in First and Second Modes with Different Aspect Ratios (AR) and without Camber/Twist Coupling

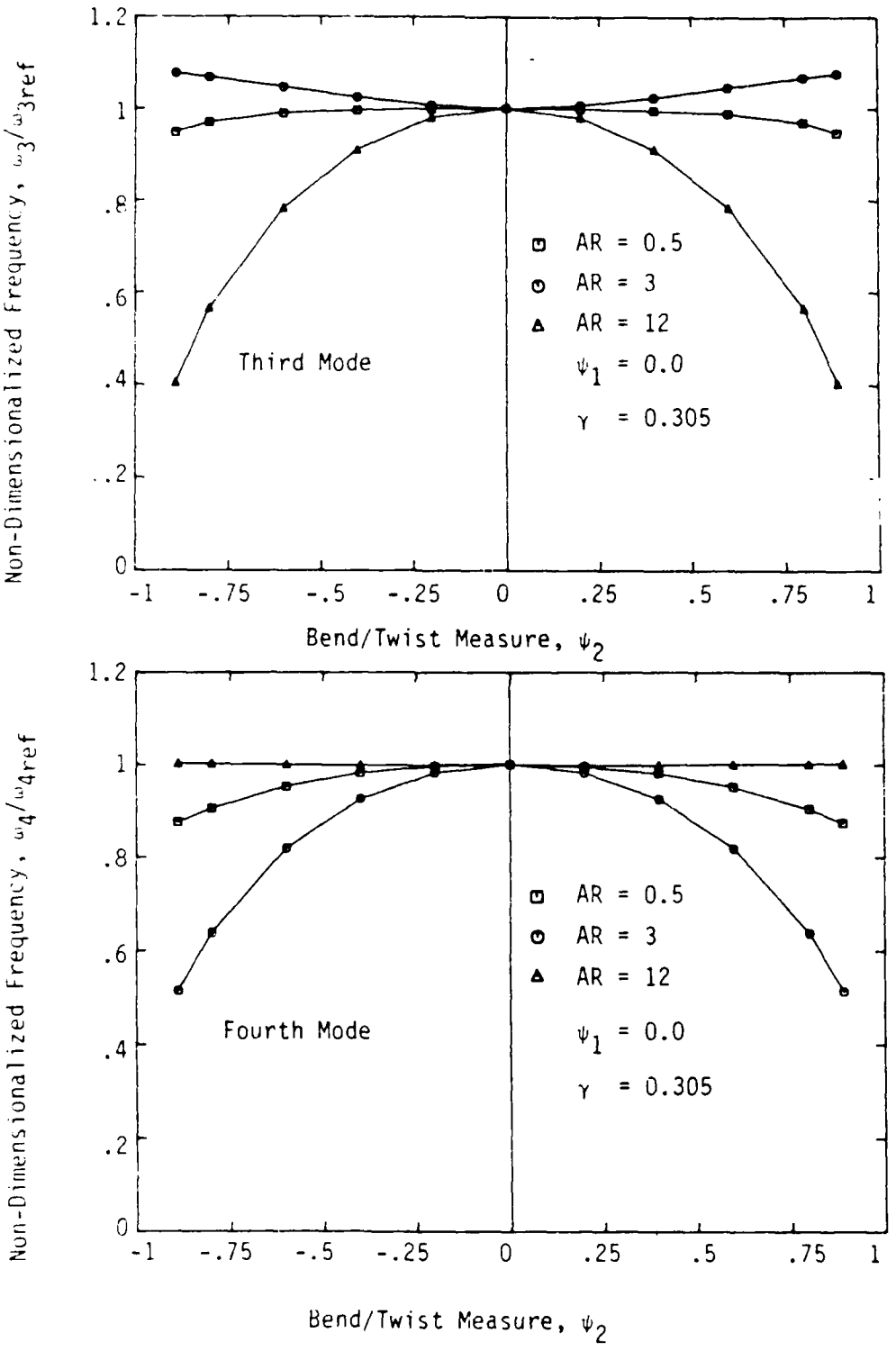

Figure 9. Frequency Variation as a Function of Bend/Twist Tailoring Parameter, ψ_2, in Third and Fourth Modes with Different Aspect Ratios (AR) and without Camber/Twist Coupling

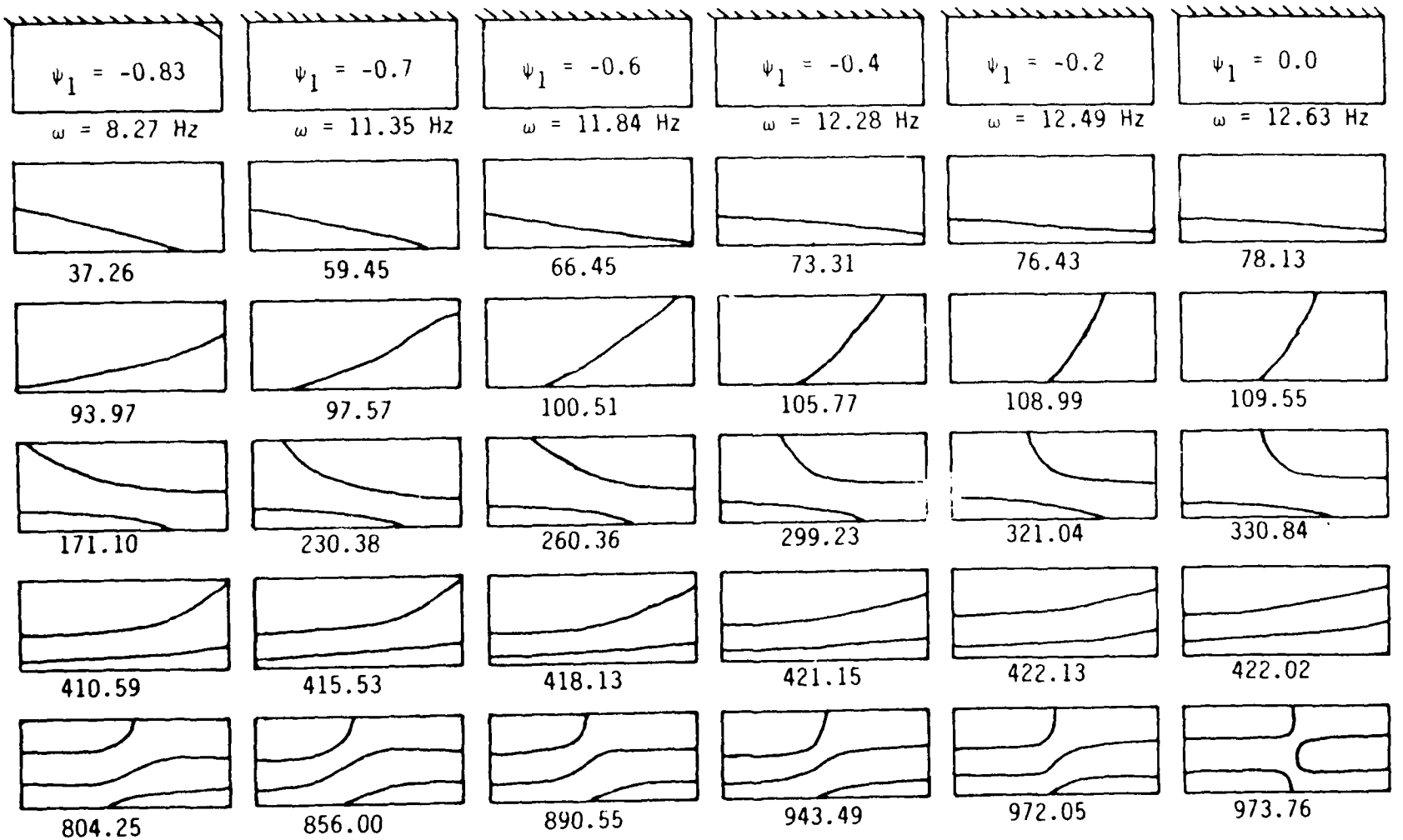

Figure 10. Effect of Tailoring Parameter ψ_1 on Nodal Patterns and Natural Frequencies. Spanwise Length Is Scaled Down. (AR = 3, ψ_2 = 0.273, γ = 0.305)

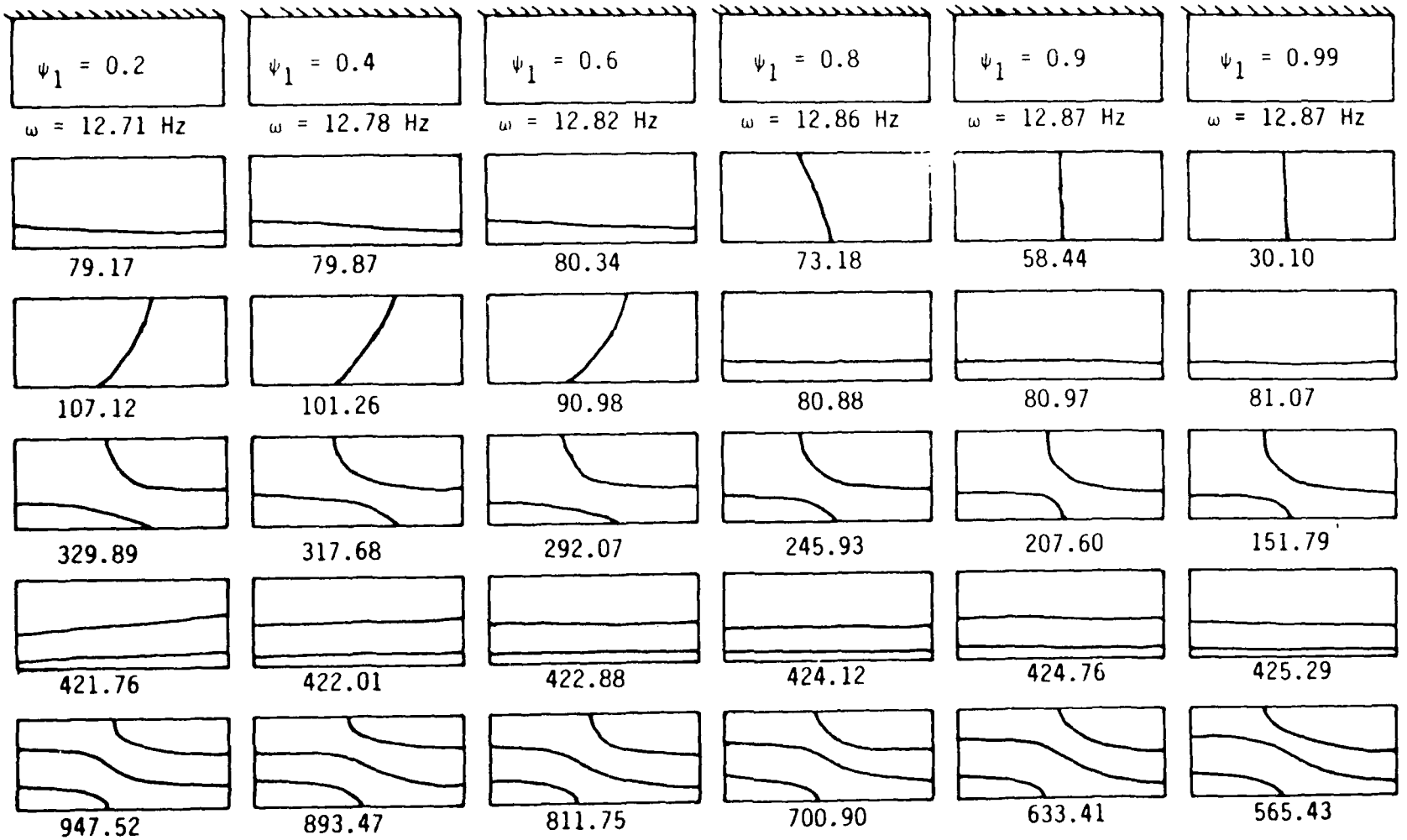

Figure 10. Continued

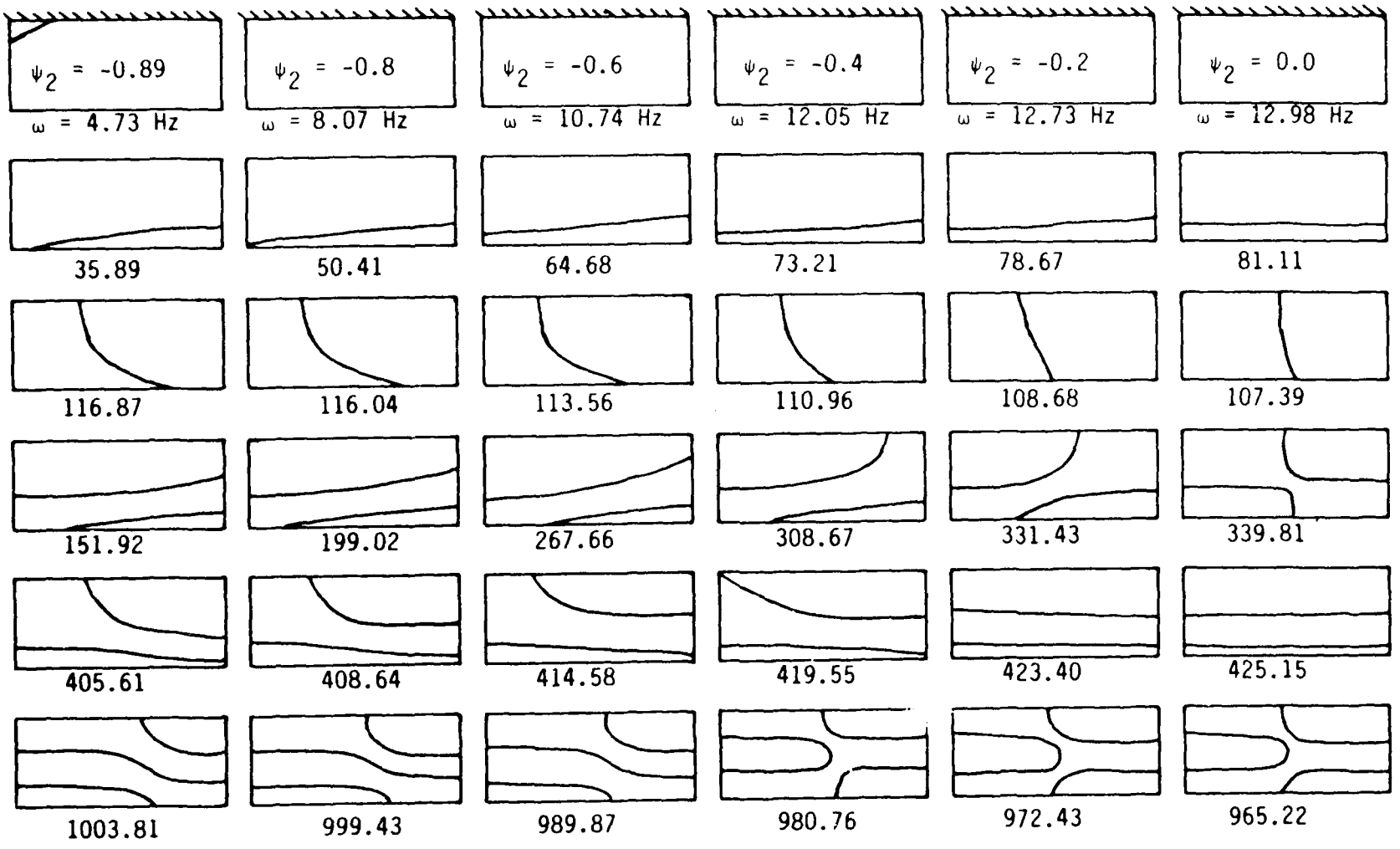

Figure 11. Effect of Tailoring Parameter ψ_2 on Nodal Patterns and Natural Frequencies. Spanwise Length Is Scaled Down. (AR = 3, $\psi_1 = 0.143$, $\gamma = 0.305$)

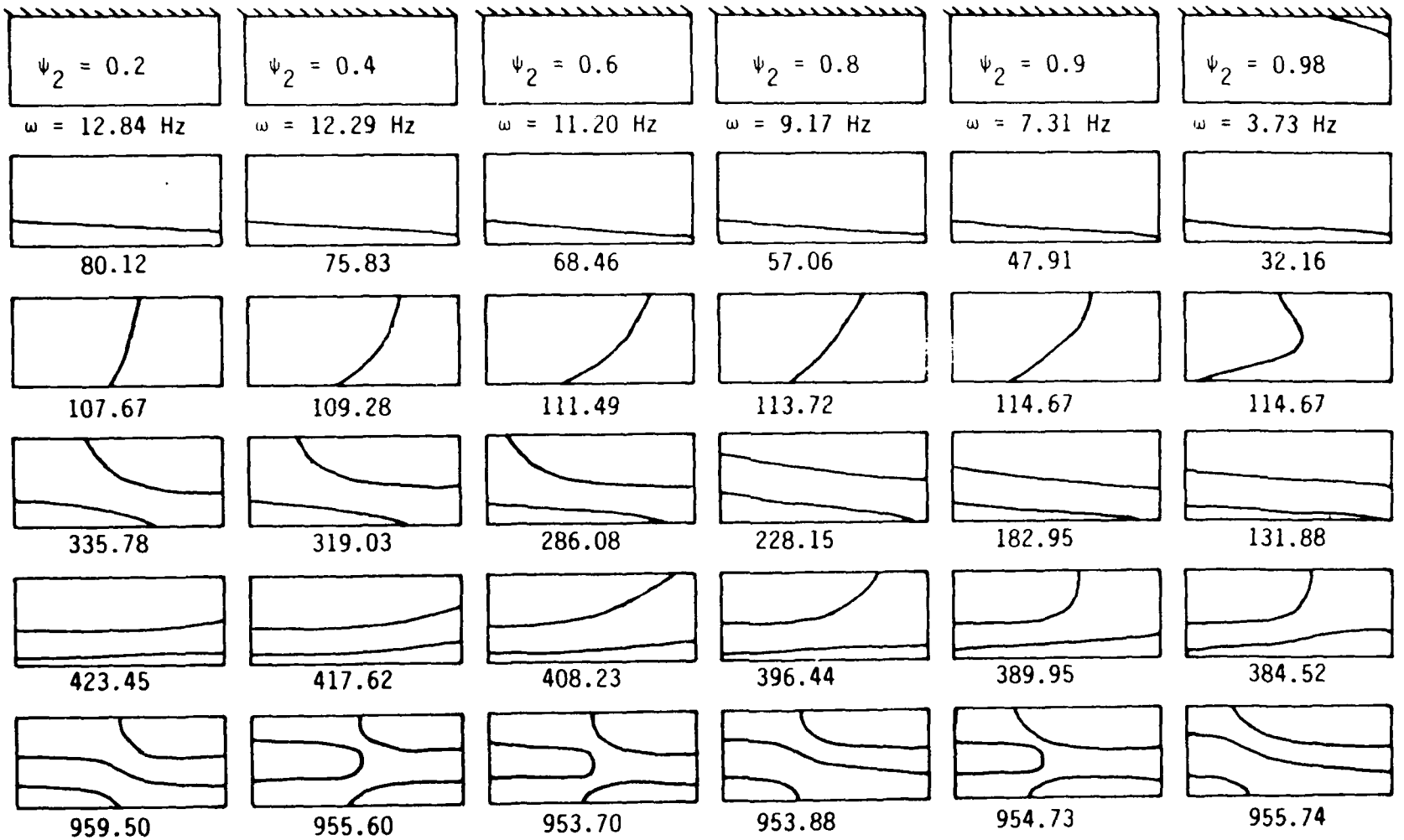

Figure 11. Continued

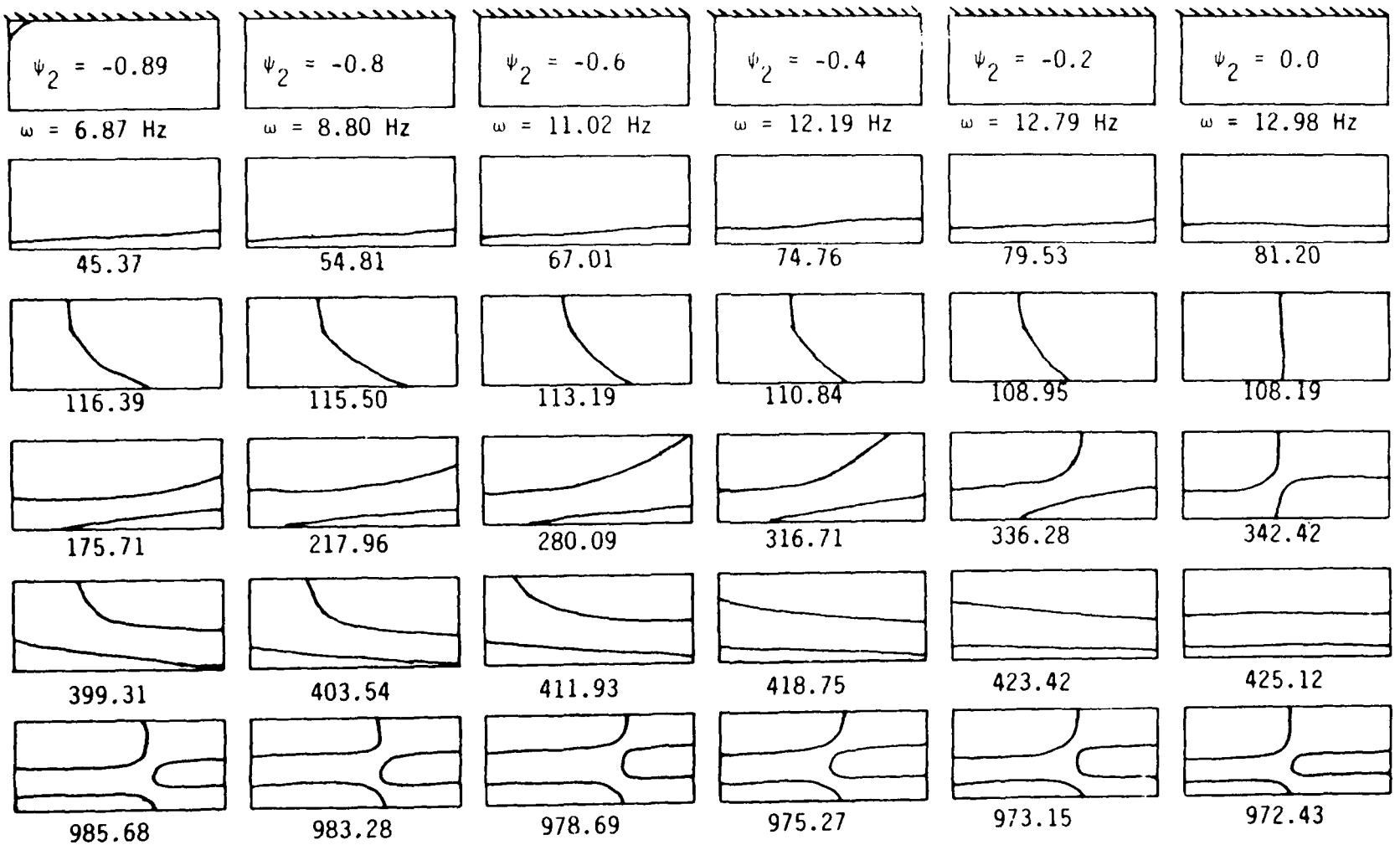

Figure 12. Effect of Tailoring Parameter ψ_2 on Modal Patterns and Natural Frequencies. Spanwise Length is Scaled Down. (AR = 3, $\psi_1 = 0.0$, $\gamma = 0.305$)

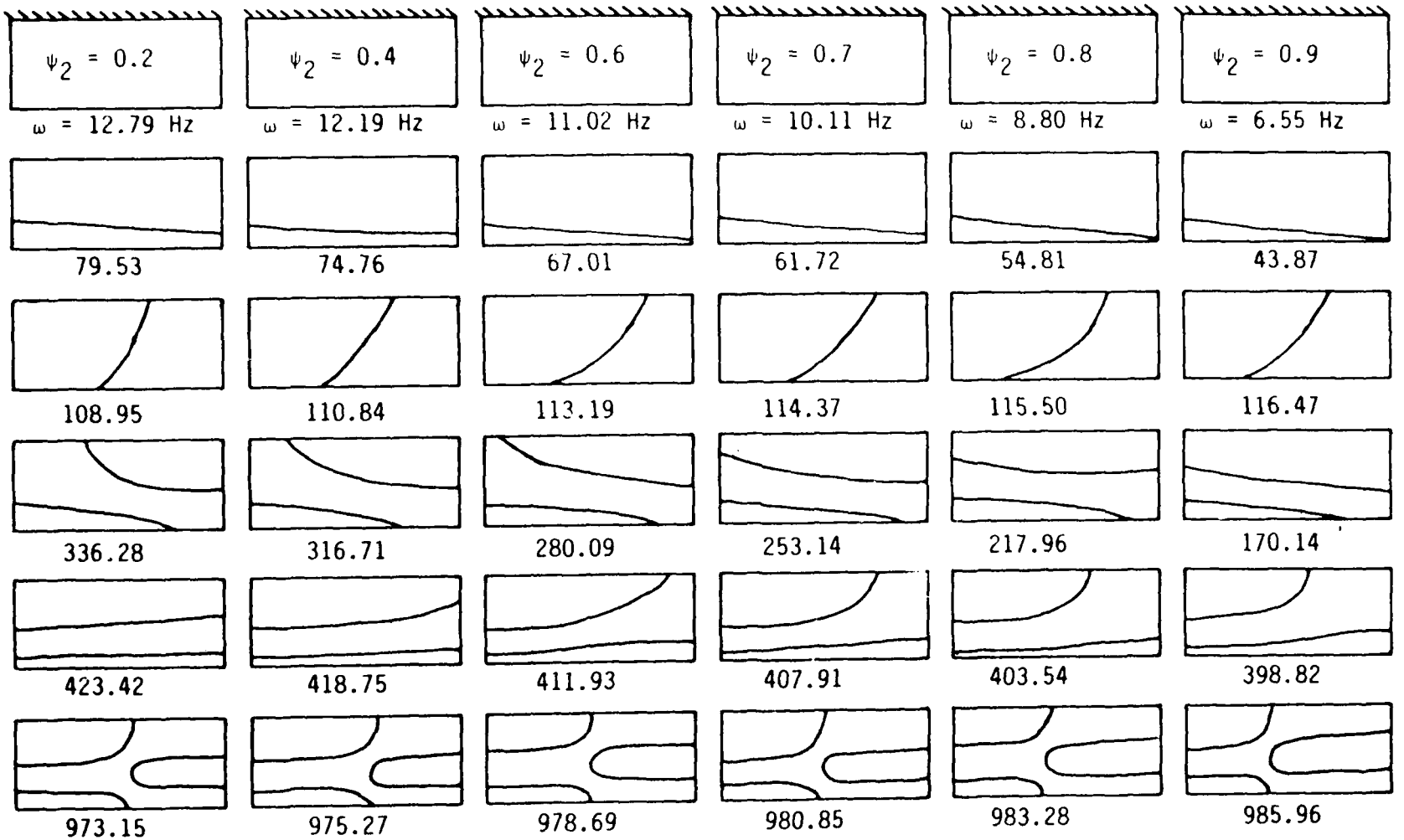

Figure 12. Continued

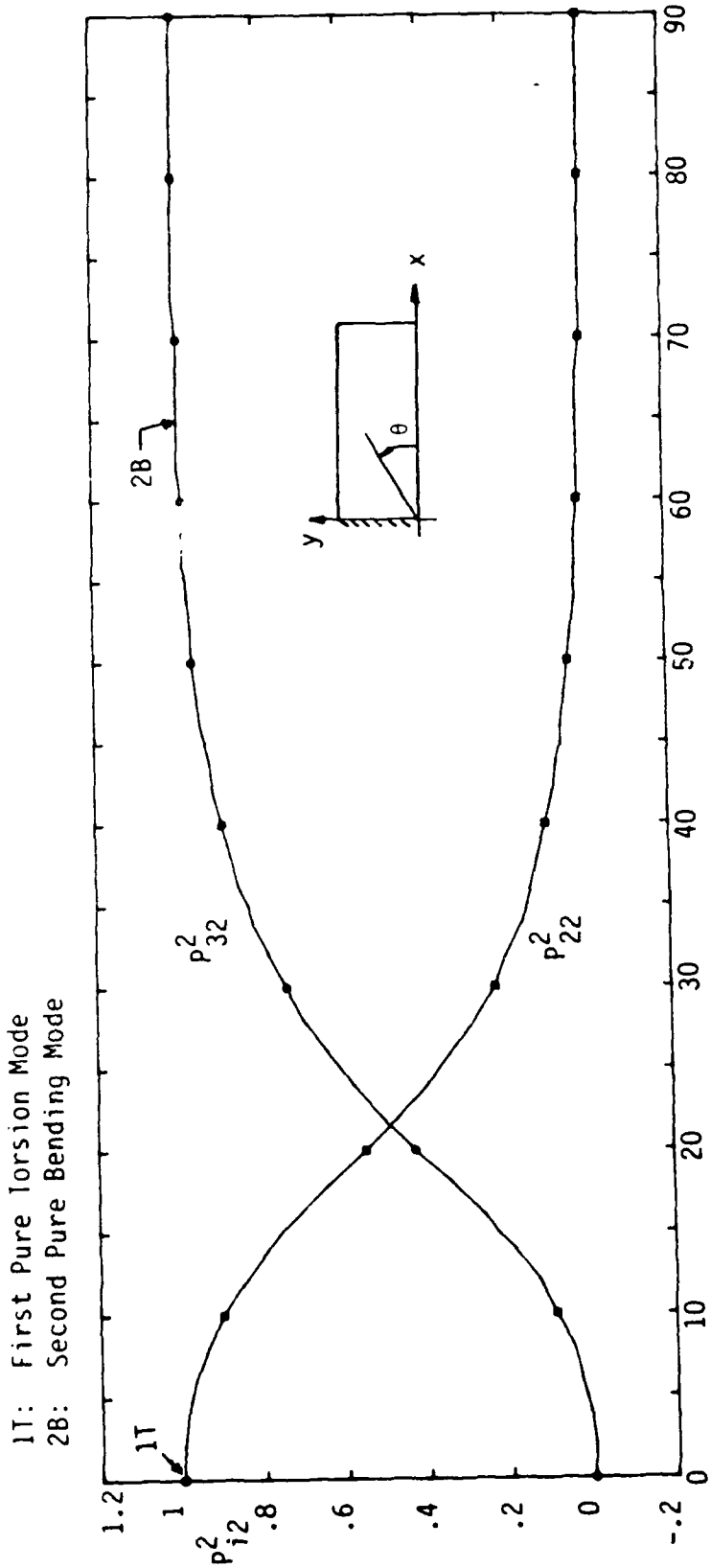

Figure 13. Change of the Measure of Kinetic Energy of Second Coupled Mode with Ply Angle

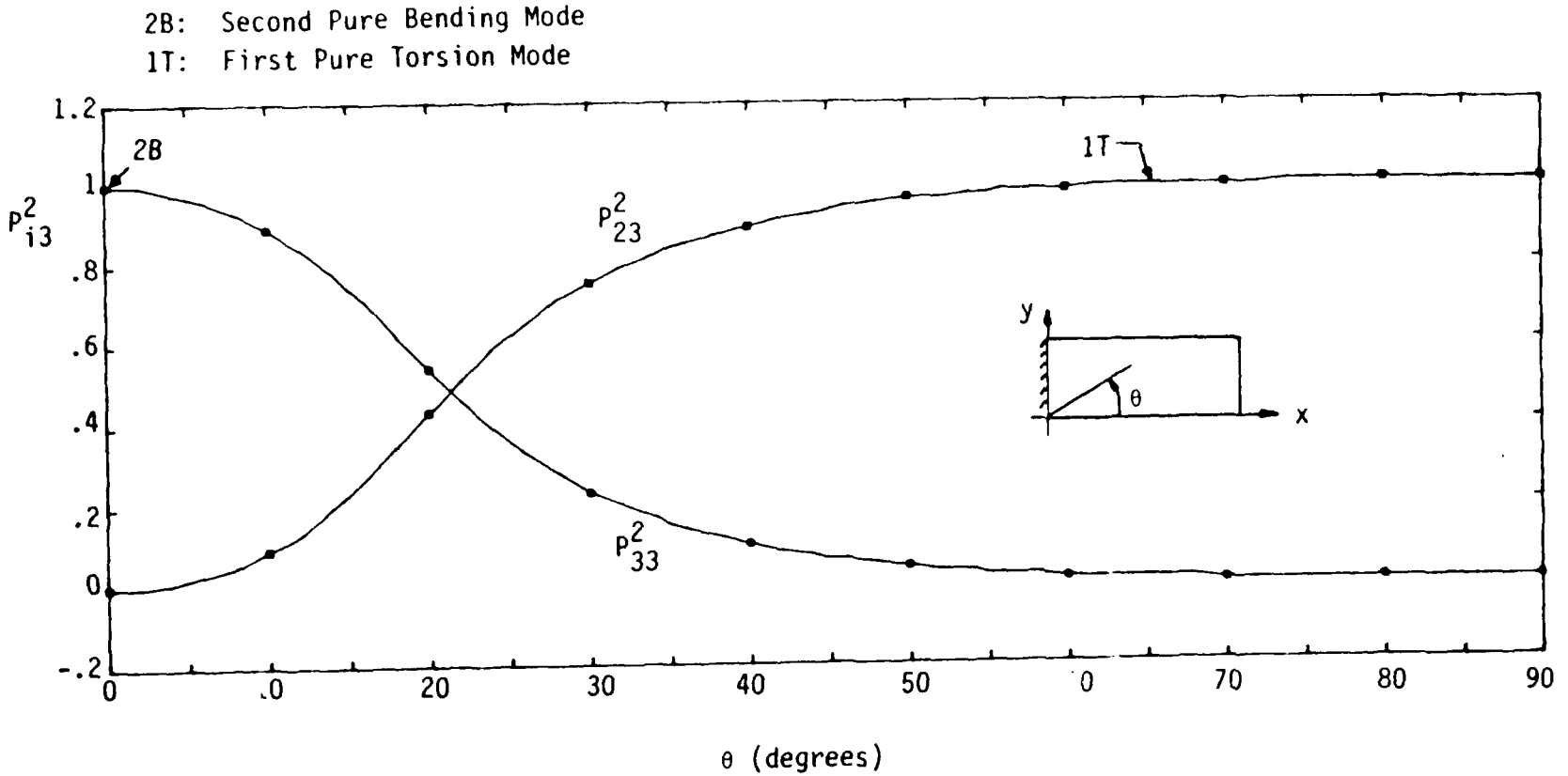

Figure 14. Change of the Measure of Kinetic Energy of Third Coupled Mode with Ply Angle

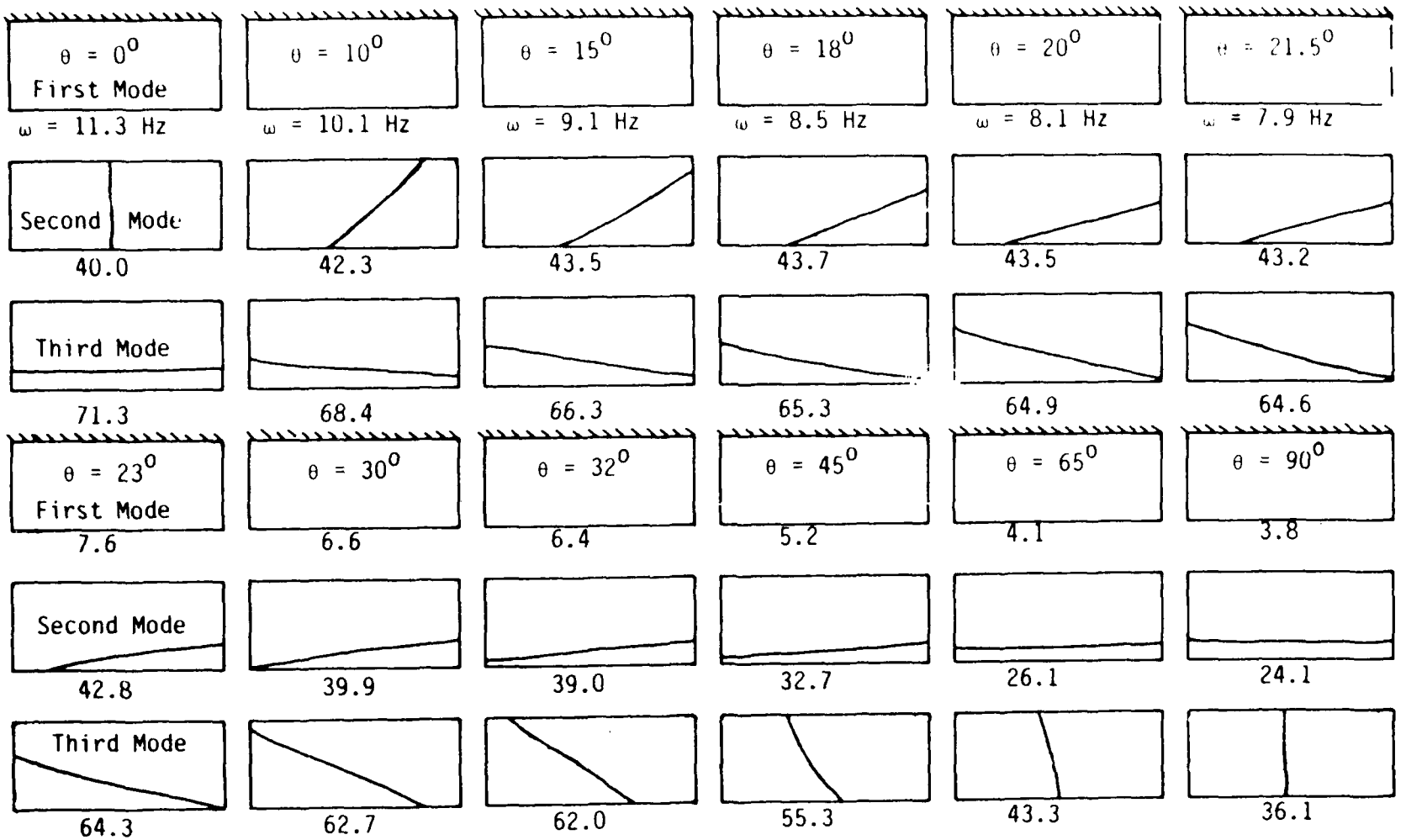

Figure 15. Nodal Patterns and Frequencies of the First Three Modes Changing with Ply Angle for $[\theta_2/0]_s$ Laminate. Spanwise Length Is Scaled Down.

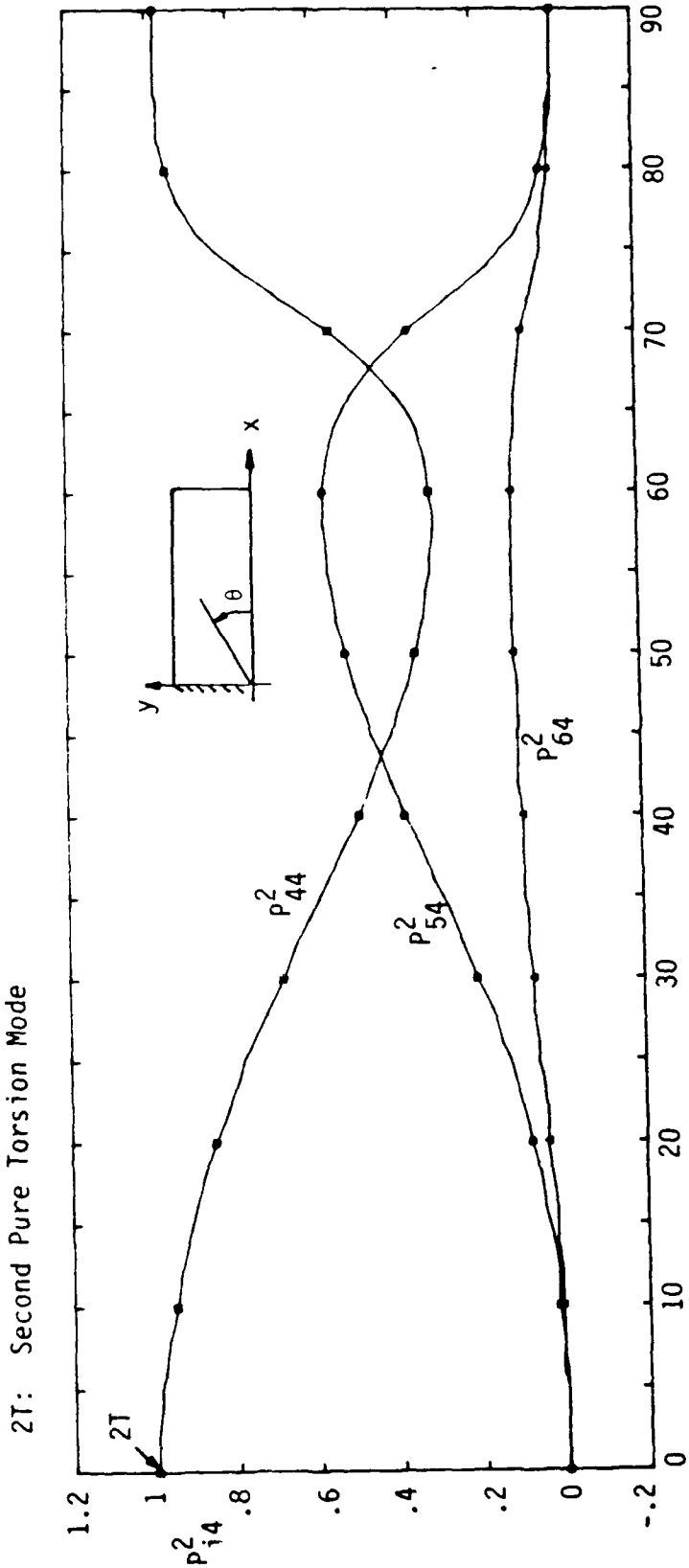

Figure 16. Change of the Measure of Kinetic Energy of Fourth Coupled Mode with Ply Angle

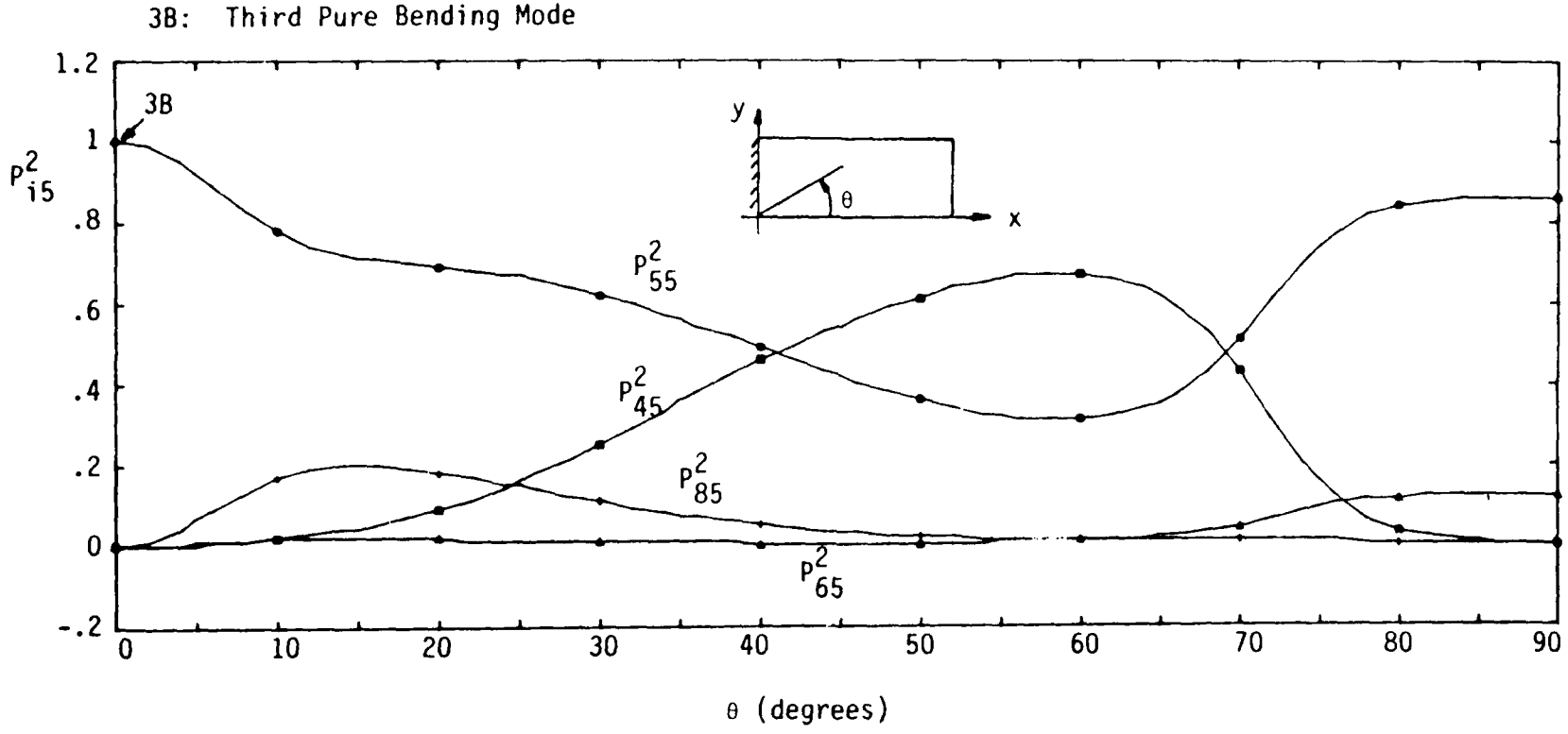

Figure 17. Change of the Measure of Kinetic Energy of Fifth Coupled Mode with Ply Angle

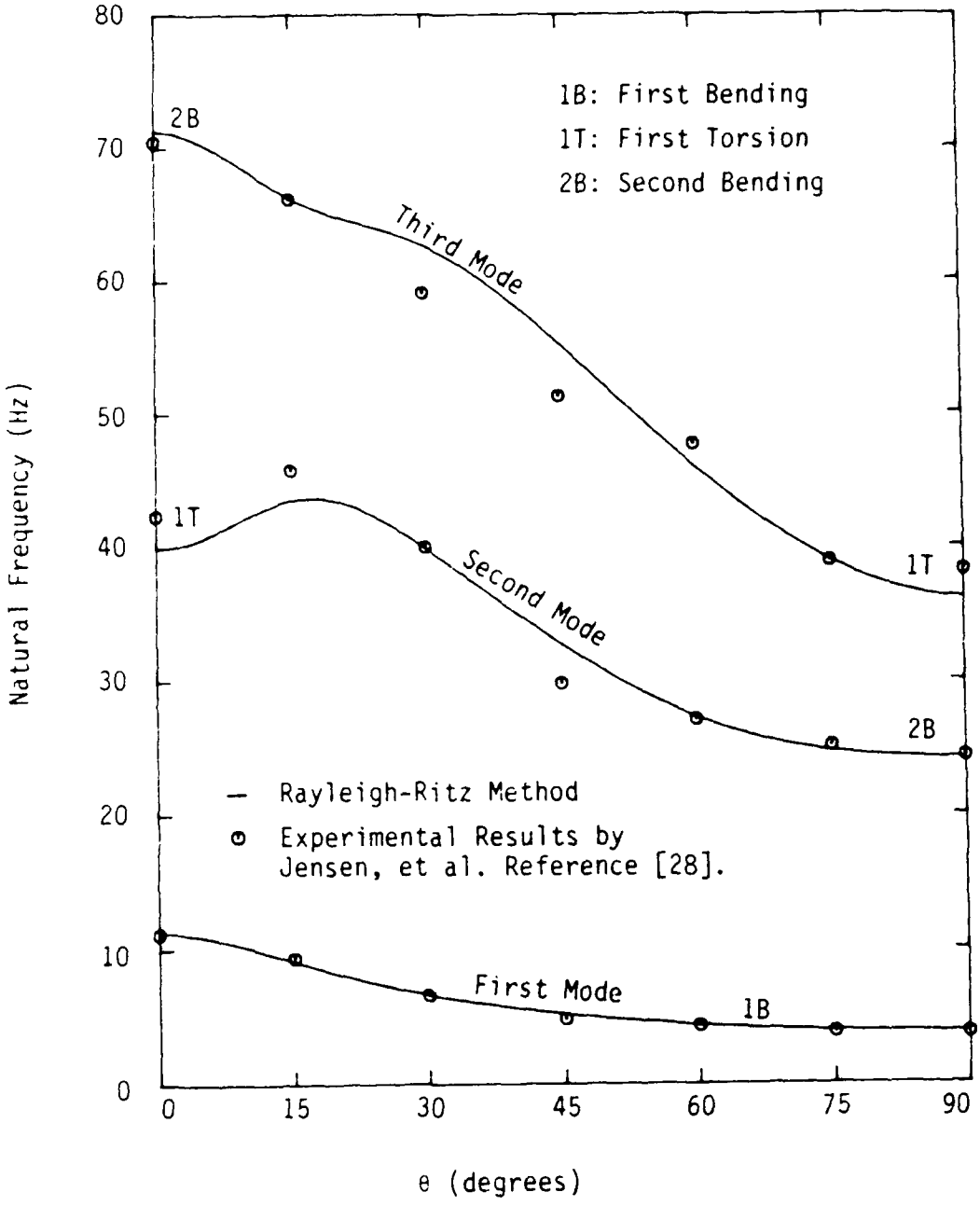

Figure 18. Variation of the Natural Frequencies of the First Three Modes with Ply Orientation in the Elastically Coupled Laminate

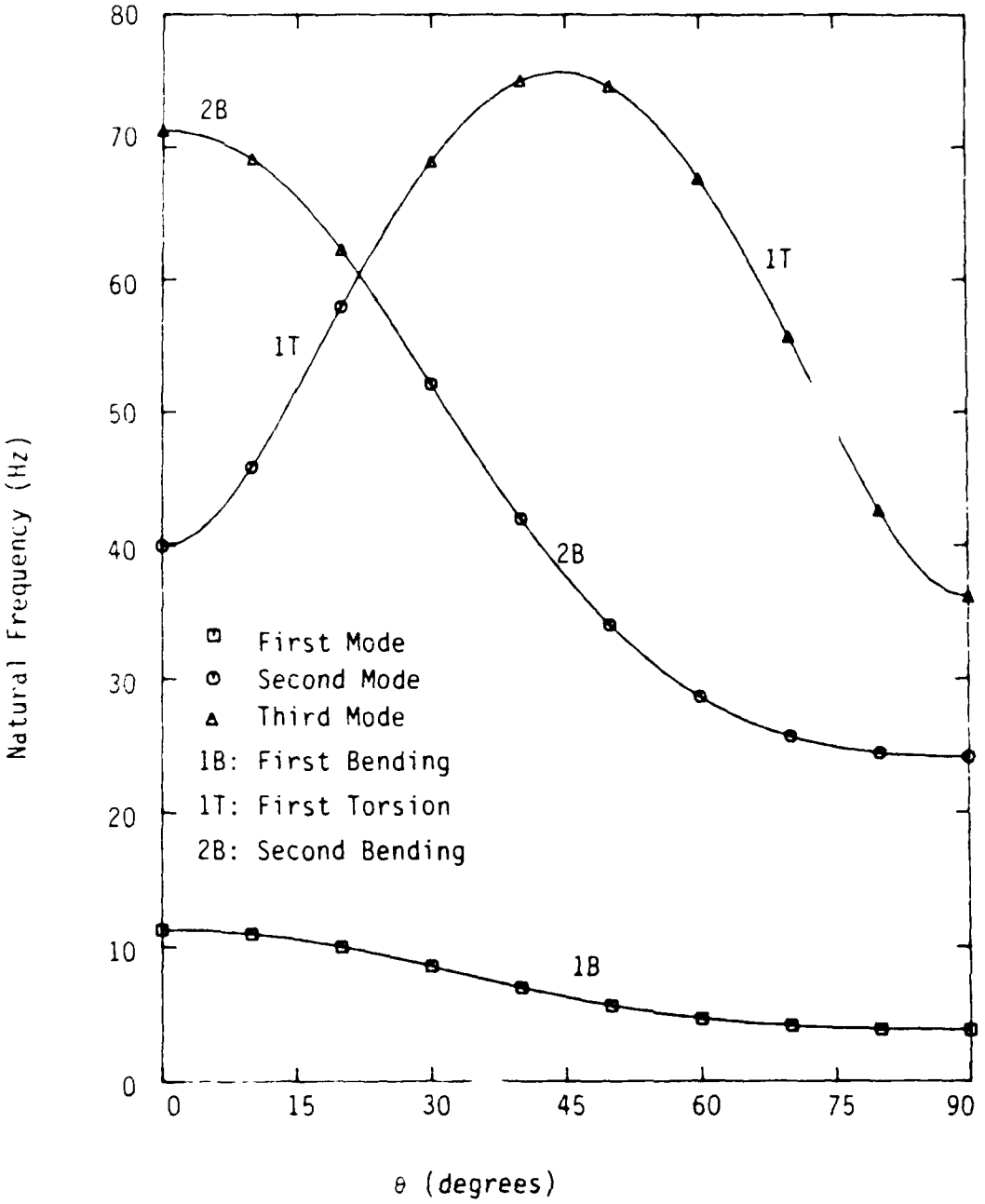

Figure 19. Variation of the Natural Frequencies of the First Three Modes with Ply Orientation in the Elastically Uncoupled Laminate ($\psi_1 = \psi_2 = 0$ for all θ)

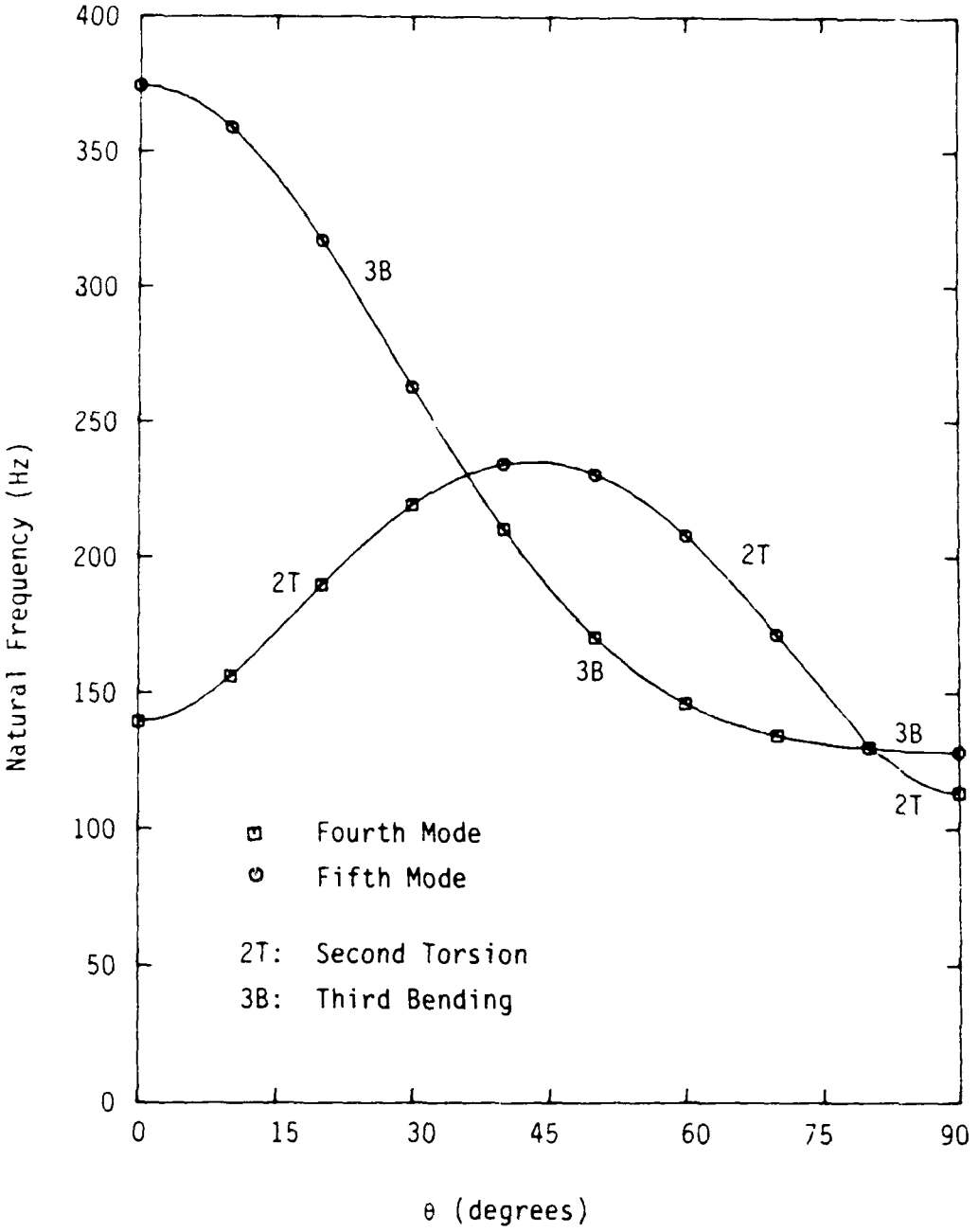

Figure 20. **Variation of the Natural Frequencies of the Fourth and Fifth Modes with Ply Orientation in the Elastically Uncoupled Laminate ($\psi_1 = \psi_2 = 0$ for all θ)**

5.5 Some Implications of Warping Restraint on the Behavior of Composite Anisotropic Beams*

Dr. Gabriel A. Oyibo**

Polytechnic University

Farmingdale, New York

5.5.1 Nomenclature

$(x,y,z,)$, (x_o,y_o,z_o) = physical and affine space coordinates, respectively

a_i = chordwise integrals

$(\Delta p, \Delta p_o)$ = differential aerodynamic pressure distributions in physical and affine space respectively

r, L_1, L_2, D^*, D_o^*, = generic nondimensionalized stiffness parameters

L_o, M_o = affine space running aerodynamic lift and moment, respectively

$\bar{U}, \bar{U}_o$ = virtual work expressions in physical and affine space, respectively

D_{ij} = elastic constants

ρ, ρ_∞ = affine space material and air density, respectively

* Research sponsored by the Air Force Office of Scientific Research (AFSC), under Contract F49620-85-C-0090 and F49620-87-C-0046. The United States Government is authorized to reproduce and distribute reprints for governmental purposes notwithstanding any copyright notation hereon.

** Associate Professor, Aerospace Engineering Dept., member AIAA

w = displacement

$\bar{h}$ = wing box depth

(h_o, α_o) = affine space bending and torsional displacement, respectively

c_o', c_o = affine space half-chord and chord, respectively

ℓ_o = affine space half-span for the wing

e = parameter that measures the location of the elastic axis relative to mid-chord

m_o = affine space mass per unit span

ω = vibration frequency

5.5.2 Introduction

The performance of modern supermaneuverable aircraft can be made to benefit a great deal from, significant advances in materials technology and the availability of more accurate aerodynamic prediction capabilities. Supermaneuverability as a design goal invariably calls for an optimization of the design parameters. Optimization may be partially accomplished for example, by using composite materials to minimize weight. Indeed, it has been known that these composite materials can be tailored to resolve the dynamic or static instability problems of these types of aircraft. The concept is referred to as aeroelastic tailoring.

While aeroelastic tailoring has tremendous advantages in the design of an aircraft, the analysis which provides the basis for the aeroelastic tailoring itself is generally very involved. This is rather unfortunate since a good fundamental physical insight of the tailoring mechanism is required for accurate and reliable results.

In this paper an attempt is made to look at some dynamic theories that can be used to understand the aeroelastic tailoring mechanism. Specifically, the accuracy of the St. Venant torsion theory which is relatively simple and frequently used in aeroelastic analysis is examined with particular reference to the effects of the wing's aspect ratio as well as other design parameters.

Although earlier studies[1,2,3] have indicated that the St. Venant's torsion theory is reasonably accurate except for aircraft wings with fairly low aspect ratios, the theory supporting that conclusion was based on the assumption that the wing is constructed of isotropic materials. Basically, the St. Venant's torsion theory assumes that the rate of change of the wing's twist angle with respect to the spanwise axis is constant (for constant stiffness and torque). This assumption is hardly accurate particularly for modern aircraft construction in which different construction materials are employed and the aerodynamic loads vary significantly along the wing's span. However, References 1-3 have shown that (in spite of such an inaccurate assumption) the main parameter that determines the accuracy of the St. Venant's theory is the wing's aspect ratio. Thus, it was determined that the theory is fairly accurate for moderate to high aspect ratio wings constructed of isotropic materials. In recent studies[4,5] however, it has been shown that for wings constructed of orthotropic composite materials, the conclusions of References 1-3 need to be modified. Rather than using the geometric aspect ratio of the wing to determine the accuracy of St. Venant's twist theory, it was suggested that a generic stiffness ratio, as well as an effective aspect ratio which considers the wing's geometry and the ratio of the

principal directional stiffness, should be considered in establishing the accuracy of St. Venant's theory.

The present paper is basically an extension of the studies that were begun in References 4 and 5. In this study the task was to examine the role of coupling (elastic coupling) on the accuracy of St. Venant's theory applied to static problems. It was discovered that coupling plays a very significant role on the accuracy of St. Venant's twist theory.

5.5.3

Formulation

Consider an aircraft wing fabricated of composite materials and mathematically idealized as a canti-levered plate subjected to forces and moments. It can be shown that the equations of motion for such a model can be described as follows.

$$a_1 h_o^{iv} + a_2 \alpha_o^{iv} + a_5 \alpha_o^{iii} + \rho_o a_1 \ddot{h}_o +$$

$$\rho_o a_2 \ddot{\alpha}_o = L_o \qquad (1)$$

$$a_2 h_o^{iv} - a_5 h_o^{iii} + a_3 \alpha_o^{iv} - a_4 \alpha_o^{ii} + \rho_o a_3 \ddot{\alpha}_o +$$

$$\rho_o a_2 \ddot{h}_o = M_o$$

where

$$a_1 = \int_{e\bar{c}_o}^{\bar{c}_o} dx_o \quad ; \quad a_2 = \int_{e\bar{c}_o}^{\bar{c}_o} x_o \, dx_o \quad ; \quad a_3 = \int_{e\bar{c}_o}^{\bar{c}_o} x_o^2 dx_o \quad ;$$

$$a_4 = 2 \int_{e\bar{c}_o}^{\bar{c}_o} D^*(1-\varepsilon) dx_o \qquad (2)$$

$$L_o = \int_{e\bar{c}_o}^{\bar{c}_o} \Delta p_o dx_o \quad ; \quad a_5 = \int_{e\bar{c}_o}^{\bar{c}_o} L_2 dx_o$$

$$M_o = \int_{e\bar{c}_o}^{\bar{c}_o} x_o \Delta p_o dx_o$$

and

$$-\infty<e<0 \quad ; \quad \bar{c}_o = \frac{c_o}{1-3}$$

$$( )' = \frac{\partial}{\partial y_o} \quad ; \quad \dot{( )} = \frac{\partial}{\partial t} \tag{3}$$

$$\bar{U}_o = \frac{U}{D_{22}}\left(\frac{D_{22}}{D_{11}}\right)^{1/4} \quad ; \quad D^* = \frac{D_{12} + 2D_{66}}{(D_{11}D_{22})^{1/2}}$$

$$\varepsilon D^* = \frac{D_{12}}{(D_{11}D_{22})^{1/2}} \tag{4}$$

$$L_1 = \frac{4D_{16}}{(D_{11}^{3/4}(D_{22})^{1/4}} \quad ; \quad L_2 = \frac{4D_{26}}{(D_{11})^{1/4}(D_{22})^{3/4}}$$

$$\Delta p_o = \frac{\Delta p}{D_{22}} \quad ; \quad \rho_o = \frac{\rho \bar{h}}{D_{22}}$$

D_{ij} are the elastic constants, ρ, is the material density, Δp is the differential pressure distribution, w is the displacement, t is the time, and $\bar{h}$ is the wing box depth.

5.5.4

Evolution of Warping Parameters

The evolution of the warping parameter with which to study the aeroelastic warping constraint phenomenon for wings fabricated of composite materials is a process that depends on the sophistication of the wing's mathematical model; whether coupling effects are included, whether the wing's chordwise curvatures are included and so on. Therefore, any warping parameter is as good as the corresponding wing's displacements assumptions. However, the virtual work equation makes it possible for the analyst to determine its effective independent variables even before the dis-

placement assumptions are made. By non-dimensionalizing the spanwise space variable in Equation (1), depending on whether one is interested in the static, dynamic, coupled or uncoupled displacements, one of the following warping parameters may be useful.

$$\lambda_c = \frac{\ell_o}{c_o} \sqrt{\frac{3}{2} D_o^*} \tag{5}$$

$$\bar{\lambda}_c = \frac{\ell_o}{c_o} \sqrt{\frac{3}{2} \left(D_o^* - \frac{L_2^2}{8}\right)} \tag{6}$$

where

$$D_o^* = D^*(1-\varepsilon) \tag{7}$$

(ℓ_o/c_o) is defined as the wing's effective aspect ratio and D_o^* and L are the generalized stiffness and coupling ratios respectively (defined in earlier work such as References 5 and 6).

Equations (5) and (6) represent the appropriate warping parameter for dynamic deformation, static displacement with elastic cross-coupling.

It was discovered in this study that evolving the warping parameter in a manner shown in Equation (1) thru (3), should enable one to effectively investigate the effects of warping on the composite wing's dynamics (or the accuracy of St. Venant's theory.) From the lamination theory for composites it is known that while D_o^* and (ℓ_o/c_o) are always positive, L can be positive or negative. However, from Equations (1) and (3), it is clear that whether a composite wing has positive or negative coupling, the warping effect (in terms of $\bar{\lambda}_c$) is unchanged.

5.5.5

Computations

By using the evolved warping parameters defined in Equations 7 and 8 and appropriate boundary conditions, the boundary value problems associated with Equation (4) are solved in a closed-form manner to determine the wing's static twist.

The wing loading conditions considered in this analysis are as follows: (a) steady state distributed twist loads and (b) steady state concentrated twist oads.

5.5.6

a. Steady distributed twist loads

For a wing with a constant uniformly distributed spanwise twisting moment, f_o resulting from a steady state coupled bending-torsion displacements, the exact closed form solutions for the mode shape α_o, satisfying the appropriate boundary conditions is given by

$$\alpha_o(y_o) = \frac{6f_o\ell_o^2}{c_o^3(4\bar{\lambda})^2}\left[y_o - \frac{\bar{y}_o^2}{2} - \frac{\sinh 4\bar{\lambda}_c y_o}{4\bar{\lambda}_c}\right. \tag{8}$$

$$\left. \frac{1}{4\bar{\lambda}_c}\left(\tanh 4\bar{\lambda}_c + \frac{1}{4\bar{\lambda}_c \cosh 4\bar{\lambda}_c}\right)\left(\cosh 4\bar{\lambda}_c \bar{y}_o - 1\right)\right]$$

Equation 8 is therefore a closed form coupled twist distribution for a composite wing with the warping effects accounted for.

where

$$\bar{y}_o = y_o/\ell_o \tag{9}$$

When equation 8 is evaluated at the wing tip and compared to an equivalent expression predicted by St. Venant's theory, the following expression is obtained.

$$\frac{\alpha_o(1)}{\alpha_o(1)_{St.V}} = 1 - \frac{\tanh 4\bar{\lambda}_c}{2\bar{\lambda}_c} - \frac{1}{9\bar{\lambda}_c^2}\left(\frac{1}{\cosh 4\bar{\lambda}_c} - 1\right) \tag{10}$$

where α_o (1) is the wing tip twist given by equation 15 while α_o (1) is the wing tip twist given by the St. Venant torsion theory. A plot of equation 10 is shown in Figure 1.

5.5.7

b. Steady state concentrated tip twist loads

If the wing is under the influence of a concentrated twisting moment, F_o at the tip as a result of a steady state coupled bending torsion displacement, the exact closed form twist distribution that satisfies these equations of motion and their associated boundary conditions is given by

$$\alpha_o(\bar{y}_o) = \frac{6F_o\ell_o}{c^3{}_o(4\bar{\lambda}_c)^2}\left[\bar{y}_o - \frac{\sinh 4\bar{\lambda}_c y_o}{4\bar{\lambda}_c} + \frac{\tanh 4\bar{\lambda}_c}{4\bar{\lambda}_c}(\cosh\bar{\lambda}_c\bar{y}_o - 1)\right] \tag{11}$$

When the twist distribution given by equation 11 is evaluated at the wing tip and compared to its counterpart predicted by the St. Venant's torsion theory the following expression is obtained.

$$\frac{\alpha_o(1)}{\alpha_o(1)_{St.V}} = 1 - \frac{\tanh 4\bar{\lambda}_c}{4\bar{\lambda}_c} \tag{12}$$

It should be noted that the ratio given by equation 12 was plotted for the real values of $\bar{\lambda}_c$ in references 5 and 6 and was shown to represent conditions where any errors resulting from using St. Venant's torsion theory are conservative (over-design rather than under-design). In this analysis equation 12 is examined when $\bar{\lambda}_c$ is imaginary, which is possible if L_2 is very large. Under such circumstances, equation 12 becomes

$$\frac{\alpha_o(1)}{\alpha(1)_{St.V}} = 1 - \frac{\tan 4\bar{\lambda}_c}{4\bar{\lambda}_c} \tag{13}$$

Figure 2 depicts the conditions given by equation 13. It is therefore seen from the figure that there are certain ranges of $\bar{\lambda}_c$ for which nonconservative errors are possible by using the St. Venant's twist theory.

5.5.8

Results and Conclusions

The results are shown in Figures 1 and 2. Figure 1 shows a comparison of the static wing tip twist obtained in the present study and that obtained via St. Venant's twist theory in the presence of statically distributed forces and low to moderate coupling. Figures 2 shows the trend for concentrated forces and substantial coupling. In Figure 1 it is seen that the presence of coupling makes the errors of St. Venant's theory worse. This seems to suggest that the more sophisticated theory is more important for wings with coupling (e.g., wings aeroelastically-tailored using *elastic cross-coupling*).

Figure 2 also shows that nonconservative errors ($\left|\frac{\alpha_o(1)}{\alpha_{o_{St.V}}(1)}\right| > 1$) are are possible.

Using Figures 1 and 2, the following conclusions can be summarized: (i) ignoring warping arbitrarily using St. Venant's theory could result in very significant errors (as high as over 80% errors) in analytical results for composite aircraft wings, (ii) warping is more important (St. Venant's theory is less accurate) for wings with coupling, (iii) St. Venant's theory (which has always been shown to be conservative[1,2]), can be non-conservative or St. Venant's approximation can lead to an unsafe design error (under design rather than over design from a stability point of view).

5.5.9
REFERENCES

1. Reissner, E. and Stein, M., "Torsion and Transverse Bending of Cantilevered Plates," NACA TN 2369, June 1951.

2. Bisplinghoff, R.L., Ashley, H. and Halfman, R.L., "Aeroelasticity," Addison Wesley, 1955.

3. Petre, A., Stanescu, C., and Librescu, L., "Aeroelastic Divergence of Multicell Wings (Taking their Fixing Restraints into Account,)" Revue de Mechanique Appliquee, Vol. 12, No. 6, 1961, pp 689-698.

4. E.F. Crawley and J. Dugundji, "Frequency Determination and Nondimensionalization for Composite Cantilever Plates," Journal of Sound and Vibration, Vol. 72, No. 1, pp. 1-10, 1980.

5. Oyibo, G.A. and Berman, J.H., "Influence of Warpage on Composite Aeroelastic Theories," AIAA Paper. No. 85-0710, April 1985.

6. Oyibo, G.A. and Berman, J.H., "Anisotropic Wing Aeroelastic Theories with Warping Effects," DGLR Paper No. 85-57, Second International Symposium on Aeroelasticity and Structural Dynamics, Technical University of Aachen, West Germany, April 1985.

5.5.10
Acknowledgements

The author is grateful to the AFOSR for sponsoring this research. He is particularly thankful to Dr. A. K. Amos, and Dr. A. Nachman, the Program Managers who monitor the research program, for their constructive criticism. He also appreciates various comments from Dr. Sinclair Scala and Mr. Julian Berman, both of Fairchild Republic Company, and Professor Terrence Weisshaar of Purdue University.

Figures

Figure 1: Wing Tip Twist Ratios for Simple and More Involved Theory (distributed load and low to moderate coupling)

Figure 2: Wing Tip Twist Ratios Comparing Simple and More Involved Theory (with substantial coupling)

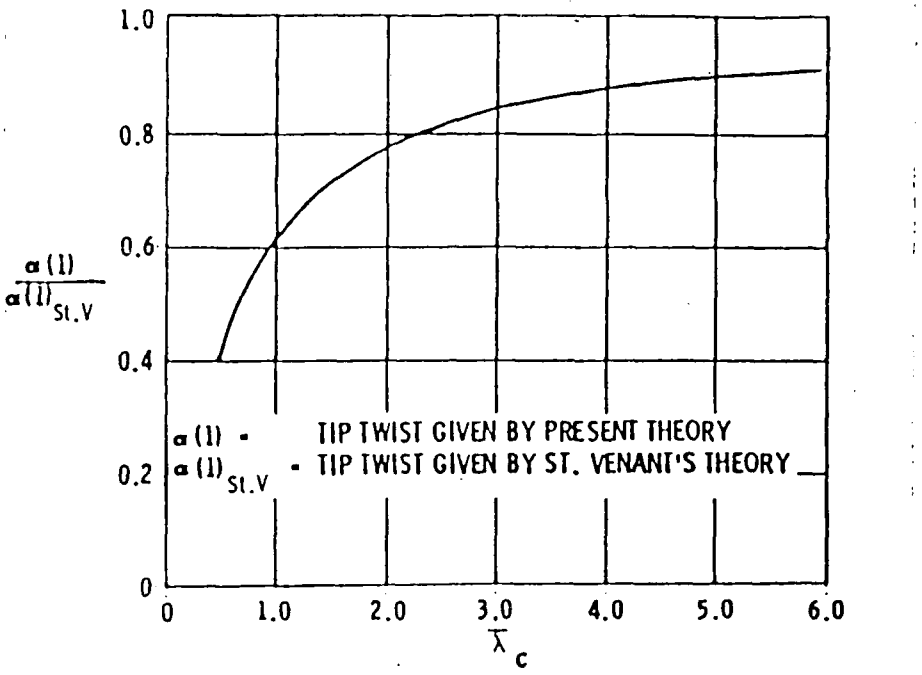
1.0
0.8
0.6
0.4
0.2
0
$\frac{\alpha(1)}{\alpha(1)_{St.V}}$
$\alpha(1)$ - TIP TWIST GIVEN BY PRESENT THEORY
$\alpha(1)_{St.V}$ - TIP TWIST GIVEN BY ST. VENANT'S THEORY
0
1.0
2.0
3.0
4.0
5.0
6.0
$\bar{\lambda}_c$

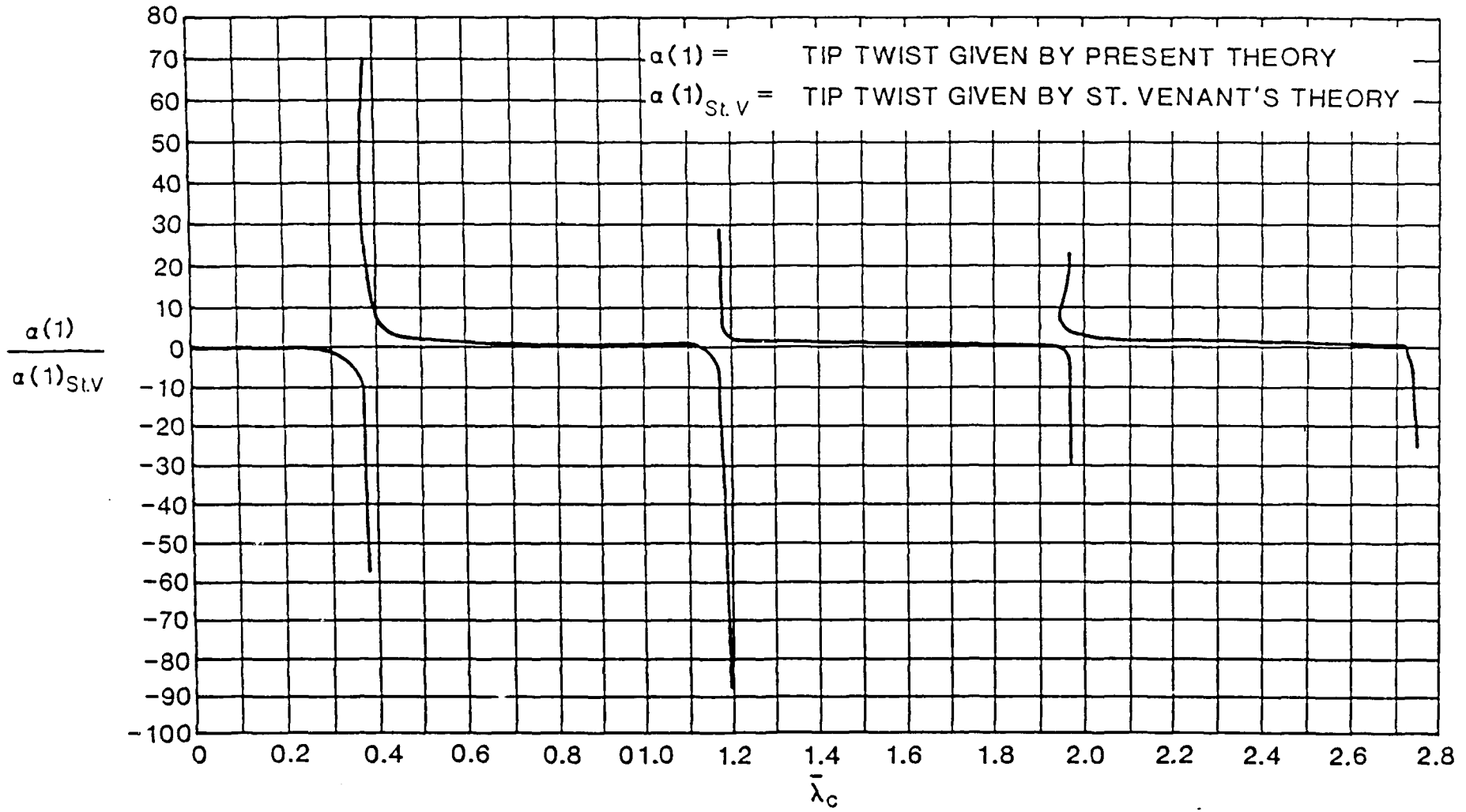
α(1) = TIP TWIST GIVEN BY PRESENT THEORY
α(1)St. V = TIP TWIST GIVEN BY ST. VENANT'S THEORY
α(1) / α(1)St.V
80
70
60
50
40
30
20
10
0
-10
-20
-30
-40
-50
-60
-70
-80
-90
-100
0
0.2
0.4
0.6
0.8
01.0
1.2
1.4
1.6
1.8
2.0
2.2
2.4
2.6
2.8
λ̄c

6.0 STATUS OF PUBLICATIONS

The significant results obtained thus far in this research program are being compiled and written up for publication in suitable technical journals. AIAA Paper No. 86-1006, a paper based on the first phase of this research has been prepared and was presented at the AIAA/ASME/ASCE/AHS 27th Structures, Structural Dynamics and Materials Conference held in San Antonio, Texas, May 19-21, 1986. A paper "Exact Solutions to Aeroelastic Oscillations of Composite Aircraft Wings with Warping Constraint and Elastic Coupling" has been submitted to the AIAA Journal. Another paper entitled "Some Implications of the Warping Restraint on The Behavior of Composite Anisotropic Beams" whose content forms the basis for this report has been accepted for publication by the Journal of Aircraft. In addition, a paper entitled "Exact Closed Form Solution for Nonlinear Unsteady Aerodynamics", which provides the basis for the proposed next phase of the program, has been accepted for publication by the AIAA Journal. Furthermore the results of the divergence study are in the process of being written up for submission to be considered for publication in a technical journal.

7.0 NAME, ADDRESS AND TELEPHONE NUMBER OF PROFESSIONAL PERSONNEL

1. Prof. Gabriel A. Oyibo,
   Principal Investigator, Program Manager
   Department of Aerospace Engineering
   Polytechnic University
   Long Island Campus
   Farmingdale, New York 11735

   (516) 755-4251

2. Prof. James Bentson, Investigator
   Department of Aerospace Engineering
   Polytechnic University
   Long Island Campus
   Farmingdale, New York 11735

   (516) 755-4390

3. Prof. Terrence A. Weisshaar, Investigator
   Department of Aeronautics and Astronautics
   Purdue University
   West Lafayette, Indiana 47907

   (317) 494-5975

4. Mr. George Papadopoulos, Graduate Student
   Department of Aerospace Engineering
   Polytechnic University
   Long Island Campus
   Farmingdale, New York 11735

   (516) 755-4367

5. Mr. John Nutakor, Graduate Student
   Department of Aerospace Engineering
   Polytechnic University
   Long Island Campus
   Farmingdale, New York 11735

   (516) 755-4367